JPL PUBLICATION 86-20

NASA/JPL Aircraft SAR Operations for 1984 and 1985

T.W. Thompson
Editor

November 1, 1986

National Aeronautics and
Space Administration

Jet Propulsion Laboratory
California Institute of Technology
Pasadena, California

NASA/JPL aircraft synthetic aperture radar imagery of Golden Gate Bridge and San Francisco; three-polarization color composite (top) and magnitude/phase image (bottom).

JPL PUBLICATION 86-20

NASA/JPL Aircraft SAR Operations for 1984 and 1985

T.W. Thompson
Editor

T. Andersen
W. Brown, Jr.
G. DiGiorgi
N. Donovan
D. Evans
T. Farr
D. Harrison
D. Held
E. McMillan
T. Miller
Contributors

November 1, 1986

NASA
National Aeronautics and
Space Administration

Jet Propulsion Laboratory
California Institute of Technology
Pasadena, California

The research described in this publication was carried out by the Jet Propulsion Laboratory, California Institute of Technology, under a contract with the National Aeronautics and Space Administration.

PREFACE

An impetus for this report was the NASA/JPL Aircraft SAR Workshop held in Pasadena, California, on 4-5 February 1986. Two recommendations of that workshop were to (1) catalog existing data and (2) document the aircraft system. This report is an attempt to satisfy those recommendations. Also, this report replaces an Aircraft SAR/Scatterometer User's Manual published in 1983 because that manual is largely out of date.

Another reason for this report was the unfortunate fire on the night of 17 July 1985 that destroyed the NASA/Ames CV-990 Airborne Laboratory and the NASA/JPL aircraft SAR. NASA is rebuilding both the Airborne Laboratory and the aircraft SAR with a goal of having them in the air again in 1987. The new systems will be modelled on what was destroyed. This report not only documents what was destroyed in the fire but also provides a model for the rebuilt radar.

The aircraft radar complements the Spaceborne Imaging Radar (SIR) Program. We at JPL conducted a major aircraft expedition in the fall of 1984 when we supplied aircraft SAR data to several SIR investigators. The next SIR flight will be SIR-C, which is scheduled for the early 1990's and will provide multiwavelength, multiple-polarization SAR data for the first time from space. The aircraft SAR provided useful inputs to the SIR Program via the multiple polarization data that have been routinely acquired since 1983. This report emphasizes the Fall-84 and Summer-85 Expeditions when the aircraft radar was equipped with microstrip antennas that permitted a direct measurement of the phase differences between the multiple polarizations.

ACKNOWLEDGMENTS

Many people contributed to the success of our aircraft radar program. First, we thank the investigators (the users) for their efforts in providing us with early indications of their data requests both during the premission planning and the postmission data-production phases. We welcome the momentum provided by the Aircraft Users Meeting held at JPL in February 1986 and the Airborne Science Meeting held at NASA Headquarters in October 1983. Both meetings provided useful insights to our operations via interactions with potential users.

The NASA/Ames Medium Altitude Missions Branch supported our efforts with a very professional operation. We thank John Reller for his careful and accurate scheduling efforts. George Grant and George Alger were excellent mission managers. We thank Bob Morrison and Gene Moniz for their support as navigators and for their work in getting to all of our data sites. We thank Fred Drinkwater and the other pilots for their help in getting the CV-990 to our sites. The NASA/Ames Medium Altitude Missions Branch was a thoroughly professional group and a pleasure to work with.

The editor wishes to thank those at JPL who played a major part in the production of data. The flight operations were supported by the untiring efforts of Elmer McMillan, Tim Miller, and Bill Fiechter. Godfrey DiGiorgi and Neva Donovan were primarily responsible for the production of the digital images. Bi Trinh, Tom Andersen, Tom Bicknell, and Dave Deats were primarily responsible for the production of the optical survey data. Gina Nelson, Annie Holmes, and Don Harrison were responsible for data archiving and distribution of products to the users. Howard Zebker, Tae Joo, Yun-Ling Lou, Godfrey DiGiorgi, and Charles Werner have produced the correlation software through many years of effort. Many members of the Aircraft Radar Group (Walter Skotnicki, Bob Blakely, George Williams, and John McCluskey) have supported many efforts that provided successful aircraft hardware. Neil Herman and Dan Held have provided invaluable guidance throughout the past few years.

Peter Mouginis-Mark of the University of Hawaii and NASA Headquarters as well as Prof. David Weissman of Hofstra University provided valuable inputs to this report. Roger Carlson of JPL provided very useful support in the production of this report.

ABSTRACT

The National Aeronautics and Space Administration/Jet Propulsion Laboratory (NASA/JPL) aircraft synthetic aperture radar (SAR) was used to conduct major data acquisition expeditions in 1983 through 1985. Substantial improvements to the aircraft SAR were incorporated in 1981 through 1984 resulting in an imaging radar that could simultaneously record all four combinations of linear horizontal and vertical polarization (HH, HV, VH, VV) using computer control of the radar logic, gain setting, and other functions. Data were recorded on high-density digital tapes and processed on a general-purpose computer to produce 10-km square images with 10-m resolution. These digital images yield both the amplitude and phase of the four polarizations. All of the digital images produced so far are archived at the JPL Radar Data Center and are accessible via the Reference Notebook System of that facility.

Sites observed in 1984 and 1985 included geological targets in the western United States, as well as agricultural and forestry sites in the Midwest and along the eastern coast. This aircraft radar was destroyed in the CV-990 fire at March Air Force Base on 17 July 1985. It is being rebuilt for flights in 1987 and will likely be operated in a mode similar to that described here. The data from 1984 and 1985 as well as those from future expeditions in 1987 and beyond will provide users with a valuable data base for the multifrequency, multipolarization Spaceborne Imaging Radar (SIR-C) scheduled for orbital operations in the early 1990's.

CONTENTS

Figures

Figures

Tables

Tables

SECTION I

INTRODUCTION

The aircraft Synthetic Aperture Radar (SAR) Program at the Jet Propulsion Laboratory (JPL) commenced in 1970 when a coherent L-band radar originally flown on an Aerobee rocket (Ref. 1) was refurbished for flights on the Ames Research Center CV-990 Airborne Laboratory. This airborne radar was flown throughout the 1970's and was a "pathfinder" for several spaceborne radars, including the Apollo Lunar Sounder in 1972, the Seasat-1 SAR in 1978, and the Spaceborne Imaging Radars (SIR-A and SIR-B) in 1981 and 1984. One research area in the 1970's was to develop a spacecraft radar for mapping Venus. In response to that goal, the NASA/JPL aircraft SAR was at L-band, a frequency that could penetrate the Venusian atmosphere. Also, this radar recorded echoes near nadir where the echo strengths were higher and represented a reasonable Venusian spacecraft geometry. The Department of Defense also developed airborne SARs in the 1960's and 1970's. These SARs tend to be X-band (to obtain higher resolution), and they observe near the horizon for tactical reasons. Several references to the NASA/JPL aircraft SAR hardware configurations in the 1970's are given in the Bibliography. Recent multi-polarization results are described in the NASA/JPL Aircraft SAR Workshop Proceedings (Ref. 2) and by Evans et al. (1986) (Ref. 3).

The NASA/JPL aircraft SAR was used in an "operational mode" from 1983 to 1985 to provide digital imagery to NASA-approved users during a number of expeditions. The recent history of this radar is given in Figure 1-1. Key events include the system upgrades in 1981-1983, the four expeditions in 1983-1985, and the rebuild currently under way. The major upgrades to the NASA/JPL aircraft SAR in the early 1980's provided the ability to interleave horizontally polarized and vertically polarized pulses. This permitted the simultaneous recording of all four possible combinations of linearly polarized waves (HH, HV, VH, and VV). Also, digital recording was accomplished by refurbishing a surplus Sabre-III high-density digital recorder (HDDR) to record the aircraft data. Furthermore, the aircraft radar was controlled via a desk-top (Hewlett-Packard) HP-9845 computer, which controlled the radar parameters (e.g., logic and gain) and provided logging of the radar state throughout its data acquisition. A handbook for this radar was published in 1983 (Ref. 4). It is largely out of date and is being replaced by this report.

The expeditions performed with this upgraded radar are summarized in Table 1-1. The first expedition with these upgrades was the Summer-83 Expedition, a 12-flight mission flown in August and September 1983. Shortly thereafter, the first digital image was produced on a JPL (Digital Equipment Corporation) VAX computer, largely through the software efforts of Charles Werner and Dan Held and through the hardware efforts of Walter Brown and others who created a fiber-optics link from the Aircraft Radar Laboratory to the VAX computer in another building at JPL. Another mission, the 11-flight, Winter-84 Expedition, was flown in February and March 1984.

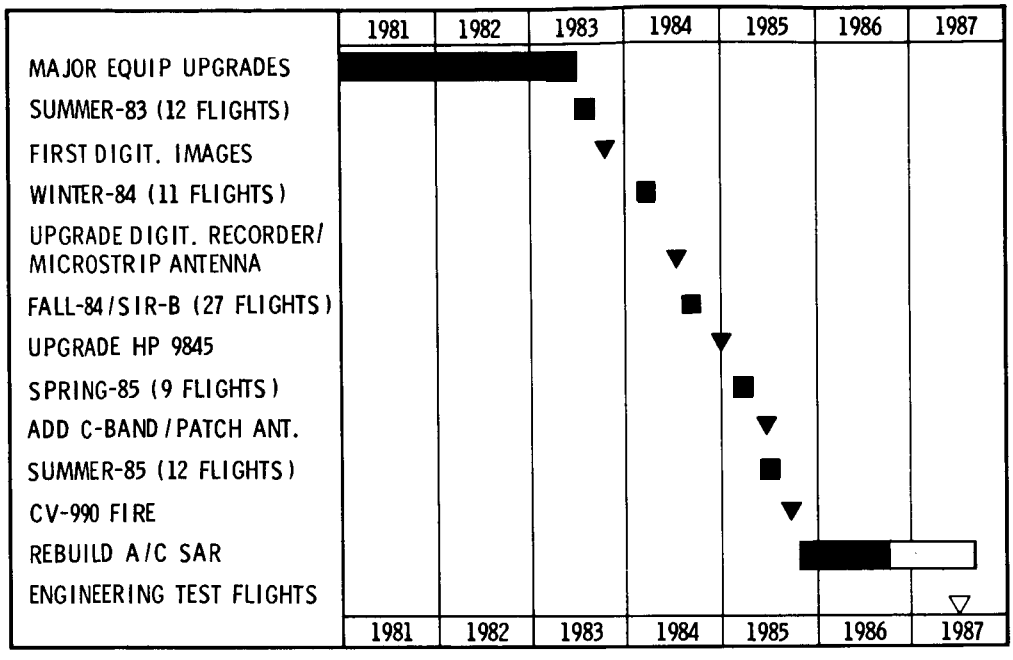

Figure 1-1. NASA/JPL Aircraft SAR Program: 1981 - 1987. Key elements include the major upgrades in 1981-1983, the four expeditions, and the rebuild, currently underway.

The next aircraft expedition was a major undertaking--the 27-flight, Fall-84 (SIR-B Underflight) mission in August through November 1984. This mission was preceded by two substantial equipment upgrades, replacement of the baggage door antenna with a microstrip antenna and replacement of the Sabre-III HDDR with a new Fairchild Model 80 HDDR. The new microstrip antenna permitted accurate measurement of phase differences among the various polarizations because the horizontal and vertical antenna elements were colocated while the horizontal and vertical antenna elements of the older baggage door antenna were not. The replacement of the HDDR greatly improved the digital data quality via error-correcting circuitry in the M-80 HDDR that did not exist on the Sabre-III HDDR.

The last expedition of the NASA/JPL aircraft SAR was the 21-flight Spring-Summer-85 Expedition from March through July 1985. This mission came to an ill-fated end on the night of 17 July 1985 when the CV-990 aircraft blew tires on its take-off roll at March Air Force Base in Riverside, California. The plane caught fire and was a total loss. Although the 19 crew members on board escaped without injury, the NASA/JPL aircraft radar equipment was also destroyed. NASA is providing funds to rebuild the equipment with the goal of operating the L-band SAR in 1987.

Table 1-1. Recent NASA/JPL Aircraft SAR Expeditions

	Aircraft Expedition			
	Summer-83	Winter-84	Fall-84-SIR-B	Spring-Summer-85
Dates	11 Aug 83-16 Sept 83	12 Feb 84-15 Mar 84	16 Aug 84-06 Nov 84	08 Mar 85-14 Jul 85
Data Flights	12	11	27	21
Investigators	19	12	29	24
Flight Requests	3	6	12	11
Sites	40	20	73	56
Along-Track Optical Coverage (km)	22,000	16,000	26,500	28,400
Along-Track Digital Coverage (km)	6,600	8,800	18,600	16,400

To complete this introduction to the NASA/JPL aircraft SAR, Figure 1-2 shows the geographic location of sites observed in 1984 and 1985 with the quadruple polarization "Quad-Pol" (HH+HV+VH+VV) data. There is a cluster of sites in the western U.S. that has been flown for JPL and SIR-B investigators. The sites in the Midwest and eastern U.S. for the most part have been flown for SIR-B investigators and for the following NASA centers: Goddard Space Flight Center (GSFC), Johnson Space Center (JSC), and National Space Technology Laboratory (NSTL). The eastern U.S. sites tend to be agricultural or forested, while the western U.S. sites tend to be geological in nature. Figure 1-3 shows the NASA/Ames CV-990 Airborne Laboratory. This was a commercial airliner (similar to the Boeing 707 or Douglas DC-8 aircraft) that was refurbished to carry scientific payloads for NASA investigators by the NASA/Ames Medium Altitude Missions Branch (MAMB).

The remaining sections of this report are devoted to the following topics. Section II describes operations in an end-to-end sense. Section III describes the aircraft hardware. Sections IV and V describe the data products. Section VI describes the location of data acquisitions and shows a few examples of typical data. Background information on flights, data, and investigators is given in Appendixes A, B, C, and D. Abbreviations, nomenclature, and acronyms are defined in Appendix E.

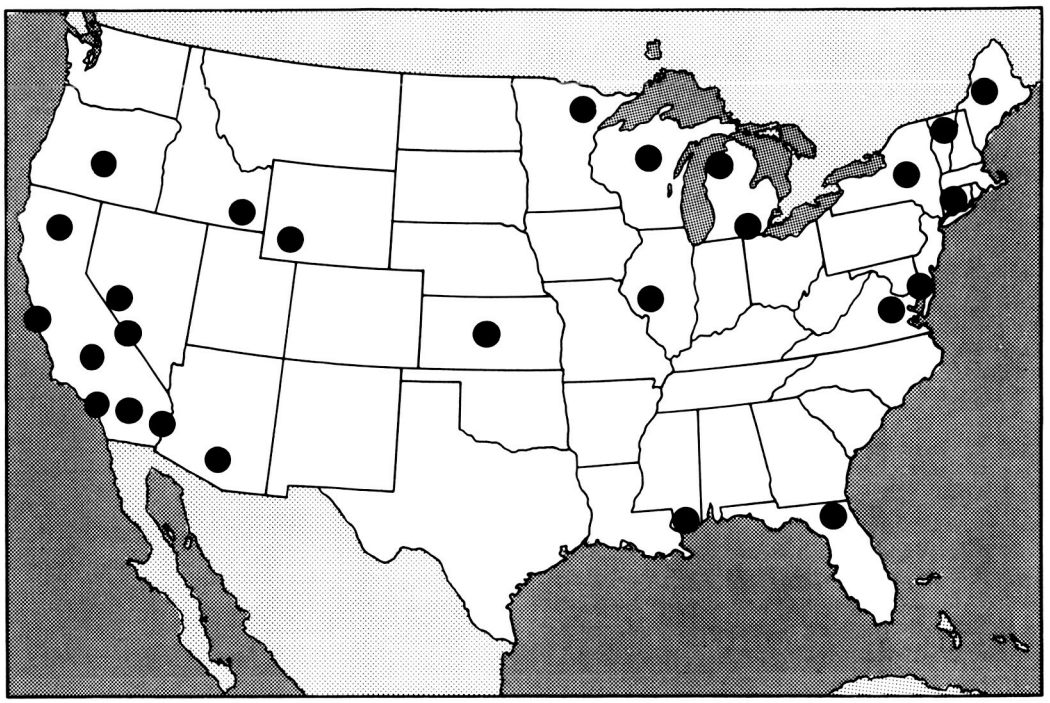

Figure 1-2. Geographic Location of Sites Observed with the NASA/JPL Aircraft Radar in 1984 and 1985. The western U.S. sites are primarily geological while the midwestern and eastern U.S. sites are primarily agricultural or forested land. More detail on site locations is given in Section VI.

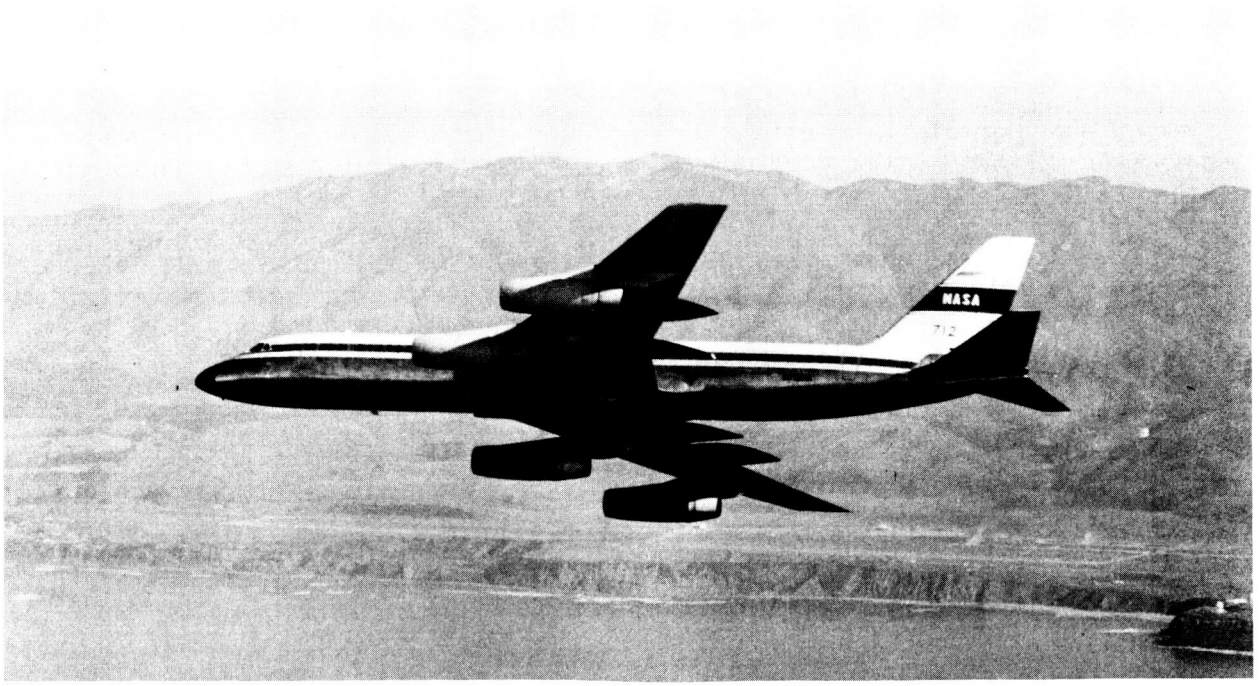

Figure 1-3. The NASA/Ames CV-990 Airborne Laboratory (Galileo II or NASA-712). Photograph courtesy of Medium Altitude Missions Branch, NASA/Ames Research Center.

SECTION II

OPERATIONS OVERVIEW

This section describes end-to-end operations. Some essence of the operations is given in Figure 2-1, which shows the aircraft SAR imaging geometry and its output in the form of radar images. The data products are images showing radar backscatter as a function of range and azimuth. The aircraft SAR geometry was defined by a broad-beam antenna, which was aligned perpendicular to the aircraft fuselage and which illuminated a swath parallel to the aircraft ground track. The antenna was 75 deg wide and was pointed 45 deg off nadir. The illuminated swath commenced near the aircraft nadir and extended off to the right side of the airplane. Normal aircraft altitudes were 7 to 13 km (20,000 to 40,000 ft); normal ground speeds were 200 to 250 m/s (400 to 500 knots (kt)). Nominal ground coverages were controlled by data recording limits. The coverages extended from directly beneath the aircraft to about 10 km to the right side of the aircraft. Nominal angles of incidence varied from 0 deg at nadir to 60 deg at the furthest recorded ranges.

Processing of radar data produces radar images as shown in Figure 2-1. Position of the echo can be located in distance from the aircraft (i.e., its slant range) and in distance along track (i.e., its azimuth). In some cases slant range is converted to ground range (the distance from nadir to the scattering element). In black-and-white renditions of a single polarization, stronger echoes have brighter, white-portrayed tones. When more than one polarization is used, the radar images can be portrayed via false-color photographs, where different polarizations are assigned different colors. Several of these false-color photographs are given in the NASA/JPL Aircraft SAR Workshop Proceedings (Ref. 2) and in the frontispiece.

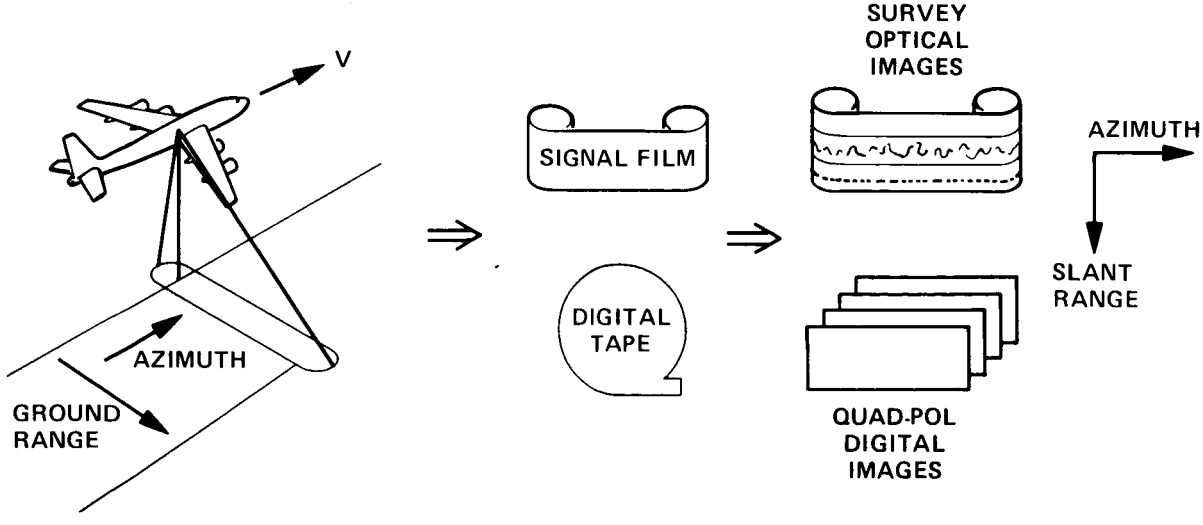

Figure 2-1. Aircraft Operations Overview Emphasizing SAR Imaging Geometries. The production of the images is described in Sections IV and V. Section VI gives examples of typical data.

While Figure 2-1 shows the core of aircraft SAR data acquisitions, more description is needed to acquaint users with the entire chain of events during data acquisitions. Figure 2-2 shows the aircraft and radar operations in an end-to-end sense. These operations were initiated by a NASA Office of Space Science Applications (OSSA) flight request for NASA/Ames CV-990 flight time and were ended with the dissemination of the data to the users. The time from flight request to data delivery was 1 to 2 years.

These data acquisitions were in the following three major phases:

(1) Premission planning
(2) Real-time (flight) operations
(3) Postmission data production and dissemination

The major steps in the premission phase included the submission and acceptance of the user's flight request and the planning of flight lines for data acquisitions. Major steps in the real-time operations included planning of flights (generation of a flight plan), flight operations where data were acquired, through shipment of data to JPL. The major steps in the postmission phase included collection and dissemination of the optical survey and digital data to the users.

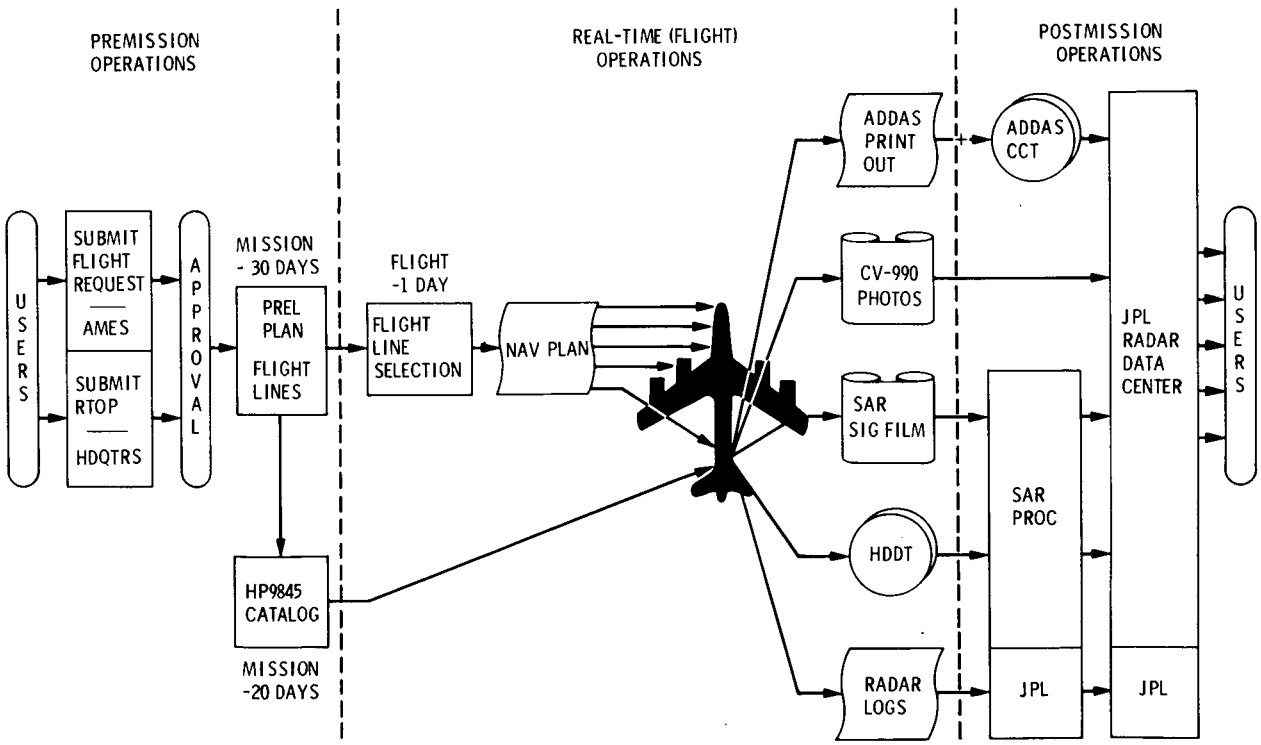

Figure 2-2. NASA/JPL Aircraft SAR End-to-End Operations. The phases were premission planning, real-time flight (data acquisition), and postmission data production and dissemination.

A. PREMISSION PLANNING

The primary purpose of the premission (planning) phase was to make optimal use of the aircraft and radar based upon the flight requests from the users. There were many requests for SAR data acquisitions on the CV-990 and still more requests for CV-990 time for other (non-radar) purposes. In order to optimize the usage of the aircraft, several flight requests were combined into missions of ten to twenty flights. Missions were defined primarily by the NASA/Ames CV-990 Program Manager (John Reller) who had the task of efficiently satisfying all of the approved CV-990 flight requests. Once a mission had been planned, specific flight lines for SAR data were defined via VAX computer programs operated by the JPL Aircraft Radar Coordinator (Tommy Thompson). Premission operations were completed when a preliminary data acquisition program was defined. Also at that time, a collection of potential SAR flight lines was forwarded to the NASA/Ames navigation and flight planners, and a matrix of SAR sites was entered into the HP-9845 for real-time data acquisition. This was accomplished about 1 month prior to the first flight of the mission. Users were expected to describe SAR lines about 2 to 3 months before data collection. User flight requests, the initiation of the entire operations process, were required by NASA about 1 year prior to an aircraft SAR data acquisition.

An overview of premission aircraft SAR planning is given in Figure 2-3. The primary output of this phase was the flight-line package used for flight planning and identification of sites during the data acquisitions. Requests for data acquisitions were compiled as a set of potential data tracks via computer programs at JPL. As shown in Figure 2-4, users provided site positions via center position in latitude and longitude, track length, heading angle of incidence, and also site elevation. This information, after review and interaction with users, was stored as "Site Matrix" in the HP-9845 computer. The planning programs at JPL also produced a listing of data tracks as pairs of waypoints for the NASA/Ames navigators.

The goal was to produce reasonable plans about 1 month before the first flight of a mission. This in turn meant that the JPL planning had to start 2 to 3 months before the first flight of a mission. Most users provided their inputs in a timely manner providing us with sufficient time to plan the real-time (data-acquisition) phase of the operations.

B. REAL-TIME (FLIGHT) OPERATIONS

The key phase of the aircraft radar operations was the flight (real-time) operations, when the SAR data were acquired on a day-by-day basis as shown in Figure 2-5. Generally, a strawman flight plan was defined by the JPL Aircraft Radar Coordinator (Tommy Thompson) and given to the NASA/Ames navigators by 10:00 a.m. preceding the day of the flight. This allowed about 6 h to generate an official flight plan for the next day's activities. Often this flight plan followed a strawman flight plan described in the preliminary flight-line package. One important deviation from this normal plan was deployments. When the aircraft was stationed away from Moffett Field, flights were conducted almost daily, so flight plans had to be generated before the first (transit) flight of a deployment.

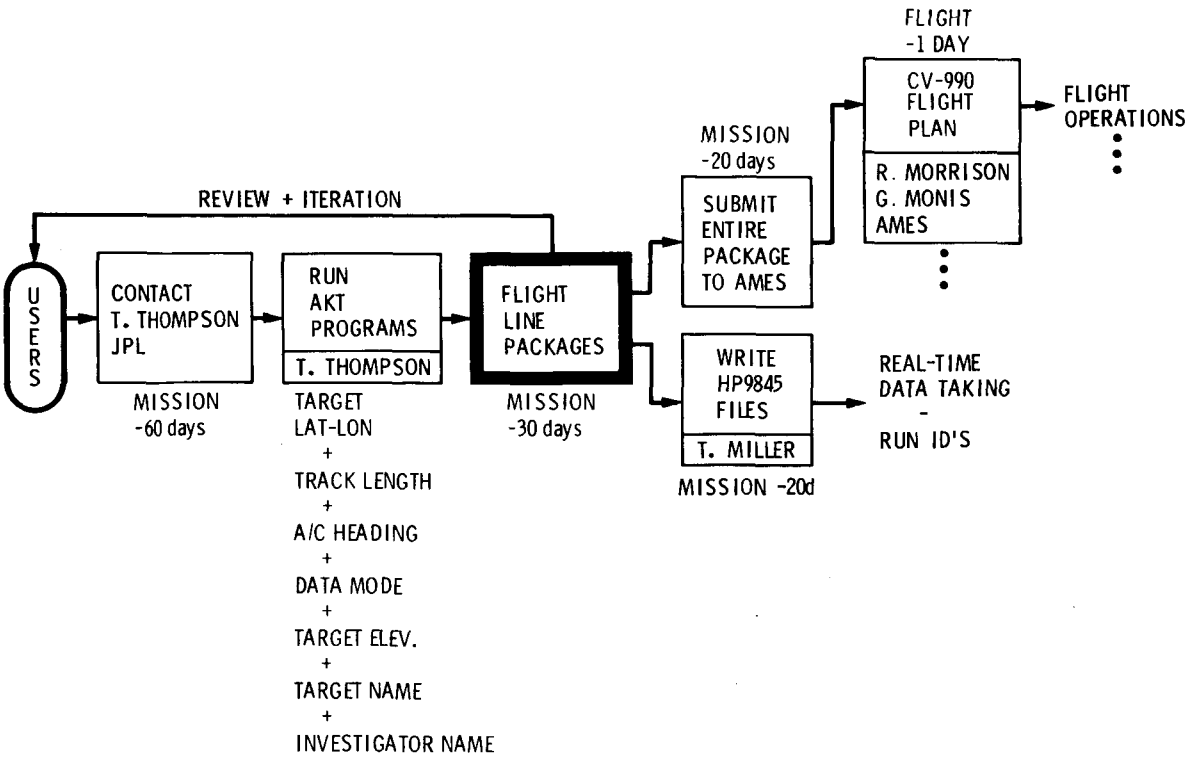

Figure 2-3. Overview of Premission Aircraft SAR Flight Line Planning. The key product was the Flight Line Package used by the CV-990 navigators and the radar computer operator.

The flight plan was a collection of flight lines, where each flight line was a CV-990 ground track described by a beginning waypoint and an end waypoint at a requested altitude. Often, flight plans had intermediate waypoints that described how the CV-990 would fly between data areas using the standard jetways for commercial airliners. On the day of the flight, the flight plan was a very important document because it was used by the pilots, the NASA/Ames Mission Manager, and the NASA/JPL radar personnel as their work plan for that day. All minute-by-minute positions were described with respect to these waypoints. Generally the CV-990 was flown sequentially through the waypoints on the flight plan. All SAR data acquisitions were logged via the waypoints the plane was flying when the data were taken.

A flight generally consisted of a number of data runs like the one shown in the lower part of Figure 2-5. During a normal data leg, the SAR data acquisition was optical survey imagery for the entire leg between the two waypoints defined by the flight plan. Digital SAR data acquisition generally started 1 min after passing the start waypoint and was completed 1 min before the end waypoint. The digital recording medium, the high-density digital tape (HDDT), was a precious commodity. Tapes were 2800 m (9,200 ft) long and lasted only 15 min at a rate of 3.05 m/s (10 ft/s, 120 in./s). Often several digital runs were recorded on a single HDDT, and the nominal 1-min pads at the

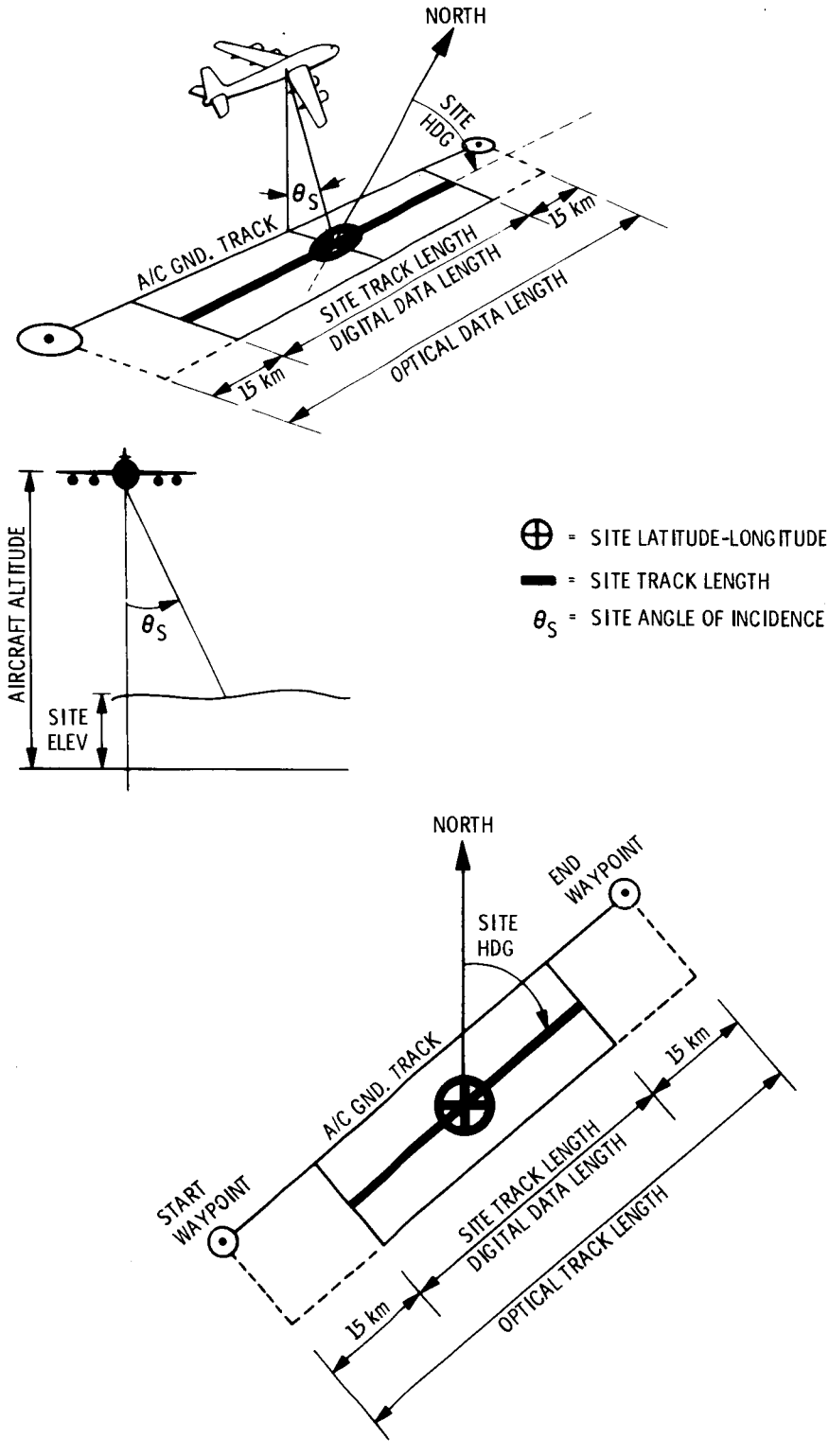

Figure 2-4. Description of Aircraft Data Acquisitions. The key information provided by the users included the site position in latitude and longitude, track length, and track direction. The key information used during the flight was the start and end waypoints.

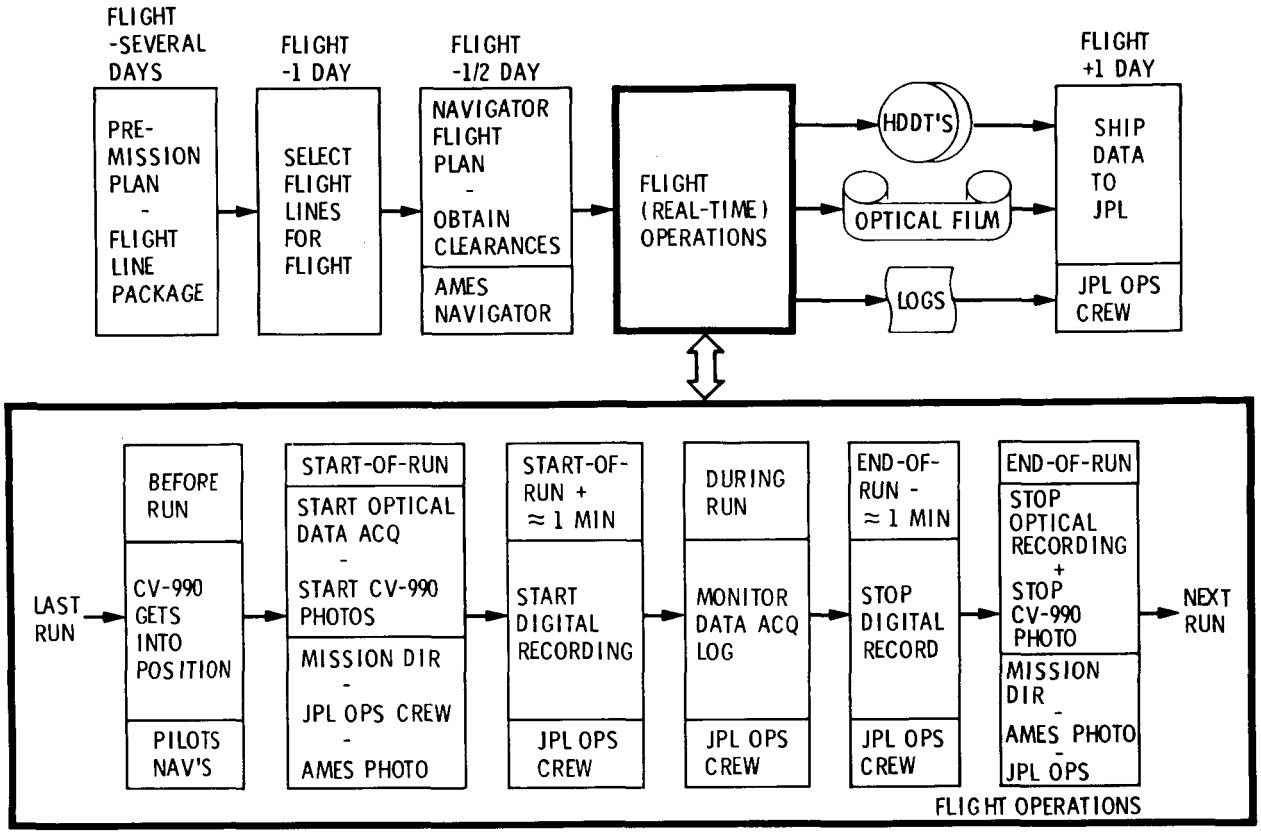

Figure 2-5. Overview of Real-Time Flight Operations. The flights were planned in a 24-h period prior to the flights. The flights were a series of data legs where the data collection started and ended at the waypoints. The data from these flights in the form of optical data logs and digital data logs were shipped to JPL for the postmission data production and dissemination.

beginning and end of a digital run were adjusted to make best use of this recording medium. The optical and digital data acquisitions were logged using the HP-9845 site matrix defined in the premission phase of operations. The flight operations ended when the data were shipped to JPL for reduction and distributions to the users.

C. POSTMISSION DATA DISSEMINATION

The postmission production and distribution of data following the flights were accomplished via the operations shown in Figure 2-6. The radar data from the flights were the raw radar data in the form of exposed optical

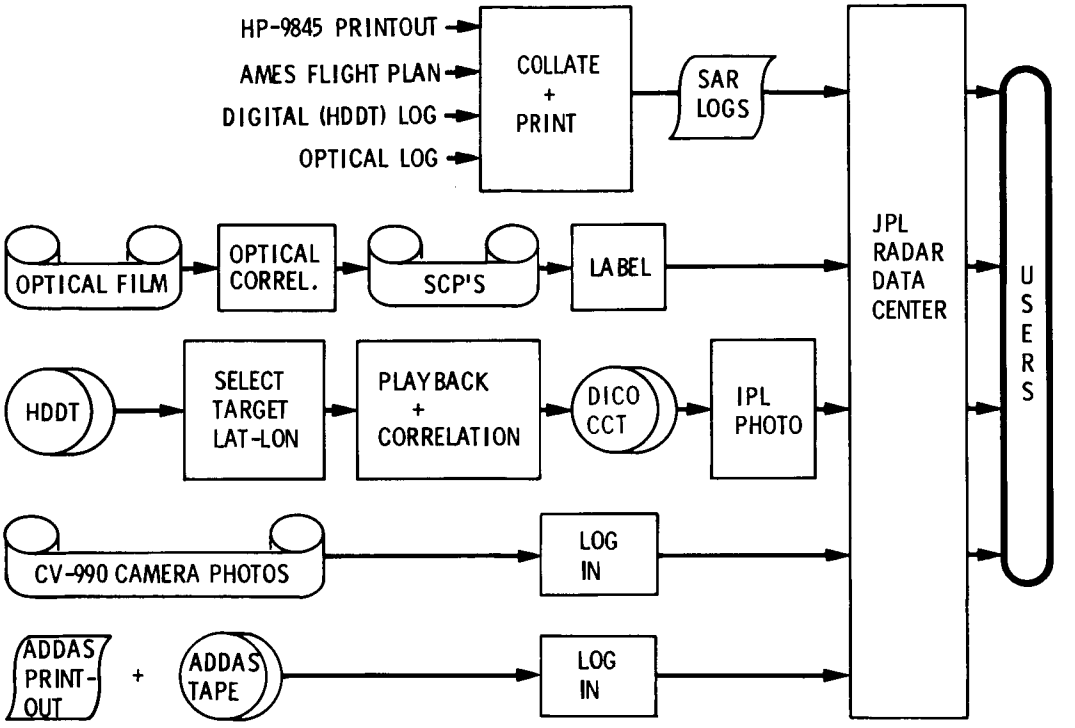

Figure 2-6. Overview of Postmission Data Dissemination. The operations included the collation of the radar logs, the production of optical survey data, and the correlation of the digital data.

signal film and recorded digital data on the HDDTs. These data were documented with logs, where the prime log was the printout from the HP-9845 computer supplemented by the handwritten logs kept by the Optical and Digital Rack Operators (Elmer McMillan and Bill Fiechter). In addition, the NASA/Ames personnel provided Airborne Digital Data Acquisition System (ADDAS) printouts, ADDAS tapes, and support photography. All of these data were shipped to JPL and archived in the Radar Data Center. This data center also collects and archives spacecraft SAR data from the JPL Seasat SAR Program and the SIR Programs. The Radar Data Center still serves as a single point of contact for aircraft SAR users after the data acquisition has been completed. All of the digital imagery is accessible via a Reference Notebook System described later in this report.

The first radar data from the flights were optically correlated survey imagery, which was produced for all data acquisitions. The first pass at optical processing was done quickly with a goal of producing quick-look images that could be used for digital image selection. It was the best medium for describing the geographic location of the radar images and was sometimes

drift (yaw) angle. The optical data are described in Section IV of this report. When areas for digital processing were located in the survey optical imagery, the computer processing for digital images was initiated. One important difference between the optical and digital imagery is that the digital images are only 11 km along track (equivalent to 40-60 s of flight) while optical images cover 4 or more minutes of real-time data acquisitions. The digital data products are described in Section V of this report.

Other data, such as support logs and photography, were archived at the JPL Radar Data Center and distributed to users. Immediately after a data flight, an aircraft SAR log was generated from the real-time HP-9845 printout, the flight plan, and the optical and digital operator logs. These aircraft SAR logs were often 50 to 100 pages in length and often distributed to users within days of the flight. The optically processed SAR SCP's were often distributed within a month of a flight. Support photography was normally done with false-color infrared (IR) film provided by the NASA/Ames Photography Group. Photography in 1983 through 1985 was generally KS-87 aerial photography, which was 12.7-cm (5-in.) format. One KS-87 aerial camera was generally a 72 deg field-of-view (FOV) aerial camera pointed at nadir; the second KS-87 aerial camera had a 36-deg FOV pointed 45 deg off nadir to the right side of the aircraft. A few flights had RC-8 or RC-9 photography; the RC-8 and RC-9 had 22.9-cm (9-in.) film. Photography for JPL users was stored at the JPL Radar Data Center, and photography for non-JPL users was generally shipped directly to those users. This support photography was generally available 1 or 2 months after a flight. In addition to the aerial photography, NASA/Ames also supplied ADDAS printouts and computer-compatible tapes (CCT's) for various aircraft parameters (such as aircraft position, altitude, and speed), and these could be used to determine a flight listing on a minute-by-minute basis.

Thus, the final phase of these operations was (and continues to be) the production and dissemination of digital SAR data. Often during a mission, a series of "quick-look" digital images was produced to assess data quality. These "quick-look" images were sometimes produced without the benefit of the optical survey imagery. Somewhat later, when optical imagery was available, the normal digital data processing commenced. As a general rule, JPL produced five images per week for a nominal allocation of five images per flight. The normal processing of a mission took 3 to 9 months. The processing of the Fall-84 (SIR-B Underflight) Mission produced 120 images; the processing of the Spring-Summer-85 digital data produced 130 images. The optical and digital processing plans and schedules were defined about 1 month after the last flight of a mission and distributed to users in a mission data plan.

SECTION III

AIRCRAFT HARDWARE DESCRIPTION

The characteristics of the aircraft radar image eventually delivered to a user depend in large part upon the radar equipment on board the aircraft. Thus, this section describes the onboard radar equipment to give users a description of what occurred during the real-time acquisition of the real data. In a broad sense, radar pulses were generated on board the aircraft and transmitted toward the earth via a skin-mounted broad-beam antenna. Then echoes from targets were received via the same antennas, converted to video frequency, and recorded on both optical and digital media. One major capability of the NASA/JPL Aircraft SAR was the ability to interlace horizontally and vertically polarized transmitter pulses and to simultaneously record both horizontal and vertical polarizations for every echo. Other major capabilities of the NASA/JPL aircraft SAR were to have computer control of many radar functions via a desk-top HP-9845 computer and to record echoes using an HDDR. The parameters for this radar are given in Table 3-1.

There were two major changes in hardware equipment in 1984 and 1985 that affect the data. These were the replacement of the High-Density-Digital Recorder (HDDR) with a newer model and the use of microstrip antennas described at the end of this section.

A. PHYSICAL LAYOUT OF THE AIRCRAFT EQUIPMENT

The radar functions were implemented via configurations suited to the CV-990 style of operations as shown in Figures 3-1 and 3-2. The heart of the radar was the radar box, which performed many functions. These included generation of swept-frequency (chirp) transmitter pulses, which were then fed to the skin-mounted antenna via a cable network. Other functions accomplished in the radar box were reception of radar echoes, front-end amplification, hetrodyning from radar frequencies (1215 to 1235 MHz) to video frequencies (1 to 20 MHz), and routing of echoes to recording equipment in racks located on the CV-990's main floor. The radar box was 0.6 • 0.6 • 1.5 m (2 • 2 • 5 ft) and mounted in the aft cargo area near the main skin-mounted antennas.

The radar box was inaccessible in normal flights, so many control and data-recording functions were performed via rack-mounted equipment on the main cabin floor. One rack housed the HP-9845 computer which both controlled many radar functions and monitored radar acquisitions. The computer acquired flight parameters from the CV-990 INS, ADDAS, and radar altimeter systems and used these parameters to control various radar functions. In particular the aircraft ground speed was used to determine the radar pulse-repetition frequency (PRF). Each polarization had a PRF of (1.5 • GS) where GS is aircraft ground speed in knots. In the Quad-Pol mode where horizontal and vertical polarization pulses were interlaced, the actual radar PRF was [3.0 • GS]. The PRF was tied to ground speed in order to facilitate processing of the data. The HP-9845 computer also used aircraft altitude and ADDAS parameters to set optical and digital recorder delays. Other functions performed by the HP-9845 computer were setting data mode, inserting site title and position into the annotator, and/or setting optical channel assignments. During a data acquisition run, the HP-9845 computer also monitored radar echo strengths and had the

Table 3-1. NASA/JPL Aircraft SAR Parameters

Parameter	Value
Frequency	1225 MHz
Wavelength	24.6 cm
Pulse length	4.9 μs
Bandwidth	19.3 MHz
Peak radiated power	4 kW
Transmitted polarizations	Horizontal and vertical interlaced
Received polarizations	HH, HV, VV, VH
Antenna azimuth beamwidth	5 deg (Summer-85, microstrip II) 18 deg (baggage door, see note) 7 deg (Fall-84 microstrip I)
Antenna range beamwidth	75 deg (all antennas)
Antenna beam center gain	18 dB (Summer-85, microstrip II) 12 dB baggage door, see note) 16 dB (Fall-84, microstrip I)
Nominal altitude	6.0 to 12.0 km
Nominal velocity	200 to 250 m/s
Pulse repetition frequency	1.5 • (aircraft velocity in knots)
Look angle range	0-60 deg
Optical sweep time	55 μs
Optical sweep film width	25 mm
DIGITAL IMAGES	
Raw data quantization	6 bits
Azimuth pixel spacing/resolution	11 m/13 m
Number of azimuth pixels	1024
Number of looks	4
Slant range pixel spacing/resolution	7.5 m/7.9 m
Ground range pixel spacing	15 m at 30 deg, 10 m at 50 deg
Ground range resolution	16 m at 30 deg, 10 m at 50 deg
Number of range pixels	927

Note: The baggage door antenna was used during the Summer-83, Winter-84, and Spring-85 Expeditions.

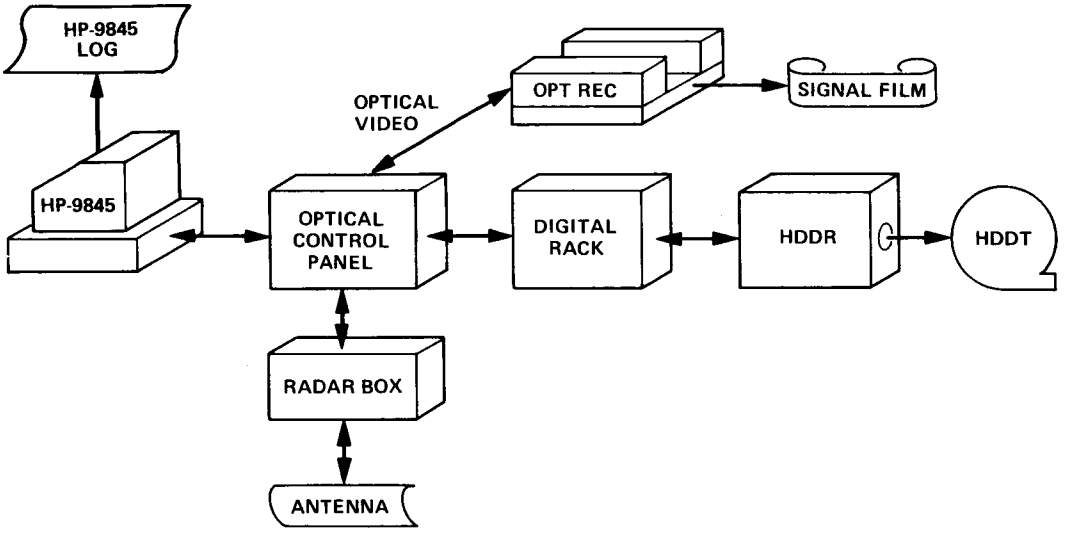

Figure 3-1. Physical Layout of the Radar Racks on the Aircraft. The antenna was mounted on the skin of the aircraft; the radar box was in aft cargo hold near the antenna; all other racks were on the cabin floor.

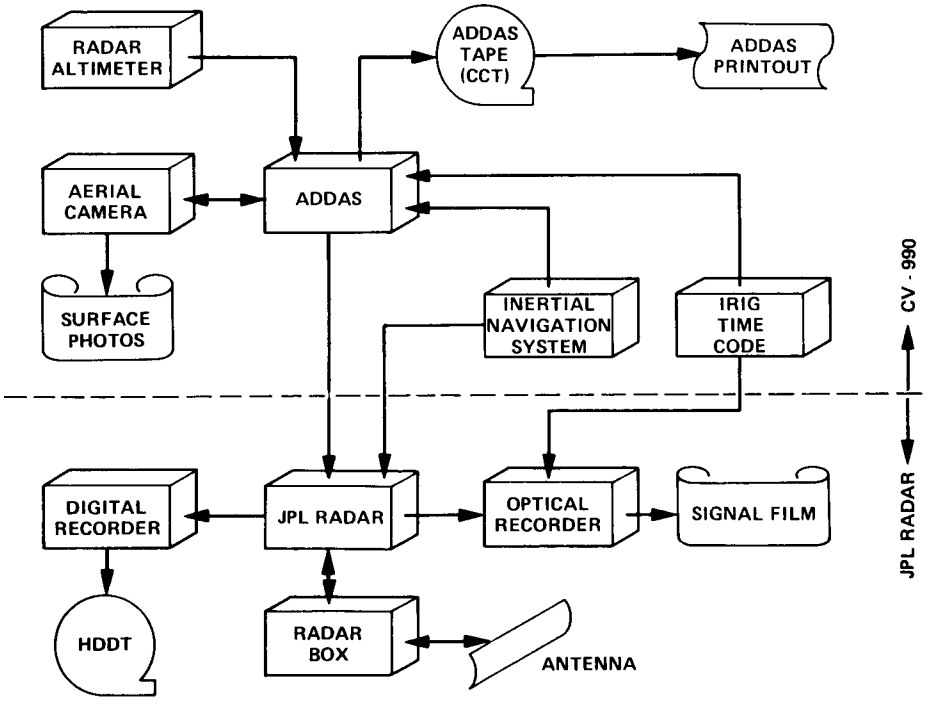

Figure 3-2. Interfaces Between the NASA/JPL Aircraft Racks and the CV-990 Aircraft. The radar used the aircraft altitude (from the radar altimeter via the ADDAS) and the ground speed (directly from the aircraft INS) as major parameters for setting up the data acquisitions. The optical recorder used the aircraft IRIG time code.

ability to adjust receiver gains accordingly. The HP-9845 computer also provided the major log for NASA/JPL aircraft SAR via its printout. Principal logging functions included the following:

(1) Optical start/stop time, location, and delay
(2) Digital start/stop time, location, and delay
(3) Transmitter forward and reverse power
(4) Echo level versus delay

Yet another rack on the main cabin floor was the optical control rack, the oldest rack in the setup. This rack controlled the radar box, the optical recorders, and the calibration and power monitoring systems. Most of the manual controls were located here as well. The stable local oscillator (STALO), the INS readout unit, the PRF generator, and the antenna switching and video distribution chassis were in the rack also. Other racks on the main floor of the CV-990 aircraft provided optical and digital recording of the echoes. The optical recording of radar echoes was accomplished via two surplus, modified military optical recorders. Each optical recorder had two 2.54-cm (1-in.) data swaths embedded in 12.7-cm (5-in.) film. Optical data were annotated in real time via an IRIG time-code repeater which transferred the CV-990 IRIG aircraft time code to a 2.54-cm (1-in.) wide block on the edge of the 12.7-cm (5-in.) data film. (This IRIG time code was subsequently transferred to the output survey imagery in postmission data processing as described in the next section, see Figure 4-4.) The optical signal film recorded on the aircraft was also annotated with a site title and geographic location although this annotation was not transferred to output optical products. There were two optical recorders yielding four channels of optical data. These four channels were normally assigned to the HH, HV, VH, and VV polarizations when Quad-Pol data were acquired. The optical recorder capacity was 58 m (190 ft) of film, and this was consumed at a rate of 3 cm (0.1 ft) per kilometer of along-track travel. Most data flights were 5 to 6 h in duration and used only one roll of film per recorder. A few flights recorded more than one roll of optical film; while in other cases, optical data from two or three shorter flights were combined on a single roll of film.

Digital recording was accomplished via two racks, one for digital sampling equipment and another for an HDDR. Functions performed on the digital rack included:

(1) Analog-to-digital conversion of the radar echoes
(2) Generation of header record annotation
(3) Digital sampling of the radar echo video
(4) Signal averaging for logging purposes (digital gate)
(5) Generation of analog check signals from a digital signal stream (video generator)

After the radar echoes were converted to a digital bit stream, the data were merged with the header information, formed into tape records, and recorded via the HDDR. Echoes were quantized at a 40-megasample/s rate with a resolution of 6 bits per sample. The HDDT is a mylar-based tape which is 2,800 m (9,200 ft) long and 2.54 cm (1 in.) wide. Twelve data tracks and two error-correction tracks were recorded. Each track had its own clock and synchronization signal. Data recording was done at 305 cm/s (120 in./s or 10 ft/s) yielding a total data time per HDDT of 15 min. Several HDDT's were

recorded on each data flight; tape changes were often done in the few minutes between data legs. This was something of a physical feat as the HDDT's weighed as much as 9.1 kg (20 lb) in the high-g regimes of the tight turns between some of the data runs.

Figure 3-2 shows the major functional interfaces between the NASA/JPL aircraft SAR and the CV-990 Airborne Laboratory. The key interface was the INS reader/repeater as the INS parameters of ground speed, roll, pitch, and yaw as well as aircraft position were important to the processing and logging of the radar data. The ADDAS provided the SAR with the CV-990 radar altimetry data, provided timing for the aerial cameras, and provided another log of aircraft position and altitude. The CV-990 IRIG time code was copied onto the optical signal films and then translated onto the optical survey images. As mentioned previously, the radar equipment was adapted to the CV-990 operation. All radar equipment, except for the skin-mounted antennas, was installed and removed from the aircraft once or twice each year. Installation of racks for a mission was a major activity normally requiring a month of premission system tests at JPL followed by several weeks of installation and flight checkout on board the CV-990 aircraft. Sensor checkout flights, the first flights of a mission, were vital to all users as they provided necessary debugging of the essentially "new" aircraft installations.

Figure 3-3 shows several of the racks as they existed during a typical installation. Figure 3-3a shows the computer control rack which contained the desk top HP-9845 computer as well as oscilloscopes, which displayed annotator outputs and echoes. The computer operator sat next to the window and kept track of data-taking progress via the displays in the rack or his view out the window. Figure 3-3b shows the optical control rack, which contained several commercial and custom-built panels. Many radar control functions could be controlled from this rack. The television screen on the top of this rack displayed ADDAS information (such as aircraft position, attitude, and altitude) and provided a means of keeping track of the progress through the flight plan. The optical control panel rack operator also sat next to the window and could visually assess the observation area. Figure 3-3c shows the two optical recorders as they were mounted on a "low boy" rack.

B. HARDWARE FUNCTIONS

Block diagrams of the radar emphasizing radar signal flow are shown in Figures 3-4 and 3-5. One major element of the hardware was the dual-receiver chain. The Receiver-A chain was normally assigned to vertically polarized echoes, while the Receiver-B chain was normally assigned to horizontally polarized echoes. The polarizations of the receivers, as well as the transmitted pulses, were recorded automatically in the header for each pulse via the formatter. Optical channel assignments, set by the HP-9845, were recorded by hand via the optical logs as well as on the HP-9845 log. During the Summer-85 Expedition, a switching panel was installed to facilitate these channel assignments; this also permitted the experimental recording of C-band echoes.

(a) COMPUTER CONTROL RACK

(b) OPTICAL CONTROL RACK

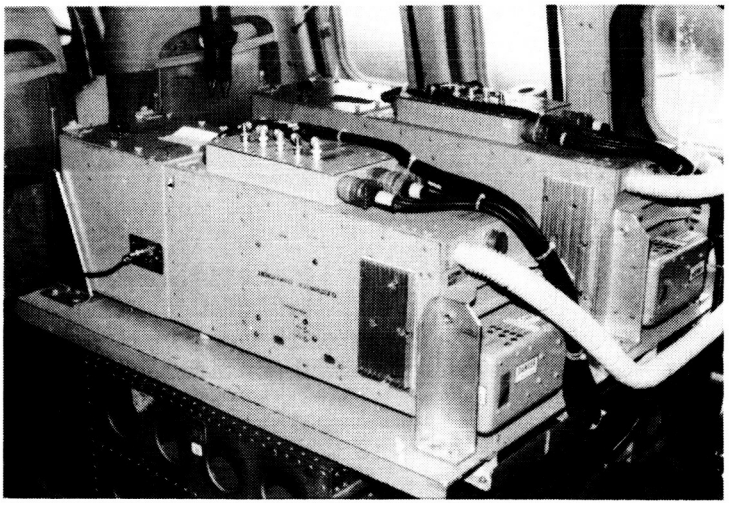

(c) OPTICAL RECORDER RACK

Figure 3-3. Aircraft Equipment Racks on Board the CV-990. The computer controlled most radar functions while the key cabin hardware elements were contained in the optical control rack. The optical recorders were military surplus adapted for use in the cabin area of the CV-990 Airborne Laboratory.

A capability of this radar was to interlace horizontally and vertically polarized pulses. This was accomplished via a diode switch which shuttled alternate pulses to the vertical and horizontal ports of the antenna. Dual-direction couplers and a circulator (to protect the receivers) were between this diode switch and the antenna port. These couplers permitted both the measurement of forward and reflected powers and the insertion of a continuous wave (CW) tone for calibration of the echoes. The switches at the antenna ports provided the mechanism for implementing various data acquisition

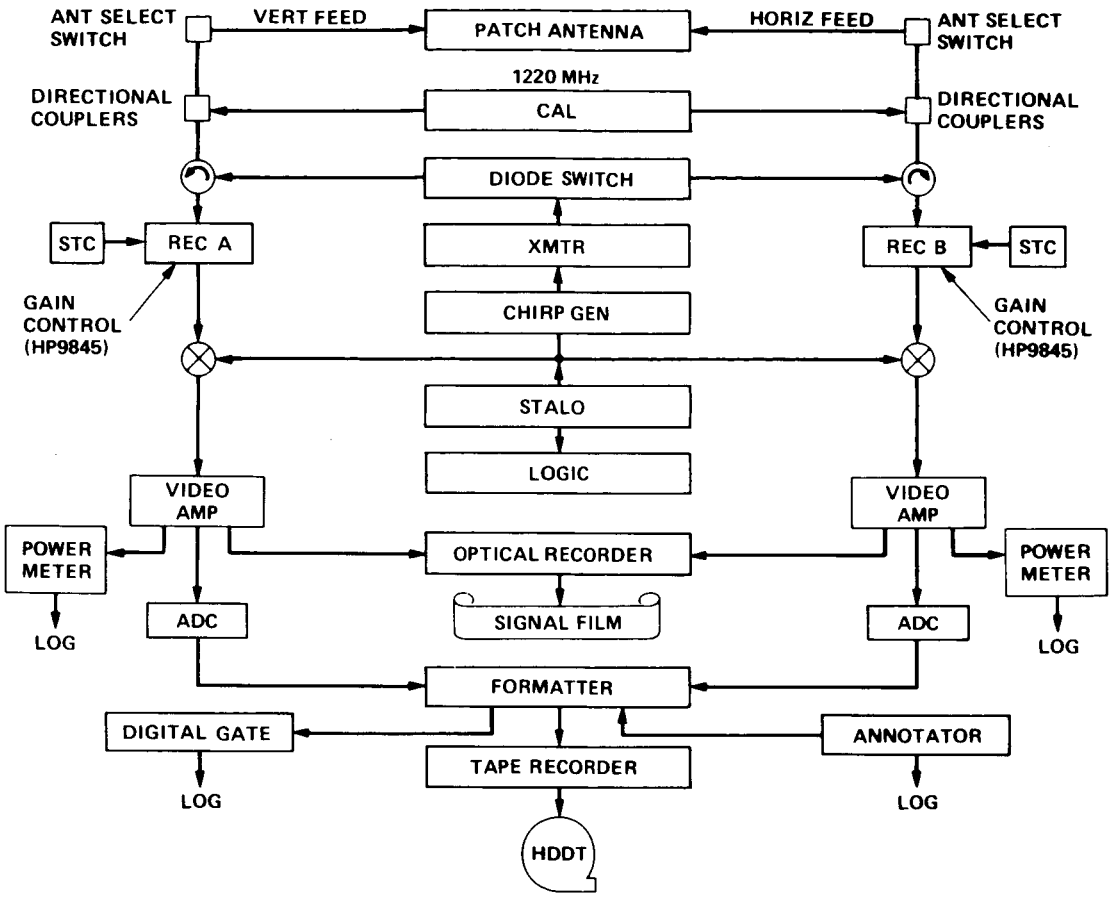

Figure 3-4. NASA/JPL Aircraft Radar Block Diagram. This figure demonstrates division of echoes into two receiver chains for vertically and horizontally polarized echoes.

modes such as along-track and cross-track interferometry, as well as a "test mode" where a dummy load replaces the antennas.

Another capability of this radar was to modulate echoes on a microsecond-to-microsecond basis via a sensitivity-time-control (STC) circuit. Empirical curves of expected received power versus incidence angle for three nominal surface roughnesses (smooth, medium, and rough) were used to generate the STC function for each polarization. Various hardware-dependent parameters were measured and factored into the calculation, such as the antenna pattern, the total system gain in each channel, and the transmitted power. The HP-9845 loaded four STC functions, one for each direct and cross-polarized combination into the random access memory (RAM) of the STC unit, which cycled through the memory continously at 1 MHz. Each RAM value in turn was then converted to an analog voltage which varied the gain of an amplifier in the receiver chain. This technique increased the effective dynamic range of the SAR.

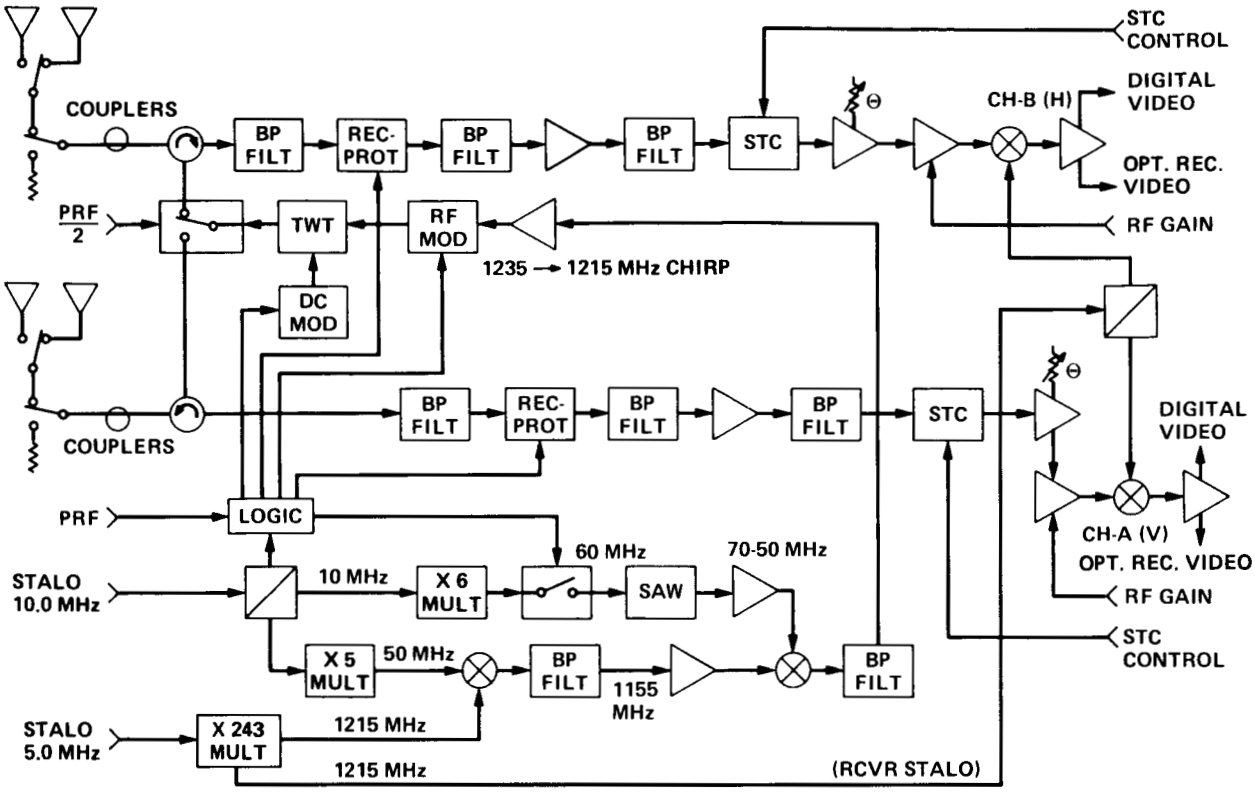

Figure 3-5. NASA/JPL Aircraft Radar Hardware Block Diagram. The key elements of this radar were its ability to switch polarizations on alternate transmitter pulses and to simultaneously record two polarizations through nearly identical channels.

C. HARDWARE SUMMARY AND DATA QUALITY CONSIDERATIONS

This section has described the NASA/JPL Aircraft SAR equipment as it existed during the expeditions flown in 1983 through 1985. This hardware was adapted to the CV-990 mode of operation where the radar consisted of several floor racks, a radar box in the aft cargo hold, and a skin-mounted antenna. The key functions of this hardware produced all four combinations of linear polarization. Echoes were modulated on a microsecond-by-microsecond basis via an STC circuit and calibrated via a CW signal fed into the receiver chain at a point near the antenna ports. The HP-9845 desk-top computer was a key element of the system, providing both logging and control functions.

There were two major hardware changes which had a profound effect on the data quality. One change was the replacement of the surplus Sabre-III HDDR with the new Fairchild model-80 HDDR prior to the Fall-84 (SIR-B Underflight) Expedition. The new HDDR had error-correcting code, which significantly improved the quality of the digital data. The new HDDR was less susceptible to data outages and degradations from mechanical shaking during

turbulence. The other significant hardware change was the replacement of the baggage door antennas with skin-mounted microstrip antennas, manufactured by Ball Brothers. The new microstrip antennas had colocated horizontally and vertically polarized radiating elements that permitted the construction of phase-difference images like those shown in the frontispiece. The radiating elements on the baggage-door antenna were 15 cm (6 in.) apart and created artificial phase differences which could not be modelled. There were two different microstrip antennas because the original microstrip antenna used throughout the Fall-84 Expedition was damaged and had to be replaced for the Summer-85 Expedition. The baggage-door antenna had to be used for the Spring-85 Expedition as it was the only antenna available.

The impact of the changes in the HDDR and antennas is shown in Table 3-2. The older Sabre-III HDDR used in the Summer-83 and Winter-84 Expeditions had poor quality digital data; the newer Model-80 HDDR used in the Fall-84 (SIR-B Underflight) and Spring- and Summer-85 Expeditions had better quality digital data. Generation of polarization phase differences is possible only with the microstrip antennas used in the Fall-84 and Summer-85 Expeditions. Thus, the best data comes from the Fall-84 (SIR-B Underflight) and Summer-85 Expeditions as shown in Table 3-2. One factor not described in Table 3-2 is the replacement of the antenna diode switch early in the Summer-85 Expedition. The new switch had better isolation between horizontal and vertical polarization and provided improved data. Users having a choice between Fall-84 and Summer-85 data should select the Summer-85 data.

Table 3-2. Major Hardware--Data Quality Factors

	Expedition				
	Summer-83	Winter-84	Fall-84	Spring-85	Summer-85
Dates	11 Aug 83- 16 Sep 83	12 Feb 84- 15 Mar 84	16 Aug 84 06 Nov 84	08 Mar 85- 24 Apr 85	21 May 85- 14 Jul 85
HDDR	Sabre-III	Sabre-III	Model-80	Model-80	Model-80
Antenna	Baggage Door	Baggage Door	Micro-strip I	Baggage Door	Micro-strip II
Digital Data Quality	Poor	Poor	Good	Good	Good
Polarization Phase Difference	No	No	Yes	No	Yes

SECTION IV

DATA PROCESSING--OPTICAL AND SUPPORT DATA

As noted in the overview of the aircraft SAR data acquisition (Section II), there were several major data products from the flights. This section describes the preliminary products, the quick-look optical survey imagery, and the supporting products such as logs and ground photography, while the next section (Section V) describes the digital imagery, the final data product. The preliminary data products described here are important because the optical-survey imagery and the logs provide the prime data for selecting areas for digital correlation. The key radar data product type described here is the quick-look optical survey image, which provides a timely indication of the geographical coverage in the digital data sets. In general, these optical survey images and logs were distributed to users before the production of digital images got under way.

A. QUICK-LOOK SURVEY OPTICAL IMAGERY

Figures 4-1 and 4-2 show an overview of the optical processing. The raw data consisted of two 2.5-cm (1-in.) swaths and an accompanying IRIG code on a 12.7-cm (5-in.) film 58 m (190 ft) long. There were two films providing four data swaths for the four possible combinations of linear polarizations. These raw data were a holographic representation of the radar image. This holograph was reduced to an optical image via the JPL aircraft optical correlator shown in Figure 4-3 and operated by Tom Bicknell, Tom Andersen, and Bi Trinh, using standard SAR optical techniques. The output of the optical correlator was an exposed image film which was developed for further processing by a D-Log E printer operated by the JPL Photo Lab (by Dave Deats and Bob Saul). The D-Log E printer removed long term (greater than a few centimeters) horizontal and lateral film density variations. Strip-contact prints (SCP's) of the D-Log E output were then annotated with site title, optical and digital run numbers, and drift (yaw) angles and distributed to users. Annotated SCPs for all data acquisitions are archived in the JPL Radar Data Center.

The optical data processing compressed the data along-film length by a factor of 20:1, yielding an along-track scale of 1:250,000. Figure 4-4 is an example of optical survey data. Optical survey processing for the recent missions was limited to one channel (normally HH or VV) to indicate geographic coverage of the digital data acquisitions. The optical and digital cross-track coverage were both near 10 km. Users should be aware that digital data acquisitions generally started 1 minute after optical data start and were terminated about 1 minute before the optical data end. Thus, the first and last 50 mm of optical survey data rarely had digital data acquisitions. On occasion, optical-only data were required on long transits between data sites to run out optical film and facilitate film changes at the end of a flight.

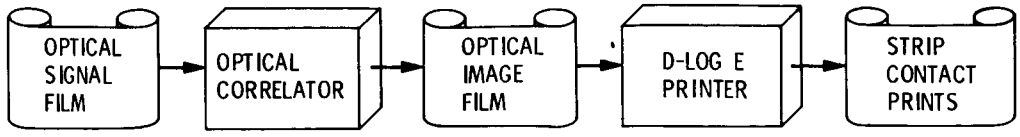

Figure 4-1. Block Diagram for the Production of Quick-Look Optical Survey Data. The input was the signal film exposed during the flights. The output was an image film produced by the optical correlator shown in Figure 4-3. The output was distributed as SCP's, a strip continuous print from the image film.

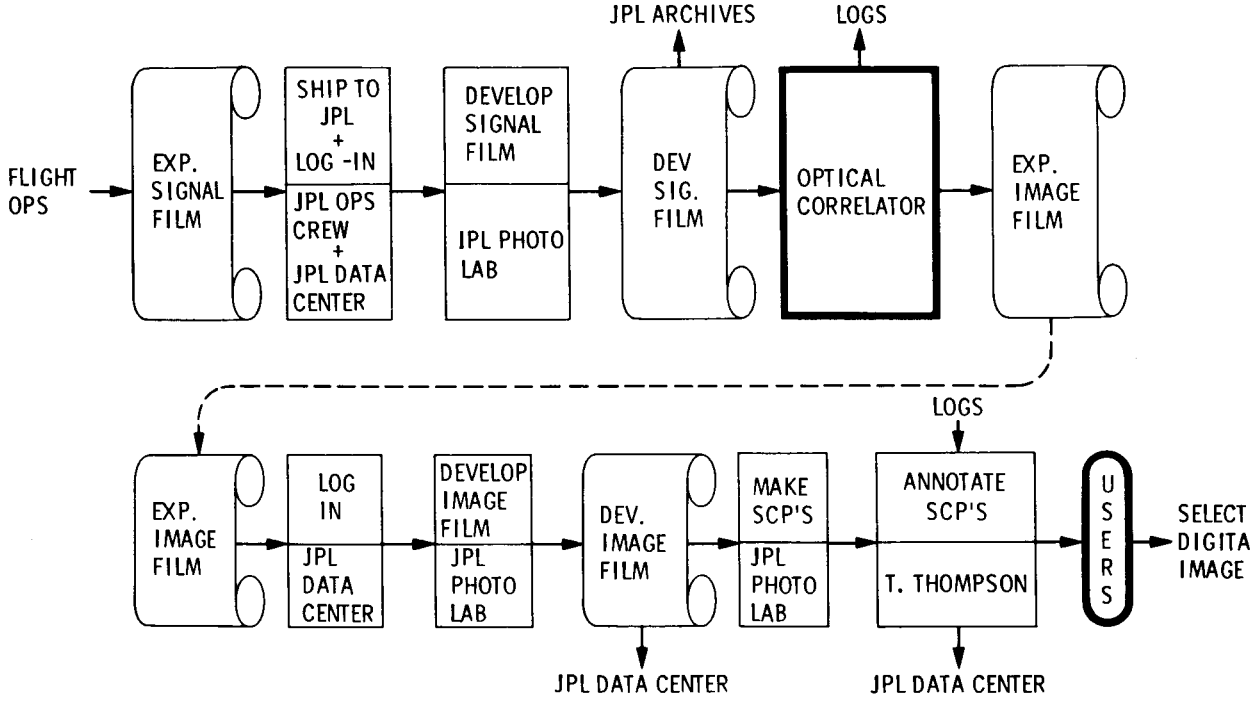

Figure 4-2. Details of Optical Survey Data Production. The input from the real-time operations was the exposed signal film; the output to the users was annotated SCPs.

B. SUPPORT PHOTOGRAPHY

As mentioned in previous sections, aircraft SAR data acquisitions were documented via ground photography from the aerial cameras that were carried on board the NASA/Ames CV-990 aircraft. The normal camera configuration was two KS-87's where one camera had a 72-deg FOV pointed at nadir, and the second camera had a 36-deg FOV pointed 45 deg off nadir to the right side of the aircraft. KS-87 aerial cameras used 12.7-cm (5-in.) film and produced

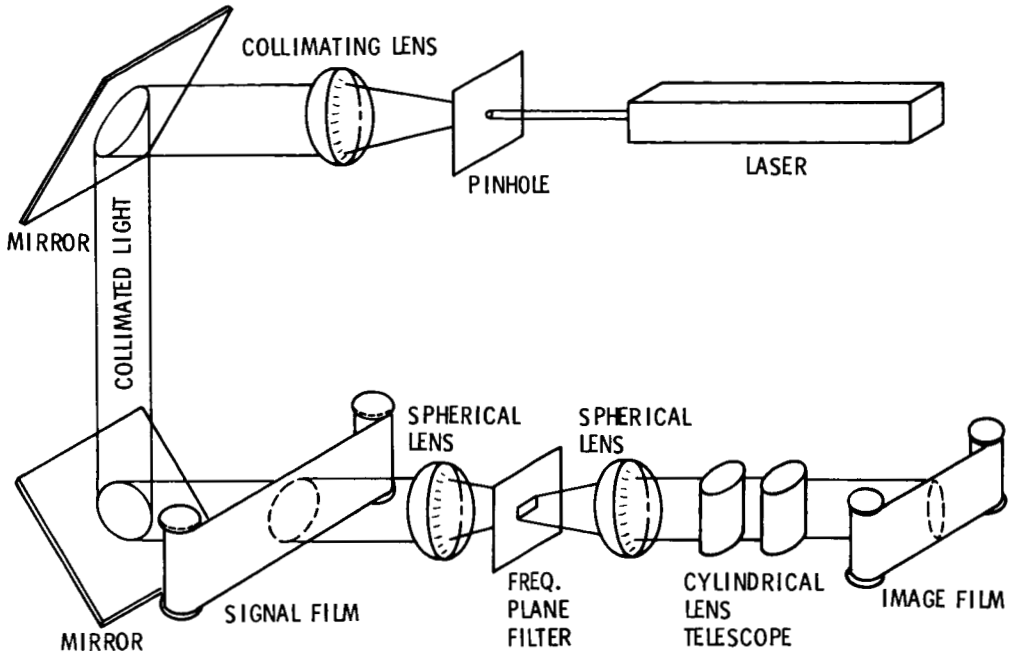

Figure 4-3. Optical Correlator Block Diagram. Focused laser light converted the holographs on the signal film to imagery. The mirrors provided a folded optical path. The frequency plane filter permitted selection of both range and azimuth bands. The output telescope expanded the image by a factor of two.

photographs like those shown in Figures 4-5 and 4-6. This KS-87 photography was normally done with false-color IR film (although black-and-white film was normally used on the checkout flights). Also, the normal picture-to-picture overlap was 10% as controlled by the ADDAS computer. There were about twice as many off-nadir photographs as nadir photographs because of the smaller FOV of that camera. On a few flights, the CV-990 photography was via RC-8 or RC-9 aerial camera with a 22.9-cm (9-in.) format and an FOV similar to those of the KS-87. This support photography was shipped to non-JPL investigators while photography for JPL investigators is stored in the JPL Radar Data Center.

C. RADAR LOGS

The radar observations were also supported by the radar logs. The major portion of the radar log was the HP-9845 printout provided by the HP-9845 operator (Tim Miller). The first entry was made at the start of the optical run, which normally occurred as the CV-990 flew past the start waypoint of a run. The second entry was made when the digital data acquisition was initiated. There were two types of data provided during the digital data acquisition. The echoes were sampled by the digital gate, providing a profile of received power over the sample interval. The other data provided during the run were intermediate positions and HDDT footages. The next-to-last entry was made at the termination of the digital recording.

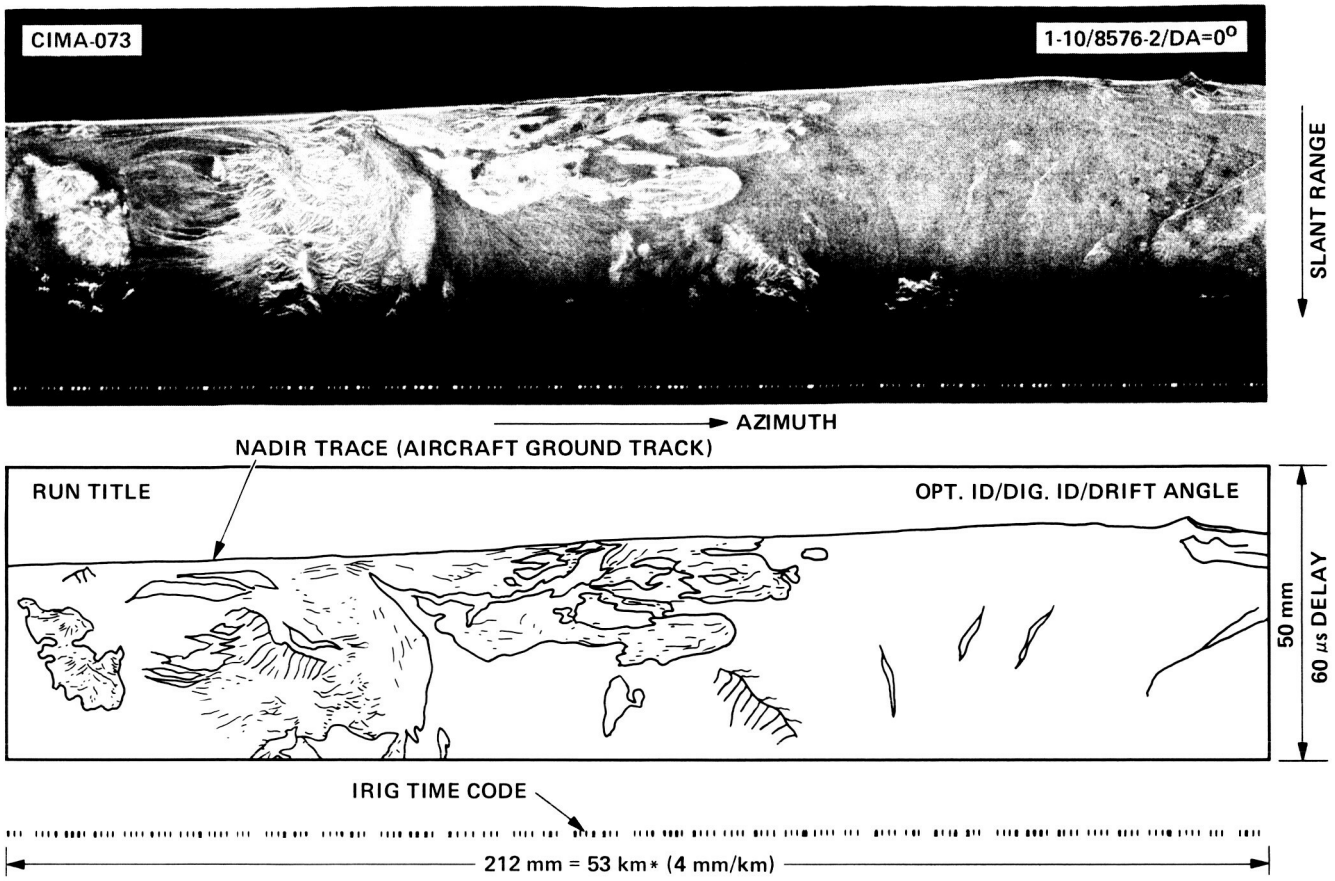

Figure 4-4. Example of Optical Survey Imagery. The azimuth scale is 1:250,000. The range coverage of the data on the ground is nearly 10 km, the nominal widths of digital images.

The final entry was made when the optical recording was terminated, and this normally occurred when the CV-990 reached the end waypoint of a run.

During the Spring- and Summer-85 Expeditions, the HP-9845 also cataloged the optical and digital data acquisitions for an entire flight. These summaries were printed out at the end of a flight--the last entries in HP-9845 printout. The HP-9845 printout normally contained 80 to 120 pages and provided a detailed view of data acquisitions during a flight. The HP-9845 computer printout was supplemented by the handwritten optical and digital logs, which detailed the optical and digital data acquisitions on a run-by-run basis. The optical log form evolved over 15 yr of usage and provided an excellent and concise insight to data acquisitions during a flight. The digital log was an adaptation of the optical log to digital recording.

The entire radar log contained the HP-9845 log, the flight plan, the optical log, and the digital log. These were collected on a flight-by-flight basis, duplicated, and distributed to investigators. The original versions of these radar logs were archived in the JPL Radar Data Center. The radar log and optical-survey imagery provide the key elements in selecting areas for digital correlation. The first step of any investigator who wants digital data from this system should be acquiring the logs and survey optical prints of sites in which he or she may be interested.

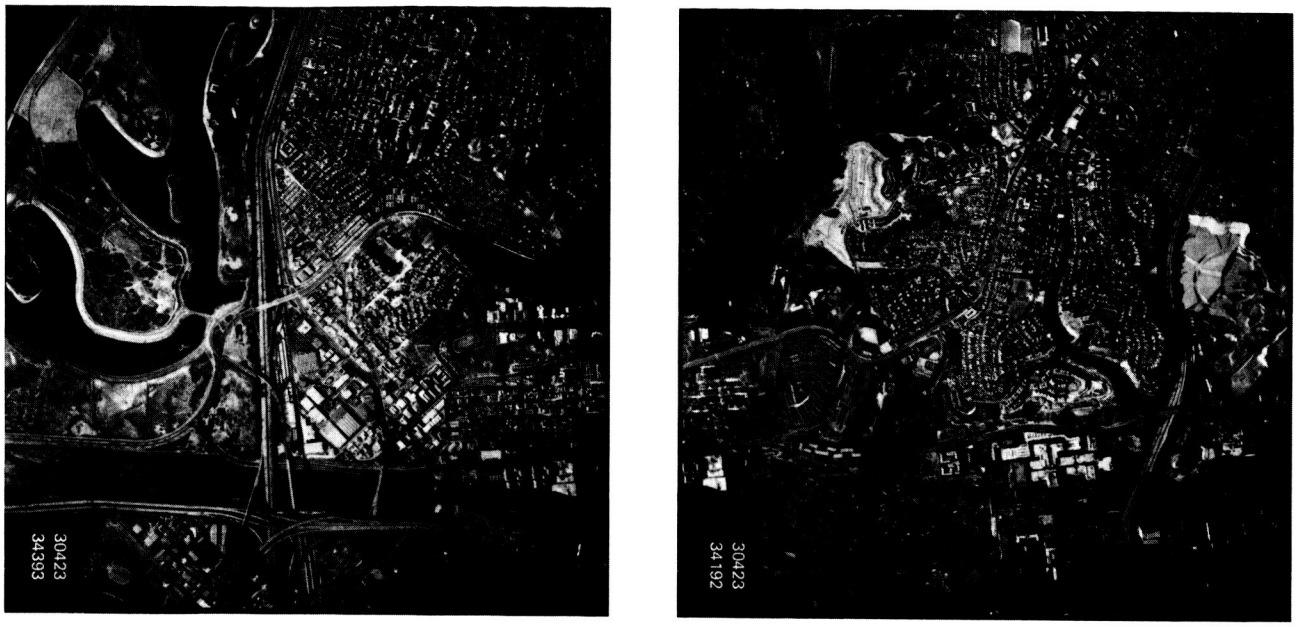

Figure 4-5. KS-87 Nadir Photography Example (San Diego Area). The photographs were taken on day of year 304 at 23:34:19.2 and 23:34:39.3.

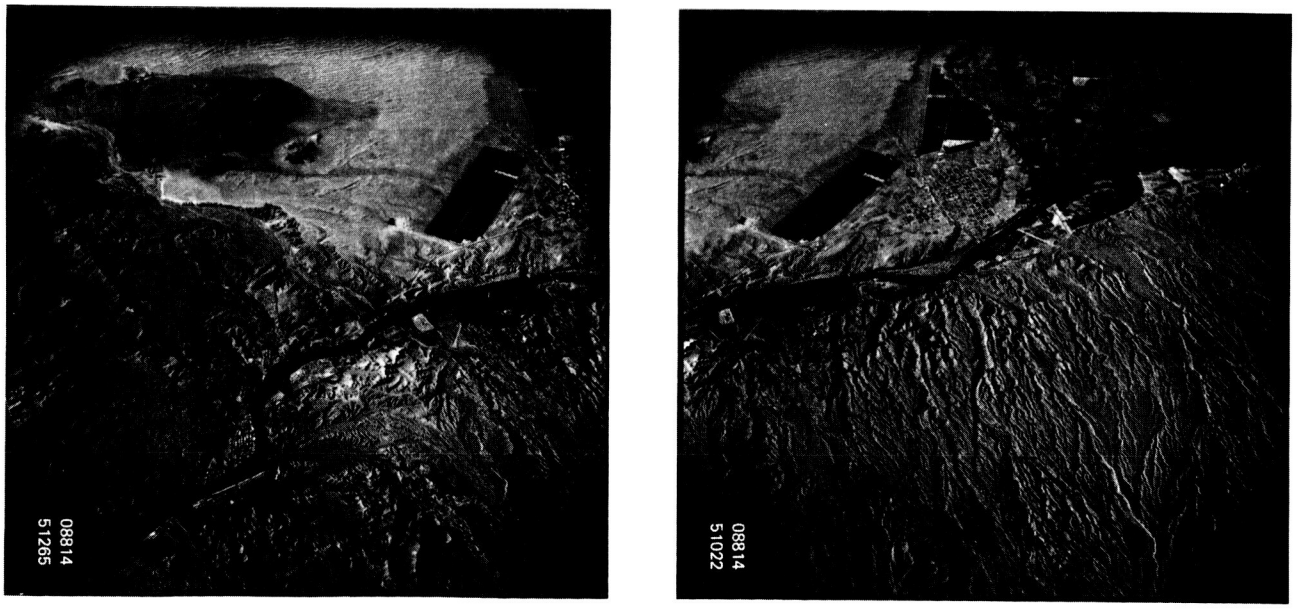

Figure 4-6. KS-87 Off-Nadir Photography Example (Colorado River between California and Arizona). These photographs show areas on the right side of the aircraft; the same areas being imaged by the radar.

SECTION V

DATA PRODUCTS--DIGITAL IMAGES

The NASA/JPL aircraft SAR data are still being used to derive digital images. As mentioned previously, the major product from the aircraft data acquisitions is the Quad-Pol digital images where the digital recordings of the echoes are converted to images via processing on a VAX computer. Overviews to this process are given in Figures 5-1 and 5-2. Figure 5-1 shows the major pieces of the hardware, and Figure 5-2 shows the interfaces with the user. Digital image production consists of five processing steps:

(1) Site selection and playback footage estimation
(2) Playback and storage on disk
(3) Digital correlation
(4) Production of photographic products
(5) Archiving and shipment of products

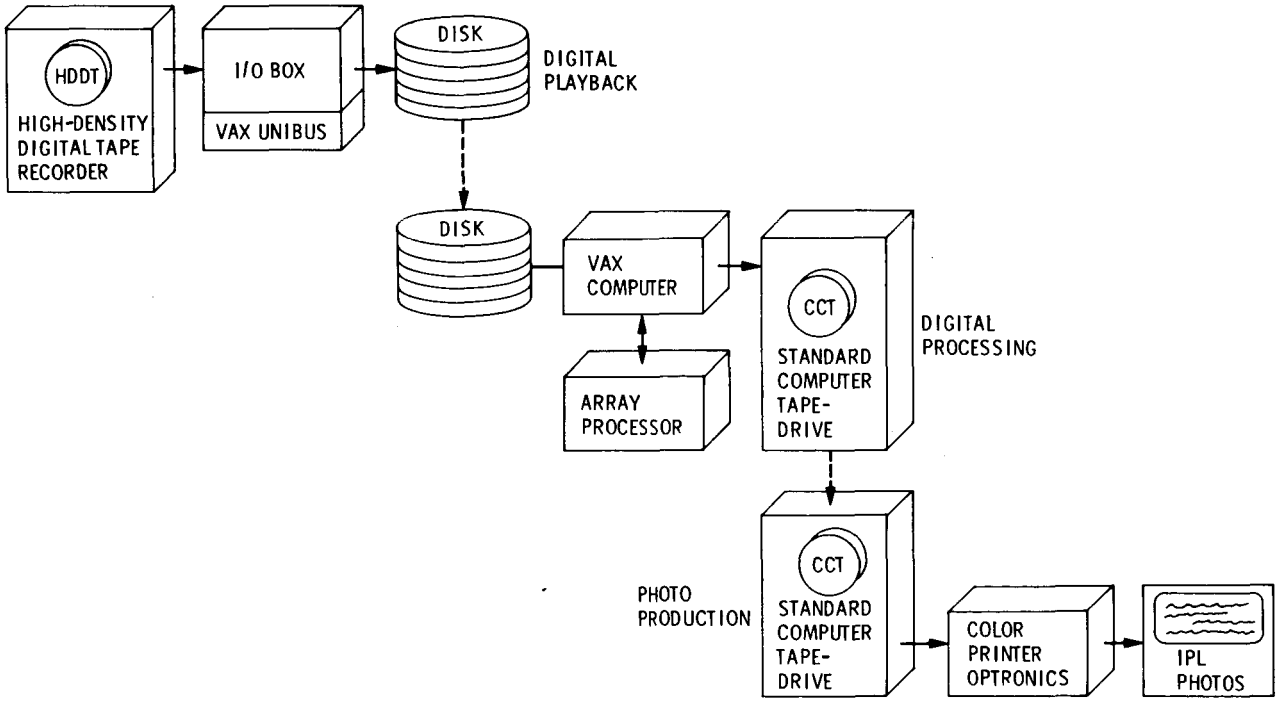

Figure 5-1. Hardware Block Diagram for Production of Digital Imagery. Steps include playback of digital data to disks in the VAX computer, production of the image converting raw data from the disk to CCT's, and production of photographic products.

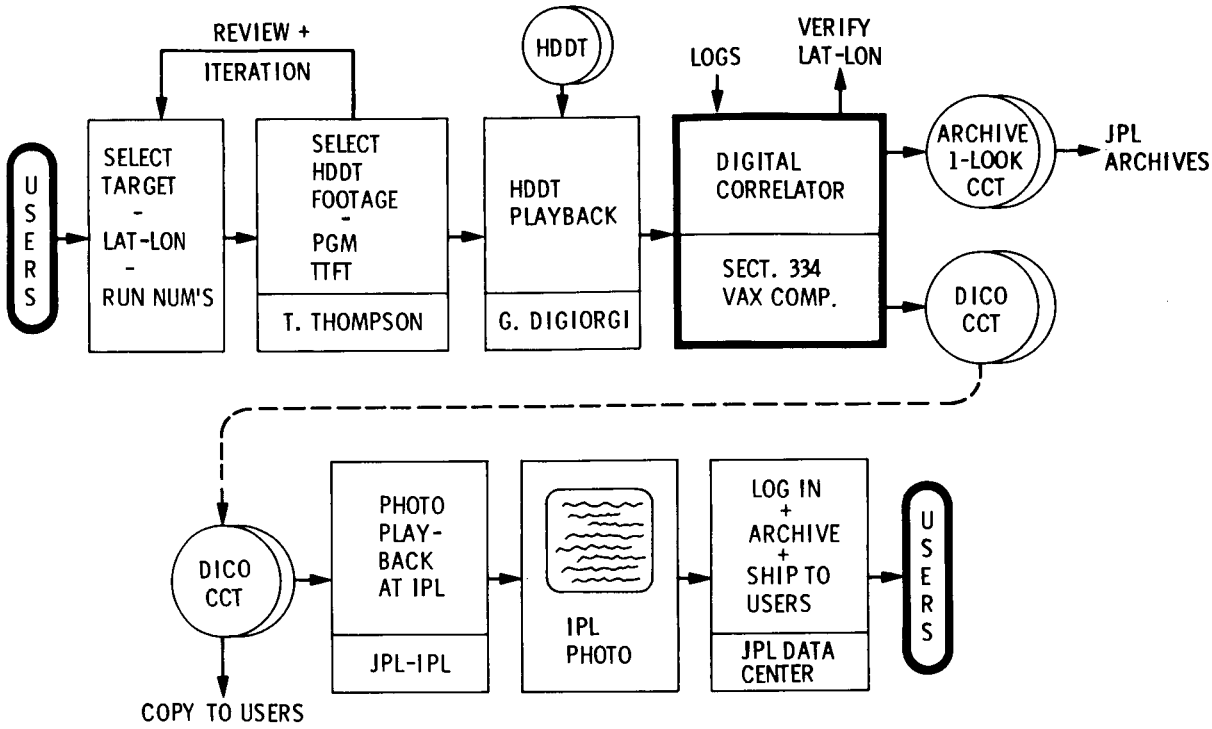

Figure 5-2. Block Diagram for Steps in Production of Digital Imagery. In addition to production steps shown in Figure 5-1, there is estimation of HDDT footage prior to playback and a logging, archiving, and distribution of imagery products after production.

Steps (2) and (3) are generally completed in 24 h while Step (4), the photographic production, requires 1 to 2 weeks. All of the digital images produced at JPL are archived in the Radar Data Center; they are accessible via a Reference Notebook System described later. The production of digital images at JPL was conducted in two periods. The digital images for the Fall-84 (SIR-B Underflight) Expedition were produced between August 1984 and August 1985. Some 120 images were produced for 21 users. The digital images for the Spring- and Summer-85 Expeditions were produced between August 1985 and August 1986. Some 130 images were produced for 23 users.

A. PLAYBACK ESTIMATION VIA PROGRAMS TTFT AND TTFTMM

The first step at JPL in the production of a digital image is the estimation of playback HDDT footages. This is accomplished via the user's input of a geographic position for the center of the image and various "log files" stored in the VAX computer. The geographic position at the center of the image is a line on the ground perpendicular to the aircraft ground track. The goal of the TTFT programs is to predict which 150 m (500 ft) of HDDT correspond to the 50 s of real-time data centered on the plane's passage over the centerline of the requested image. The key time and tape footage corresponds to when the aircraft was abeam of the centerline of the image.

The basic input to the TTFT programs is a latitude and longitude position provided by the user. Background inputs to the TTFT programs were provided by three VAX data sets corresponding to the optical, digital, and HP-9845 logs as shown in Table 5-1. To communicate between these logs and the requested position, the TTFT programs require other information which identify day, optical run, and digital run. After all the pertinent information is stored in the computer, the TTFT programs basically reconstruct the plane's ground track on a second-by-second basis and find the point of closest approach to the requested target. The ground track is reconstructed from the times and positions given in the HP-9845 log file. Although the HP-9845 log file essentially records the plane's position from the INS, there may be 1- to 2-km differences between the plane's true position and the INS position.

A second method of computing playback tape footages has evolved in response to both the INS position-error problem as well as ease of identifying areas for playback from the optical survey data. Here a center-of-image is identified by its position from the start (left-hand edge) of the optical image. This position is compared with the plane's position at the start and end of the optical data runs given in PLOG8X.DAT, and the latitude and longitude of the center-of-image is computed. This position computed from position on the optical image is then handled in the computer as if it were a map position as described previously.

B. DIGITAL PROCESSING

The NASA/JPL aircraft digital correlator is a software and hardware instrument implemented on a general purpose VAX 11/780 computer supplemented with a Floating Point Systems 120B array processor and several disks. This subsection describes the sequence of processor steps necessary to reconstruct the image from the "signal" state of reformatted data.

The starting point of the digital data production is the HDDT data. The SAR digital data collection system wrote a serial stream of six-bit input data using a 14-track HDDR. The input data stream was split into 12 parallel data streams and, along with the tracks of error correction data, written on an HDDT at a speed of 305 cm/s (120 in./s, 10 ft/s). The first processing step is to load this raw data onto the VAX computer. This is accomplished through the use of a dedicated VAX DR11W interface board, a high-speed 12-line parallel fiber-optics link, and custom driver software. A large volume of data is needed for the production of images because all the reformatting and prefiltering operations are performed in the VAX computer. This restricts the image frame to about 11 km in azimuth, dependent upon actual ground speed. The data are loaded into a series of forty-nine 8.2-megabyte files as a serial stream, recombined from the 12 parallel streams of the tape recorder. This playback requires approximately 35 min with the Fairchild M-80 HDDR, and it corresponds to 60 s of real-time data.

Following a successful playback, the next step is reformatting the data to line up all the transmit/receive events, in essence producing a digital equivalent of the optical signal film. The reformatting includes conversion of six-bit bytes to standard eight-bit bytes of VAX-11 FORTRAN.

Table 5-1. VAX Computer Log Data Files

Optical Logs (PLOG8X.DAT)	Digital Logs (DLOG8X.DAT)	HP-9845 Logs (HPLOG8X.DAT)
Day	Day	Day
GMT	HDDT Reel	HDDT Reel
Latitude	HDDT Run	HDDT Run
Longitude	Site-Name	GMT
Site Title	Investigator	Latitude
Aircraft Track	Footage	Longitude
Optical Roll	GMT	Ground Speed
Optical Run		Barometric Altitude
Footage		Radar Altitude
Delay		Pitch
Channel Polarizations		Roll
Drift Angle		Yaw

Note: GMT = Greenwich Mean Time

This requires another 30 min of processing time and typically produces 40 reformatted output files. The digital header is stored in the first 32 bytes of each receiver event in subcommutated form, and the data are truncated at 4096 bytes per receive event.

The next processing step produces a series of four one-look, high-resolution digital images, one each for the four polarizations of the Quad-Pol data. Each image is a set of four disk files. Each pixel is represented by a double-precision complex number. There are 4096 azimuth pixels with a spacing of 2.75 m and 927 slant range pixels at a spacing of 7.5 m. Processing here includes header extraction, azimuth prefiltering, STC estimation, root mean square (RMS) estimation and radiometric calibration of each polarization, as well as range and azimuth compression. Subsequent processing of this one-look data sums four adjacent azimuth pixels producing the four-look digital images that are delivered to users and archived at JPL. Processing steps here include annotation, incoherent integration of the one-look data, and ground-range rectification. The phase difference between the two principal polarizations (HH and VV) is extracted by an additional processing step. This processing is done at night as a batch job.

Following the overnight batch processing, the next processing steps provide the products delivered to the users. These steps include verification of the output, plotting of the RMS and STC estimates, and printing of the header record, as well as production of the archive and DICO CCT's. Verifying the correlation is done by examining the output listings of the reformatter, the STC estimates, the RMS estimates, and the digital header listing and by visually inspecting the image outputs on a Ramtek high-resolution color-graphics display.

One measure of data quality is provided by the listing from the reformatting at the start of processing. The reformatter writes a listing of missing lines based upon whether it was able to find the correct codes at the expected intervals in the input stream. It generates "fake" lines of all zeros to replace missing elements. Large numbers of missing lines degrade image quality and data authenticity, particularly if a large number of missing lines occurs in a small number of groups. Nominally, data are accepted with missing line counts less than 40, and distributed grouping. Correlations exhibiting more than 70 missing lines are generally rejected and a new attempt to transfer and process the data is performed. In a few cases, where some documented real-time condition of the radar in the data collection phase has acted on the recorded data stream to degrade it, the processed image is accepted as of sufficiently good quality even if the missing line counts are high.

A careful inspection of the digital header listing can reveal other problems with the data collection at some point in the subsystem interfaces. The digital header listing also contains important parameters used in the correlation and calibration process with regard to the aircraft attitude and motion. If any of those values depart significantly from the expected values, the processing can be rerun with the corrected parameters based upon other sources in our logs. The RMS and STC estimate plots are inspected because they indicate the derived values for total received power and attenuation curves used in data collection.

All of the digital images are displayed on a Ramtek graphics display and checked visually for anomalies and other image degradation. Various programs implementing color overlaying and other analytical techniques are utilized to look for anomalies and interesting features of the image. At this point, the average magnitude value is inspected for each polarization. The expected relative magnitudes for a calibrated Quad-Pol image should be $HV \cong VH$ and $HH \cong VV \cong (2 \bullet HV)$.

Following these inspections, the digital image is archived by writing the four-look output files and the phase difference output files to a 1600-Bpi tape. The tape format is compressed from the disk file format to minimize space: the 1025 records by 8192 byte disk file is written to 205 records by 40960 bytes on tape. Using this packing strategy, we are able to fit 41 megabytes of imaging data on one 1600-Bpi tape. On a few occasions the set of one-look data files is also saved in the same formats on 6250-Bpi tape.

In addition to archiving the digital image, photographic DICO tapes are created by finding the average magnitude of the four-look image file and scaling that average to be the mean value for an eight-bit gray scale, compatible with the DICO and Optronics machines the IPL uses for creating the negatives. The resulting output values are written to tape as byte records for reading: there are a number of possible paths for this process to take, so the actual on-tape format is listed on the tape label for each image output. This is the standard distribution media delivered to users, and each of the outputs is described later under Digital Image Products (Subsection V.C).

The digital images in slant-range format can be described as four 927 (range) by 1024 (azimuth) pixel arrays where each of the four images represents the HH, HV, VH, and VV polarizations, respectively. The 1024 azimuth pixels represent some 11.2 km along track direction (i.e., in that direction parallel to aircraft defined by the aircraft's ground track). The 927 range pixels represent some 8.8 km in distance from the aircraft starting from the first sample in time delay. In this slant range representation, the range pixel spacing on the ground is [9.498 m/sin (angle of incidence)]. Slant range pixels are not evenly spaced on the ground because the angle of incidence varies from near zero for the earliest echoes near nadir to 60 deg for the latest echoes at the furthest ranges of the scene. To compensate for this distortion, a geometric rectification based on a "flat earth" model is performed. This rectification will have up to 1024 range pixels if enough data exist in the 927 slant-range pixels. Rectified images have a square ground pixel of 10.98 by 10.98 m. The formula for this ground-range pixel rectification is:

$$R_g^2 = R_s^2 - H^2 \qquad (1)$$

where

R_g = distance on the ground from the aircraft's nadir to the pixel in question

R_s = observed slant-range from the aircraft to pixel in question

H = aircraft altitude

The translation of slant-range to ground-range images uses linear interpolations. The phase difference image is not rectified since interpolation destroys phase differences. The relationship between the various parameters associated with the ground-range rectification is shown in Figure 5-3. The photograph annotation, as well as the header listings, gives the aircraft altitude, the key parameter in the geometric rectification equation.

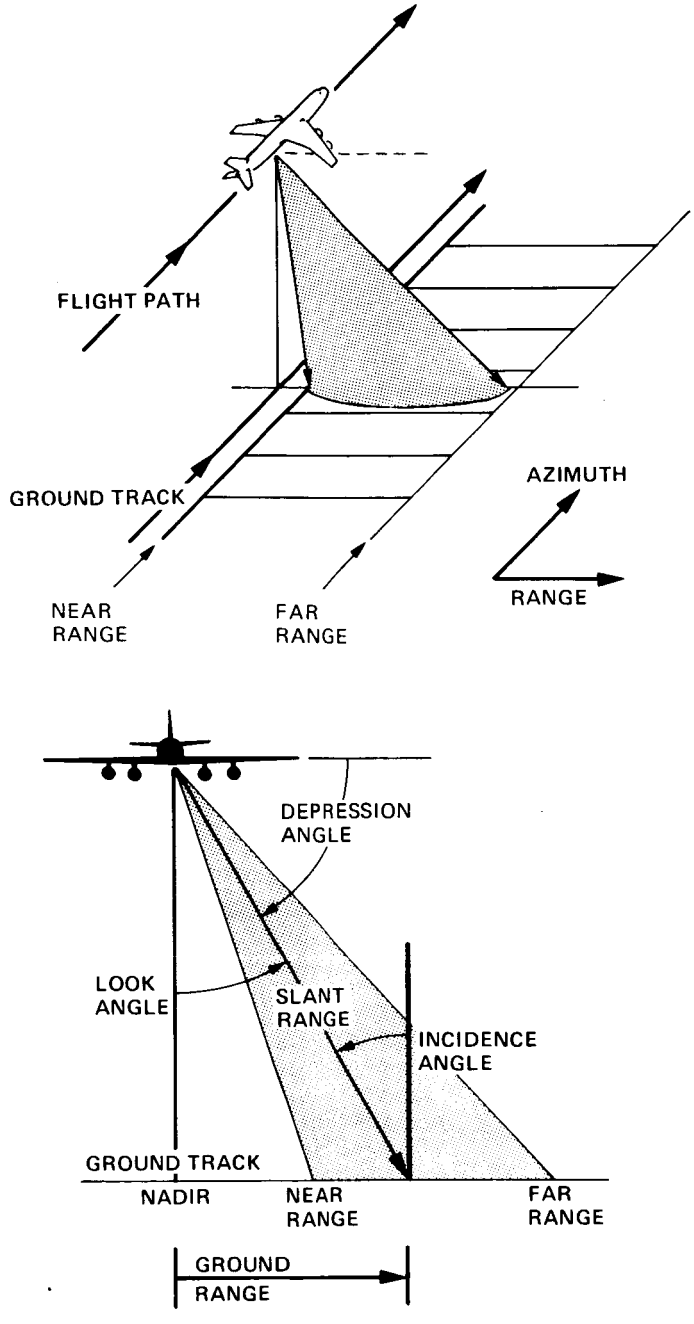

Figure 5-3. Geometry for Geometric Rectification of Digital Images. Elements in the radar image (the pixels) are located in the orthogonal coordinates of ground or slant range and azimuth. The geometry of the scattering element with respect to the radar is described by an incidence angle that is related to the complementary look and depression angles.

C. DIGITAL IMAGE PRODUCTS

The output products from the digital correlator include the following:

(1) DICO CCT
(2) IPL photographs
(3) Header listing
(4) STC and RMS estimation plots

The DICO CCT, output product (1), is shipped to the user and not archived at JPL. Output products (2), (3), and (4) are produced in duplicate; one set is sent to the user, and one set is retained at the JPL Radar Center.

The DICO CCT and IPL photographs are two versions of the same product as shown in Figure 5-4. The DICO CCT contains seven files where the first file is used to generate a black-and-white four-polarization check print like that shown in Figure 5-5. Files 2, 3, and 4 on the DICO CCT form the false-color Quad-Pol power-amplitude photograph, while files 5, 6, and 7 of the DICO CCT form a false-color phase-difference photograph. The radar image for each of the four polarizations is a 927-line by 1024-sample array for a slant-range image and a 1024-line by 1024-sample array for a ground-range image. When annotation is added to these images, they exist as 1280-line by 1024-sample arrays.

The Quad-Pol black-and-white mosaic combines four of these arrays with a 100-line and 100-sample spacing yielding a 2660-line by 2148-sample array. Each pixel in this array is related to surface cross-section (sigma-zero) via the following:

$$\text{Sigma-zero} = [20 \log (\text{DN}/\text{Scale Factor})] + (\text{K}) \qquad (2)$$

where DN is the digital number (0-255) for that pixel. The Scale Factor is determined by the correlator operator to keep the output pixel values between 0 and 255, the range needed for the photographic displays. These Scale Factors are in the photograph header. As our digital correlator is "compensated," the output numbers are only proportional to sigma-zero, and factor (K) is unknown.

False-color photographs of the radar images are produced by combining three 1280-line by 1024-sample arrays such that they are colored blue, green, and red. Files 2, 3, and 4 form a power-amplitude false-color photograph where the square-root of the HH, VV, and VH polarizations are assigned to the colors blue, green, and red. Files 5, 6, and 7 form a phase-difference false-color photograph where brightness in the photograph is controlled by the average powers in the HH and VV polarizations and where color is controlled by the phase difference between the HH and VV voltage phasors. Examples of these two types of false-color photographs are given in the frontispiece.

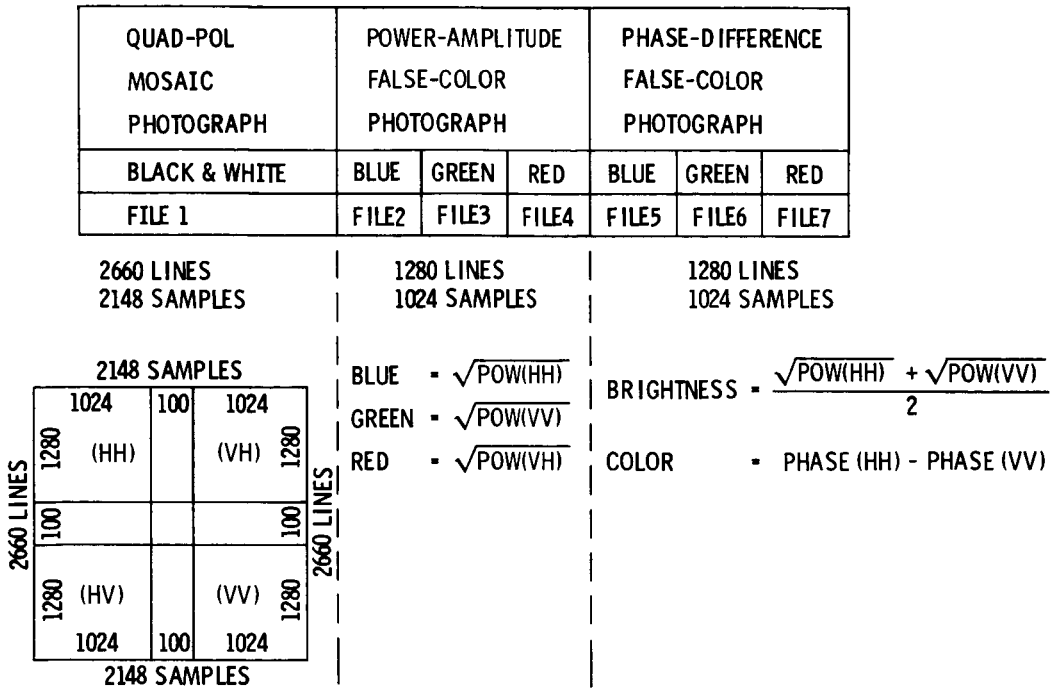

Figure 5-4. DICO Tape/IPL Photograph Format. The computer tape has seven files. The first file is a Quad-Pol mosaic like that shown in Figure 5-5. The remaining six files produce two color photographs like those shown in the frontispiece.

In addition to these IPL photographs and the DICO CCT's, users receive a header printout and STC/RMS estimation plots like those shown in Figures 5-6 and 5-7. The digital header printout is a decoded ASCII listing of the digital annotation recorded during data collection. It contains information concerning flight parameters of the aircraft in attitude and position as well as relative position to the specified investigator target. Additionally, information reflecting the state of various setup parameters of the SAR system is recorded: operational mode, gain curve settings, user, operator, etc. Of primary interest to the user are the drift angle and digital delay. All of these parameters refer to the center frame of the image.

The drift angle (or yaw of the aircraft relative to the ground track) is a critical parameter to the correlation because it determines how far from the Doppler centroid processing will occur. The operational processor, until the summer of 1986, made no correction for drift angle; therefore, data authenticity degrades as drift angle increases.

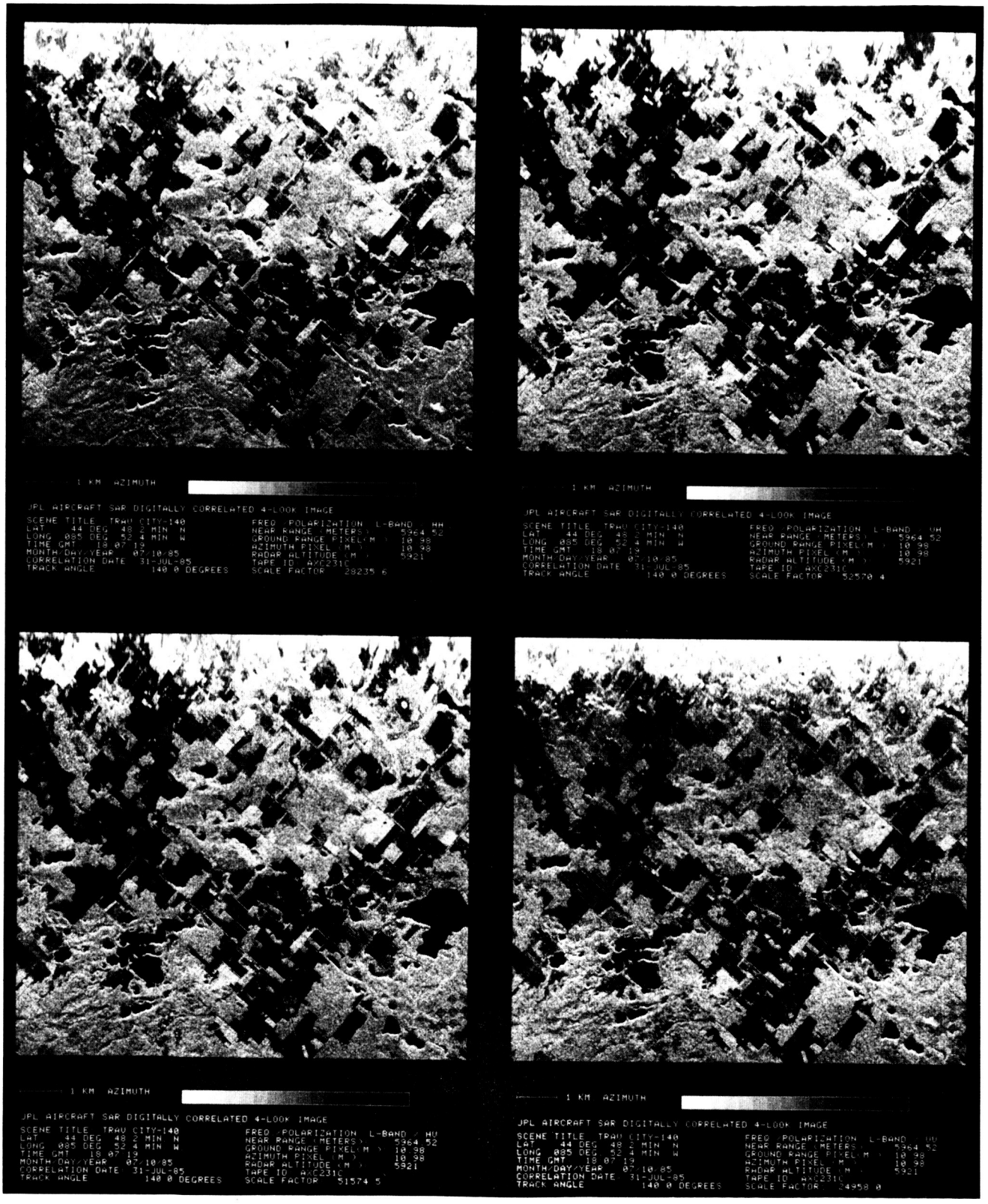

Figure 5-5. Example of Quad-Pol Power Black-and-White Mosaic, File 1 of DICO Tape. (See Figure 5-4.) The images for the four polarizations are 1024 x 1024 pixel arrays supplemented with the annotation shown.

```
NUMBER OF ERRORS DETECTED =    0
FIRST FRAME COUNT =    182545
DISTANCE TO GO          0017.9 NAUTICAL MILES
TIME TO GO              002.3 MIN.
CROSS TRACK DEV.        000.1 NAUTICAL MILES
DESIRED TRACK ANG.      140.1 DEGREES
TRACK ANG. ERROR        -000.1 DEGREES
DRIFT ANGLE             -03.6 DEGREES
ALIGN STATUS            067
LAT     44 DEG.  48.2 MIN.  N.
LONG   085 DEG.  52.4 MIN.  W.
GROUND SPEED            0461 KNOTS PER HOUR
TRACK ANGLE             140.0 DEGREES
TRUE HEADING --> 143.5 DEG.
WIND SPEED              070 KNOTS PER HOUR
WIND ANGLE              299 DEGREES
DAY OF YEAR:   191
TIME GMT:   18:07:19
PRESSURE ALTITUDE       20034 FEET
RADAR ALTITUDE          19426 FEET
AIRCRAFT PITCH          01.8 DEG. UP
AIRCRAFT ROLL           00.5 DEG. LEFT
DIGITAL DELAY           054 MICROSECONDS
MONTH/DAY/YEAR:   07/10/85
RUN NUMBER 04
DIGITAL SWATH WIDTH 060 MICROSECONDS
ANTENNA = DOOR
PRF FREQUENCY IS CONTROLLED BY INS
TARGET LATITUDE         42 DEG.  21.5 MIN.  NORTH
TARGET LONGITUDE        085 DEG.  52.4 MIN.  WEST
TARGET ELEVATION IS 01000 FEET
TARGET LOOK ANGLE = 35 DEGREES
SCENE TITLE: TRAV CITY-140
INVESTIGATOR: DOBSON-ULABY
OPERATOR: Tim Miller
OPTICAL RECORDER DELAY = 038 MICROSECONDS
FIXED GAIN:   HH = 505  HV = 515
FIXED GAIN:   VH = 529  VV = 494
RECHIRP DELAY = 450 MICROSECONDS
INJECTED SINE WAVE FREQ. = 005000 MHZ.
HORIZONTAL (LEFT) FORWARD POWER = 65.64 DB
HORIZONTAL (LEFT) REVERSE POWER = 52.93 DB
VERTICAL (LEFT) FORWARD POWER = 64.69 DB
VERTICAL (LEFT) REVERSE POWER = 51.58 DB
CAL CHAN 0
ATTENUATOR SETTING 45
CAL POWER    0.1 DBM
STC DELAY 53
```

Receiver Gain Curves

Step #	VV	HH	VH	HV
0	53.2	54.0	61.4	62.5
1	53.6	54.0	61.4	62.5
2	53.8	54.5	61.4	62.5
3	54.0	54.5	61.4	62.5
4	54.2	54.9	61.4	62.5
5	54.6	55.4	61.4	62.5
6	54.9	55.4	61.4	62.5
7	54.9	55.9	61.4	62.5
8	55.6	55.9	61.4	62.5
9	55.6	55.9	61.4	62.5
10	56.0	56.5	61.4	62.5

Figure 5-6. Example of Header Printout. Important parameters include the aircraft position and attitude given as LAT, LONG, GROUND SPEED, TRACK ANGLE, RADAR ALTITUDE, AIRCRAFT PITCH, AIRCRAFT ROLL, DRIFT ANGLE.

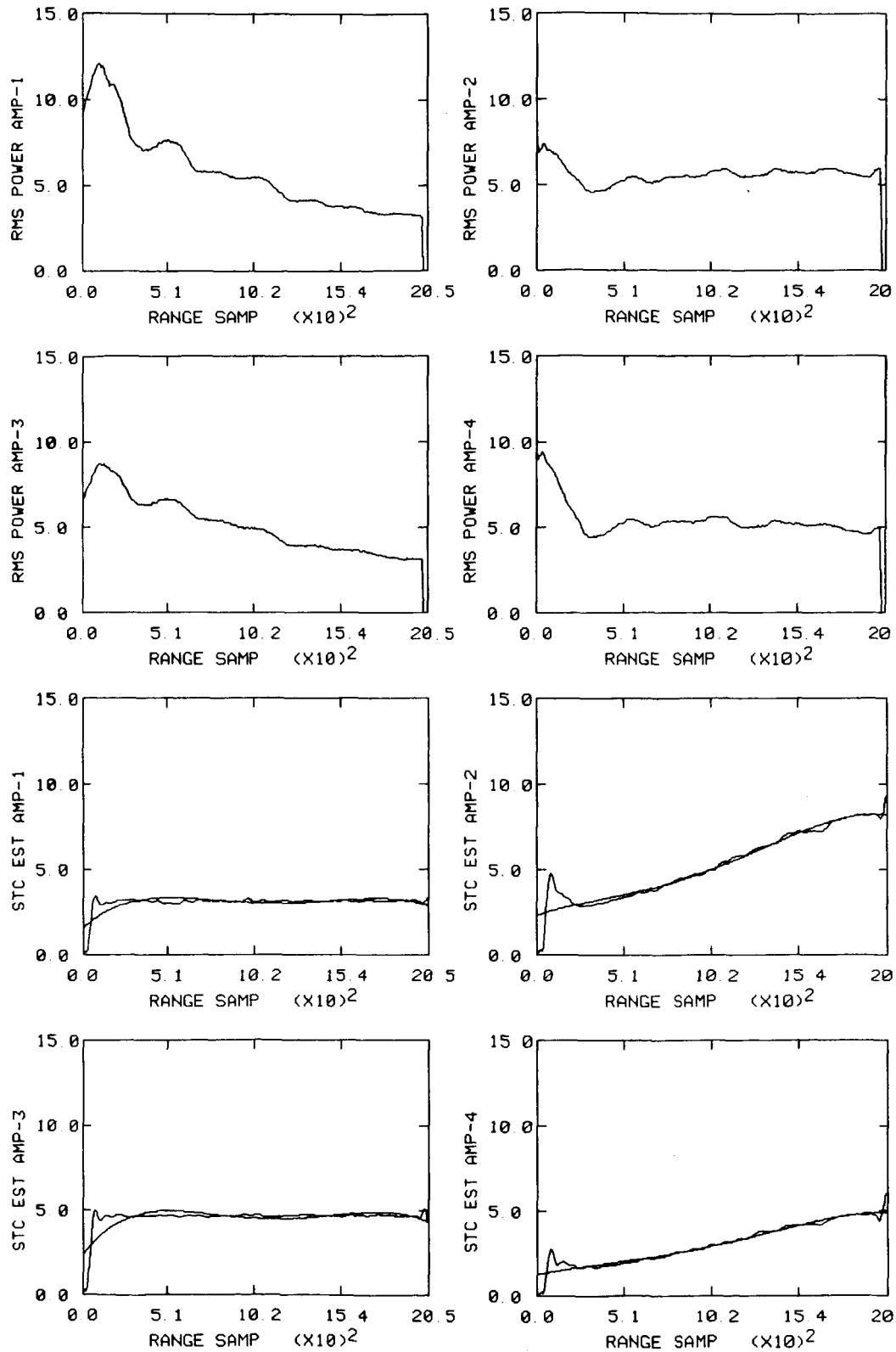

Figure 5-7. Example of STC and RMS Estimation Plots. The STC estimate is the average STC compensation applied to the echoes. The RMS estimate is echo power as viewed by the radar; it includes STC, range factor, and antenna gain.

The "digital delay" refers to the time in microseconds from the anticipated start of a receive event to the point at which recording of the digital data actually begins. Using this digital delay, the distance to the first line in range can be calculated by the following formula:

$$\text{near range (in meters)} = [[(\mu s \text{ of DD}) - 14.21] \bullet c]/2 \qquad (3)$$

where

DD = digital delay from the header
14.21 = μs of system offset (constant)
c = speed of light in m/μs

Look angles, depression angles, and incidence angles for a particular pixel position can then be calculated utilizing the radar altitude information and the "flat earth" model shown in Figure 5-3.

The STC and RMS plots provide information about average signal levels as a function of range. The STC plots are an estimate of the CW calibration signal that was inserted in the radar receiver chain at a point between the antenna port and the front-end switches. They are derived in the processing by a narrow-band software filter centered on the calibration-tone frequency. A "correct" set of STC plots would be the "inverse" of sigma-zero modulated by the range factor and the antenna gain. The RMS plots are an estimate of the received power as a function of range. They include the STC modulation as well as the range factor and antenna gain effects. If the STC were perfect, the RMS plots would be flat. Any large deviations of the RMS power from a flat curve would indicate areas where either saturation occurred (for large RMS values) or the echo was not adequately sampled (for low RMS values).

D. DIGITAL DATA SUMMARY

The production of digital images for the Fall-84 (SIR-B Underflight) and Spring- and Summer-85 Expeditions has produced some 250 images for 46 users between August 1984 and August 1986. The steps needed to produce these images are the following:

(1) Collection of request from the user
(2) Estimation of playback footage
(3) Production of the digital image
(4) Production of photographic products and dessimination of the data to the requestor

The products delivered to the users include the DICO CCT and corresponding black-and-white and color photographs described above. JPL maintains two archives of this data. The basic image data in the form of four-look floating point files is stored in an off-site computer tape library. The IPL photographs are archived in the JPL Radar Data Center and are available to any requestor.

All of the duplicate photographs are archived in the Radar Data Center using a Reference Notebook System. Also, a data base exists in the JPL VAX computer; this data base allows rapid access to the photographs in these notebooks. The reference notebooks are accessed via book and page numbers; and each notebook has a table of contents. Sorts of the data base provide listings by corelation date, title, or tape number. The sorts, by correlation date and title, are given in Appendix C.

In general, correlations which have AXK serial numbers should be recorrelated to take advantage of the compensation correlations described above. Correlations with AXC serial numbers can be duplicated from the archive tapes without new correlations. Thus, many existing digital images can be reproduced with little effort, and this Reference Notebook System provides users with easy access to the existing data.

SECTION VI

DATA ACQUISITION SUMMARY

The data acquired from 1983 through 1985 (summarized in Appendixes A, B, and C) represent some 189 sites for 84 investigators, a substantial amount of data. However, as mentioned previously, the Fall-84 (SIR-B Underflight) and Summer-85 Expeditions produced superior data because these two expeditions were equipped with a microstrip antenna and the Fairchild Model-80 HDDR (see Table 3-2). The microstrip antenna provided straightforward measurement of the phase differences between the polarizations, and the Model-80 HDDR provided superior digital data quality via its error-correcting codes. Consequently, the remainder of this report discusses only the digital data acquired in the Fall-84 (SIR-B Underflight) and Summer-85 Expeditions. This still represents a substantial amount of data because these two expeditions had 39 flights to 116 sites for 31 investigators.

Two methods are used to describe the data acquisitions. The first method uses track plots of digital data to give the geographic location of the data. The second method uses survey optical mosaics and typical digital images of a few sites to give an overview of the appearance of sites in the radar images. Both methods concentrate on those sites that were observed on multiple tracks.

A. TRACK PLOTS

Track plots were generated for some 20 sites observed with multiple passes during the Fall-84 and/or Summer-85 Expeditions. Figure 6-1 gives the location of these track plots while Tables 6-1, 6-2, and 6-3 list these sites. Often several targets appear in a single plot, and flight directions are given where possible. The order of the track plots in the following pages is from west to east (left-to-right on standard maps).

As mentioned previously, the western U.S. targets tend to be geological in nature for primarily JPL investigators. The midwestern and eastern U.S. targets tend to be agricultural or forested in nature and to be used by non-JPL primary investigators (either SIR-B investigators or those from the NASA Goddard, Johnson, and NSTL Centers).

Figures 6-2 through 6-6 show a number of sites located in California and Nevada. Many of these were flown in the Fall-84 Expedition for SIR-B investigators. The Los Angeles site in Figure 6-5 covers an urban area (San Francisco provides another urban area since it was observed on several checkout flights because it was close to the NASA/Ames CV-990 base at Moffett Field). The Raisin City site in Figure 6-3 is an agricultural site that was observed on many flights. The Snake River Plain and Wind River Basin, in Idaho and Wyoming, shown in Figures 6-7 and 6-8, complete the geologic sites in the western U.S.

Figures 6-9 through 6-12 show sites in the Midwest. These tend to be forested sites. Other forested sites include the NSTL site in Mississippi and the Jacksonville Forest site located in northern Florida near the border of Georgia. (See Figures 6-13 and 6-14.) The Supersite in Illinois, the location of crossing orbital SIR-B coverage, was agricultural. (See Figure 6-12.)

Figures 6-15 through 6-18 show various sites in the eastern U.S. The Winchester, Virginia site has excellent coverage of the Appalachian Mountains, while the Blackwater River in Maryland was a wetland site. (See Figure 6-15.) The New England and upstate New York sites are forested sites.

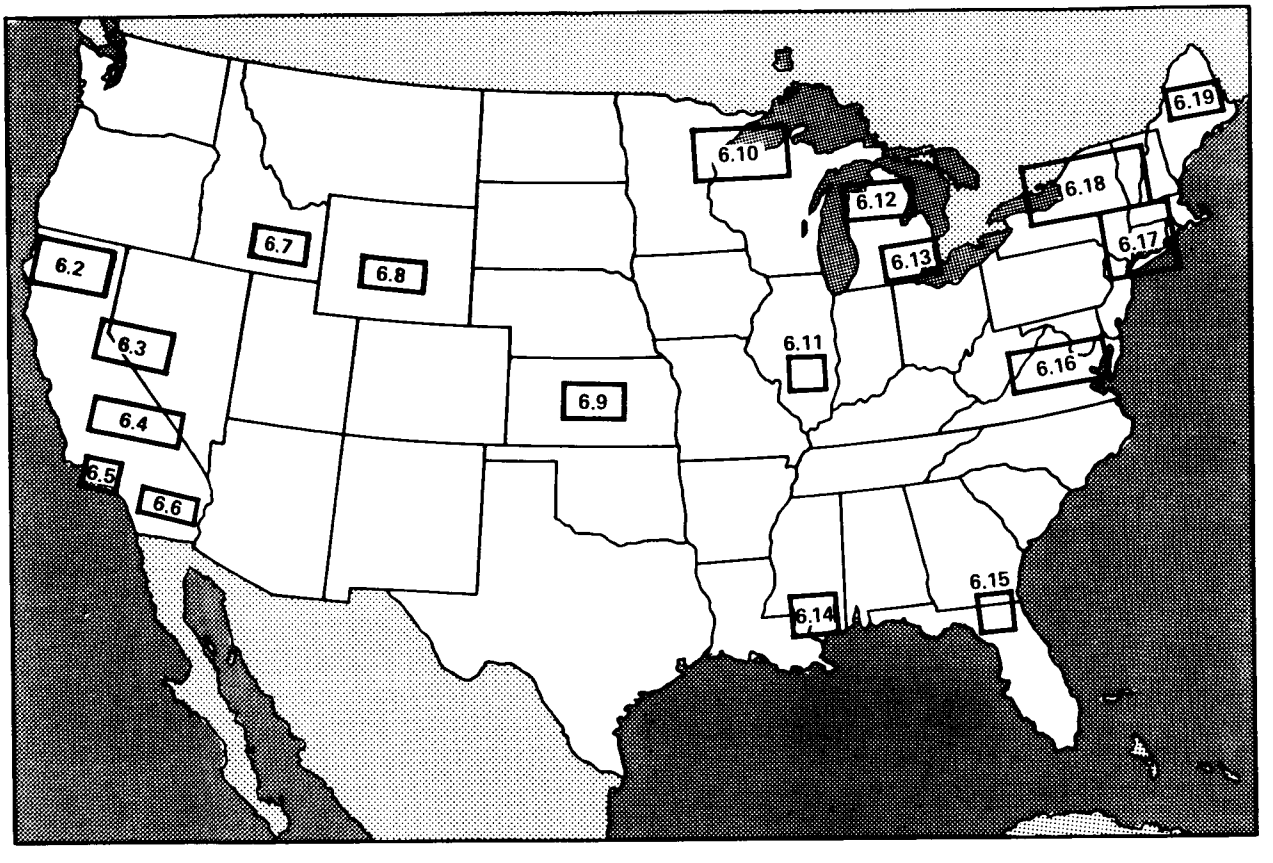

Figure 6-1. Geographic Locations of the Track Plots in Figures 6-2 through 6-18. The track plot numbers progress from west to east.

Table 6-1. Track Plot Summary

Figure	Target	Discipline	Investigator(s)
6-2	Northern CA, SIR-B	Geology, Forestry	Various
6-3	Raisin City, CA	Agriculture	Paris (JPL), Held (JPL)
	Owens Valley, CA	Geobotany	Rock (JPL)
	Death Valley, CA	Geology	Farr (JPL)
6-4	SIR-B, NV	Geology	Taranik (U of NV),
		Geology	Parr (AS Corp)
6-5	Los Angeles, CA	Land Use	Wasowski (Notre Dame)
6-6	California Desert	Geology	Various
6-7	Snake River, ID	Geology	Farr (JPL)
6-8	Wind River, WY	Geology	Evans (JPL)
6-9	Konza Grasslands, KS	Hydrology	Schmugge (GSFC)
6-10	Ely Pines, MN	Forestry	Pitts (JSC)
	Ottawa National Forest, MI-MN	Forestry	Hoffer (Purdue)
6-11	SIR-B Supersite, IL	Calibration, Agriculture	Dobson (U of MI)
6-12	Traverse City, MI	Land Use	Dobson (U of MI)
6-13	Ann Arbor, MI	Land Use	Dobson (U of MI)
6-14	NSTL, MS	Forestry	Wu (NSTL)
6-15	Jacksonville Forest, FL	Forestry	Hoffer (Purdue)
6-16	Winchester, VA	Geology	Masuoka (GSFC)
	Blackwater River, MD	Hydrology	Ormsby (GSFC)
6-17	Cockaponset, CT	Forestry	Paris (JPL)
	Albany, NY	Forestry	Paris (JPL)
6-18	Upstate New York	Forestry	Paris (JPL)
	Vermont Forests	Forestry	Paris (JPL)
6-19	Moosehead, ME	Forestry	Hoffer (Purdue)

Table 6-2. Track Plots for the Fall-84 (SIR-B Underflight) Expedition

Date	Site	Investigator
840911	NASA-NSTL, MS	Wu (NSTL)
840914	Jacksonville Forest, FL	Hoffer (Purdue)
840916	Winchester, VA	Masuoka (GSFC)
	Blackwater River, MD	Ormsby (GSFC)
840920	Connecticut and Upstate NY	Paris (JPL)
840921	Ely, MN	Pitts (JSC)
840926	Shasta, CA	Simonett (UCSB)
	Medicine Lake, CA	Kaupp (Univ. of Arkansas)
	Northern California	Farr (JPL)
940928	Death Valley, CA	Farr (JPL)
	Nevada SIR-B	Taranik (U of NV)
	Raisin City, CA	Paris (JPL)
841008	Supersite, IL	Dobson (U of MI)
841010	Supersite, IL	Dobson (U of MI)
841013	Wind River, WY	Evans (JPL)
841017	Raisin City, CA	Held (JPL)
841018	Windriver, WY	Evans (JPL)
	Snake River, ID	Farr (JPL)
841019	Raisin City, CA	Held/Paris (JPL)
841024	Glass Mountain, CA	Simonett (UCSB)
	Shasta, CA	Simonett (UCSB)
	Cinder Cones, CA	Blom (JPL)
841025	Goldstone, CA	Held (JPL)
	Cima Volcanics, CA	Farr (JPL)
	Kelso Dunes, CA	Blom (JPL)
	Pisgah Lava, CA	Farr (JPL)
	Means Valley, CA	Evans (JPL)
841104	Los Angeles, CA	Wasowski (Notre Dame)
841106	Goldstone, CA	Zebker (JPL)
	Cima Volcanics, CA	Farr (JPL)
	Kelso Dunes, CA	Blom (JPL)

Table 6-3. Track Plots for Summer-85 Expedition

Date	Site	Investigator
850612	Konza Grass, KS	Schmugge (GSFC)
850614	Konza Grass, KS	Schmugge (GSFC)
	Ann Arbor, MI	Dobson (U of MI)
850616	Vermont Forests	Paris (JPL)
850617	Traverse City, MI	Dobson (U of MI)
	Konza Grasslands, KS	Schmugge (GSFC)
850618	Konza Grasslands, KS	Schmugge (GSFC)
850621	Wind River, WY	Evans (JPL)
	Snake River, ID	Farr (JPL)
850627	Owens Valley, CA	Rock (JPL)
	Cima Volcanics, CA	Farr (JPL)
	Vidal Junction, CA-AZ	Farr (JPL)
	Pisgah Lava, CA	Farr (JPL)
	Raisin City, CA	Paris (JPL)
850710	Ely Pines, MN	Pitts (JSC)
	Ottawa Forest, MI-MN	Hoffer (Purdue)
	Traverse City, MI	Dobson (U of MI)
850713	Upstate New York	Paris (JPL)
	Moosehead Lake, MN	Hoffer (Purdue)
	Cockaponset, CT	Paris (JPL)
850714	Raisin City, CA	Paris (JPL)
850714	Raisin City, CA	Paris (JPL)

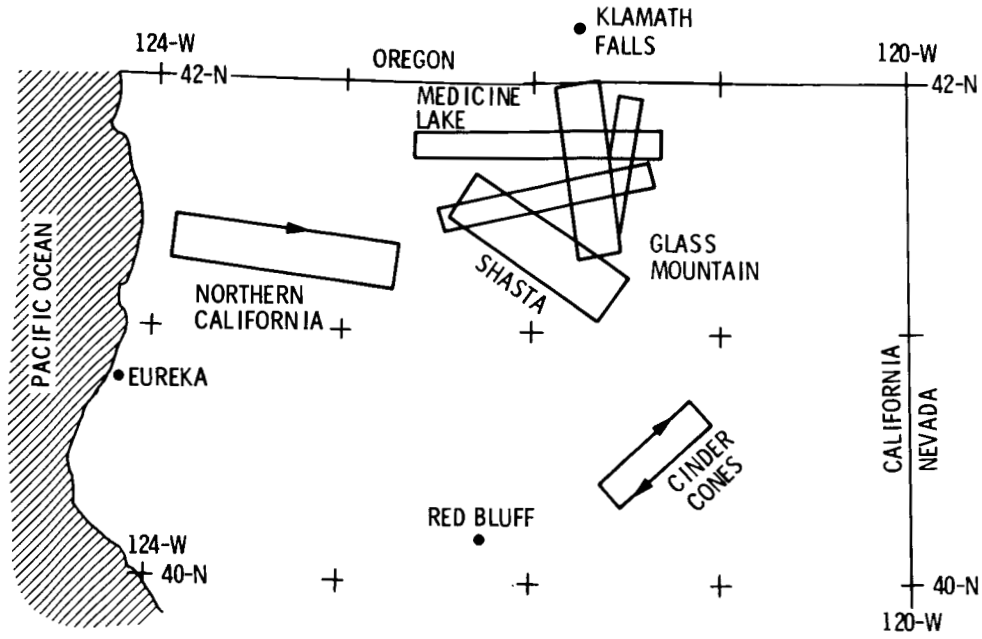

Figure 6-2. Track Plots for Northern California. These data support SIR-B and were flown on 840926 or 841024.

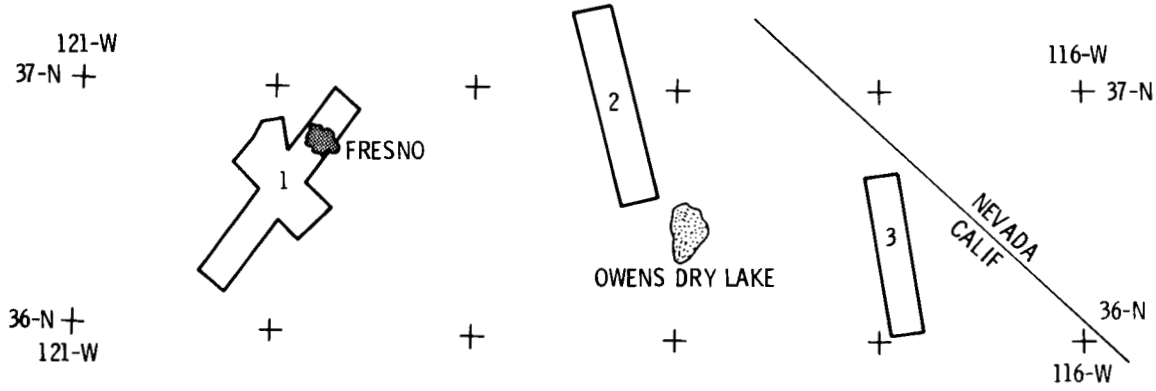

Figure 6-3. Track Plots for Central California:

(1) Raisin City (Several Flights in 1984 and 1985)
(2) Owens Valley (Several Flights in 1984 and 1985)
(3) Death Valley (Flown 840928).

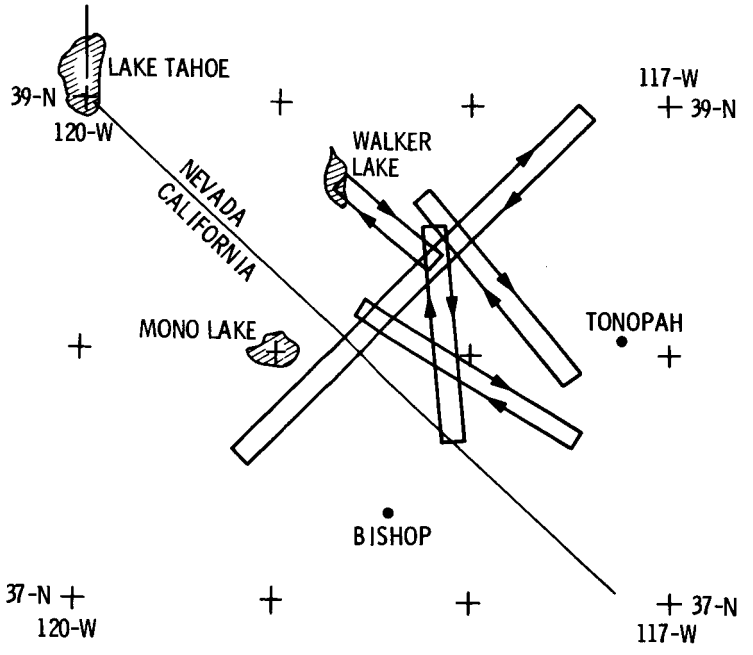

Figure 6-4. Track plots for Nevada SIR-B Sites (Flown on 840928)

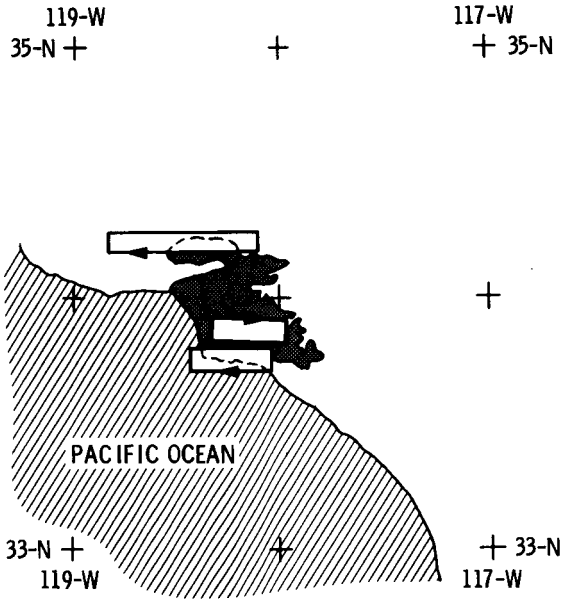

Figure 6-5. Track Plots for Los Angeles, California (Flown on 841104)

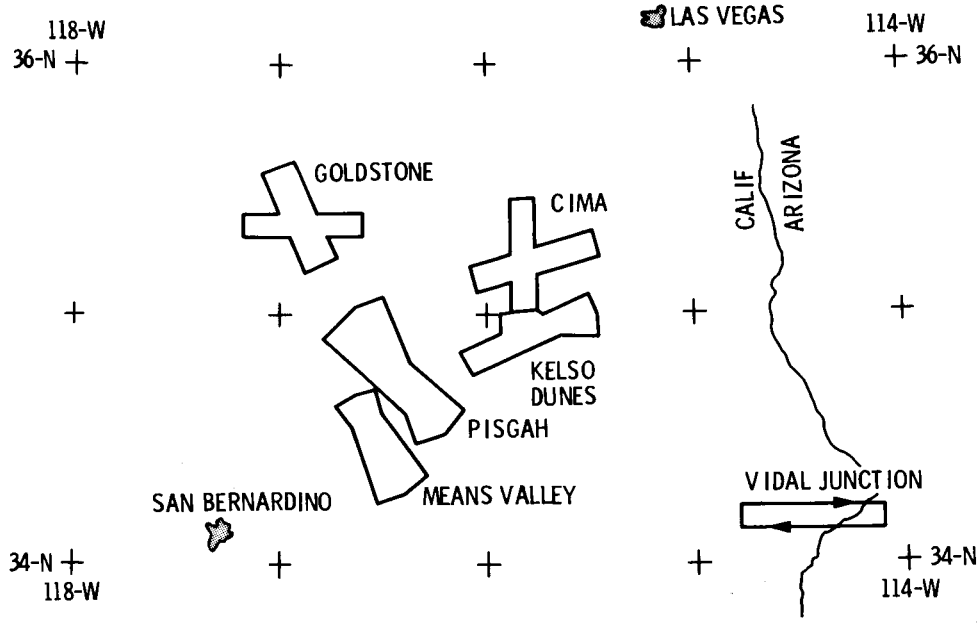

Figure 6-6. Track Plots for the Southern California Desert. This, the densest coverage for 1984 and 1985 expeditions, was flown on various dates.

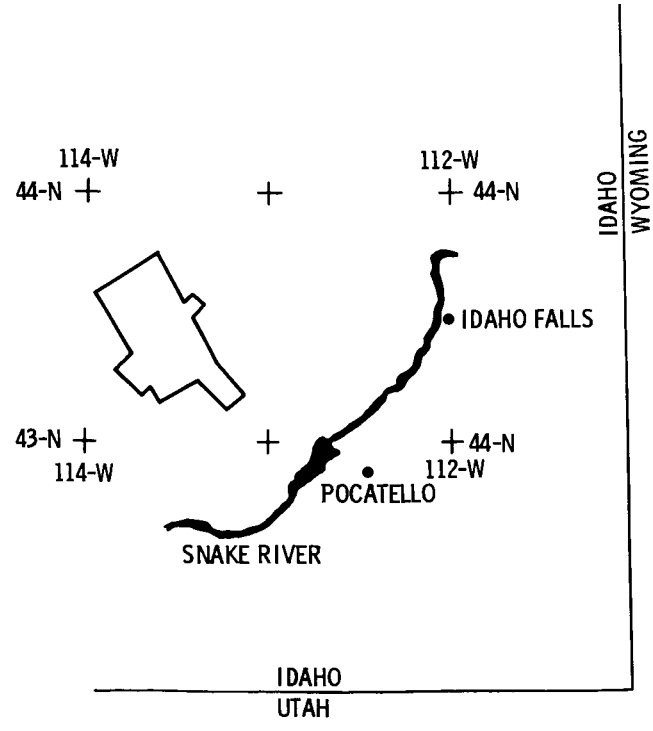

Figure 6-7. Track Plots for the Snake River, Idaho (Flown on 841018 and 850621)

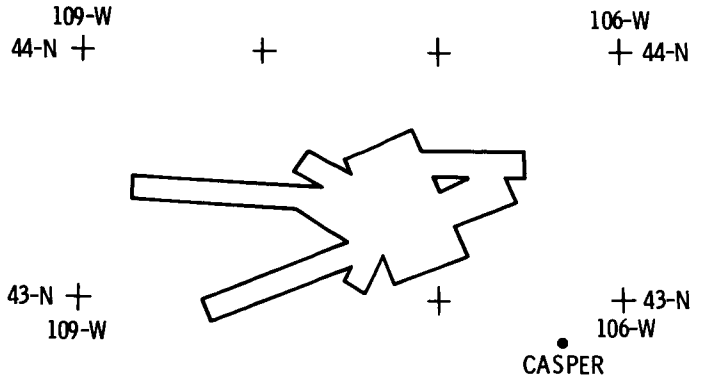

Figure 6-8. Track Plots for Wind River, Wyoming (Flown on 841013, 841018, and 850621)

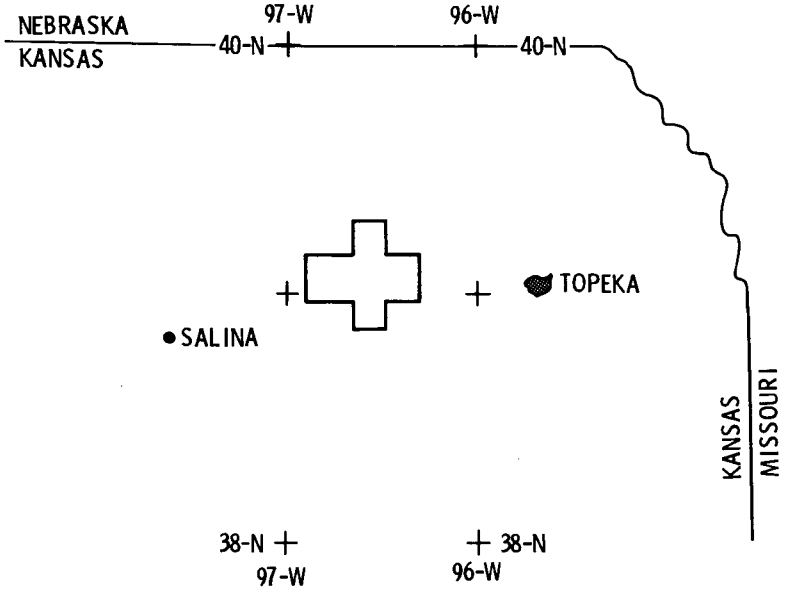

Figure 6-9. Track Plots for the Konza Grasslands, Kansas. These were flown on 850612, 850614, 850617, and 850618. The first two (850612 and 850614) were flown in the north and south directions. The last two (850617 and 850618) were flown in the east and west directions.

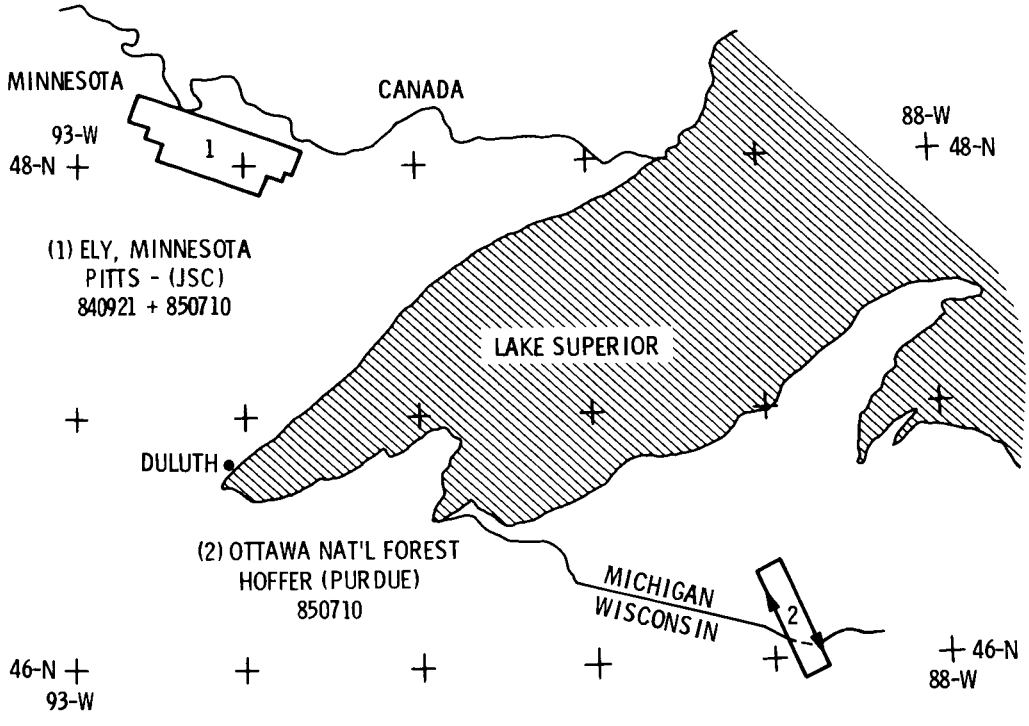

Figure 6-10. Track Plots for the Ely Pines Site, Minnesota(1) and Ottawa National Forest Site(2) on the Border of Michigan and Minnesota. The Ely Pines Site was flown on 840921 and revisited on 850710. The Ottawa National Forest Site was flown on 850710.

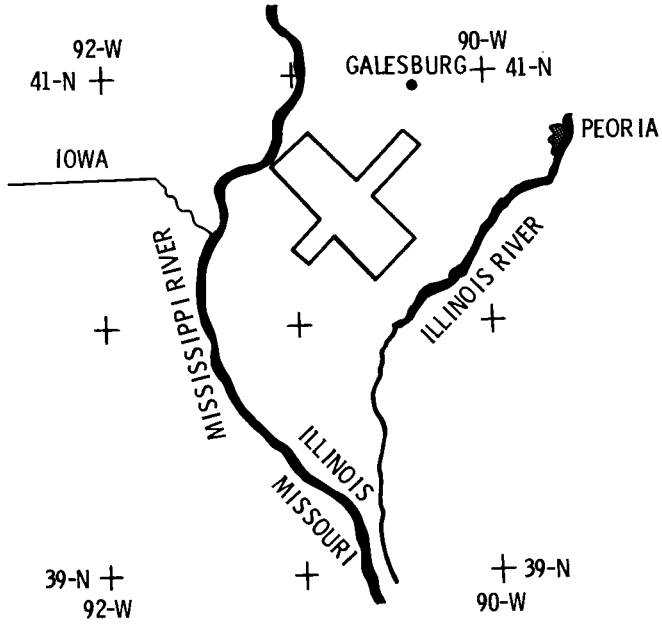

Figure 6-11. Track Plots for the SIR-B Supersite, Illinois. Although this site was flown daily for 4 days, there are useful data only for 841008 and 841010.

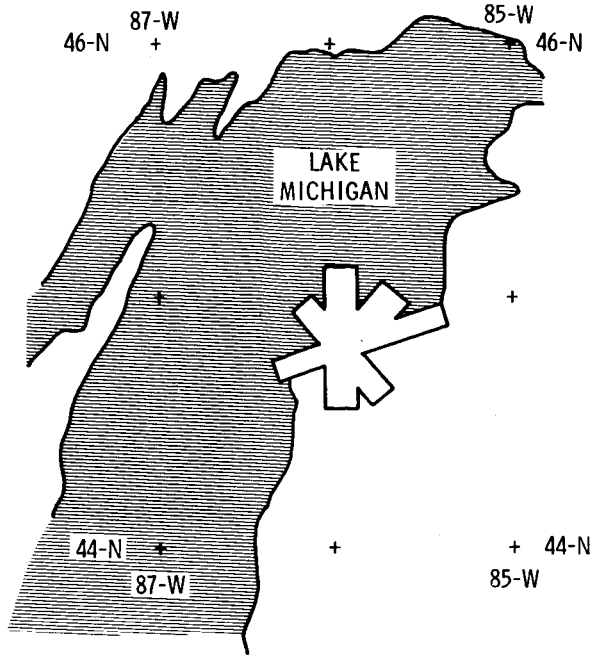

Figure 6-12. Track Plots for Traverse City, Michigan. This site lies east of Green Bay, Wisconsin, and was flown on 850617 and 850710.

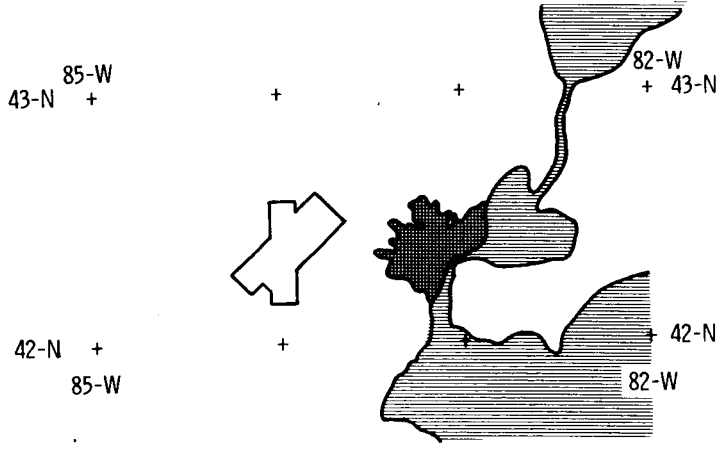

Figure 6-13 Track Plots for Ann Arbor, Michigan. The Ann Arbor site which is west of Detroit was flown on 850614. There were six lines in total, three each with headings of 0 deg and 45 deg.

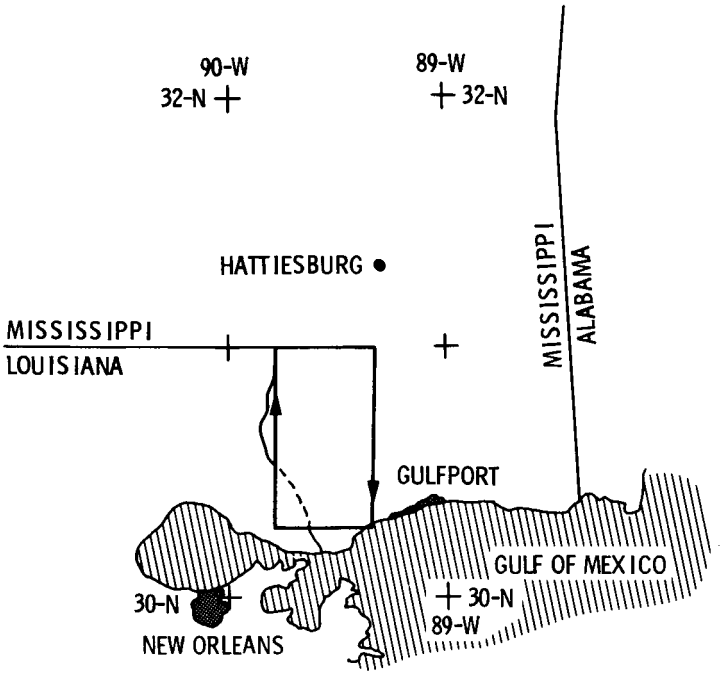

Figure 6-14. Track Plots for the NSTL Site, Mississippi. There were eight legs in total, four each with headings of 360 deg (due north) and 180 deg (due south). This site was flown on 840911.

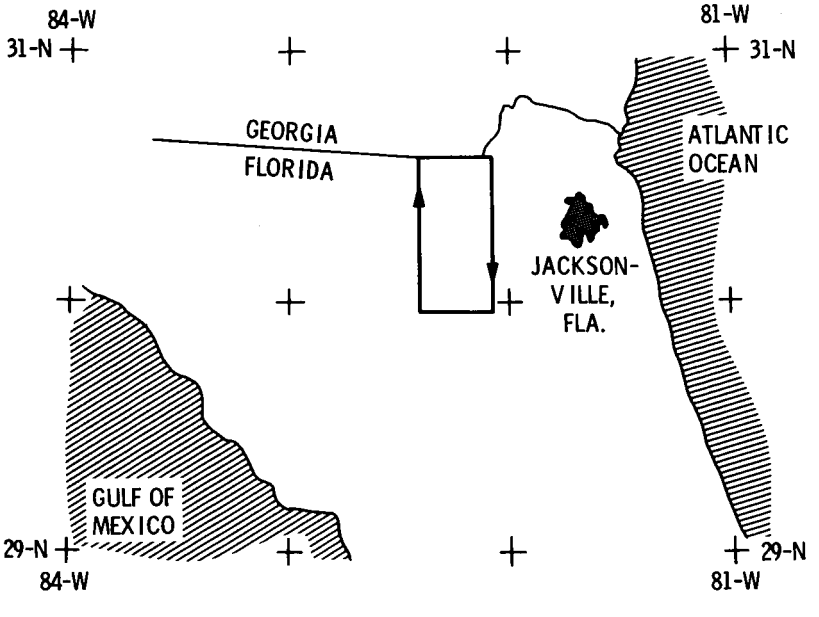

Figure 6-15. Track Plots for Jacksonville Forest Site, Florida. Site flown on 840914 with six total legs, three each at headings of 180 deg (due south) and 360 deg (due north).

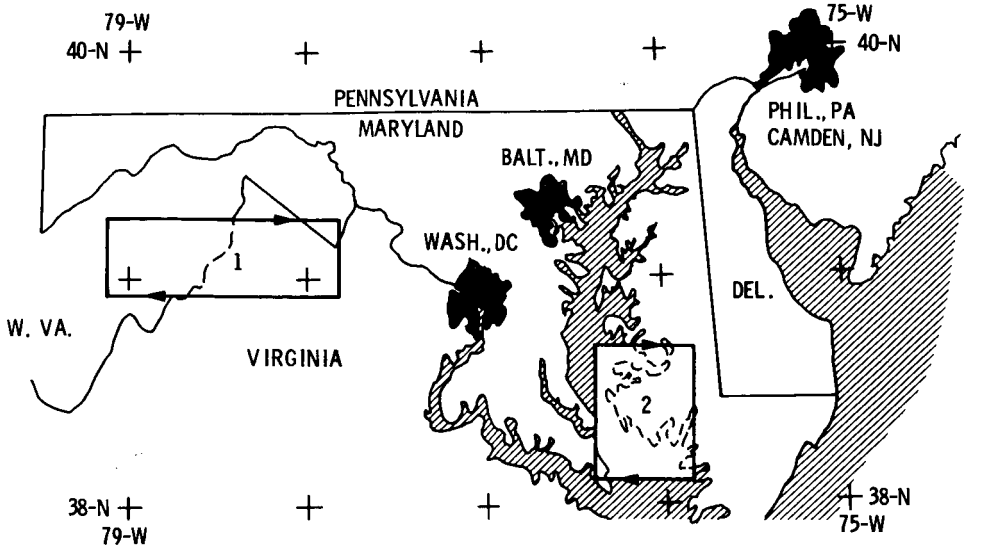

Figure 6-16. Track Plots for the (1) Winchester, Virginia and (2) Blackwater River, Maryland Sites. Sites were flown on 840916; both had eight legs, with four each at headings of 90 deg (due east) and 270 deg (due west).

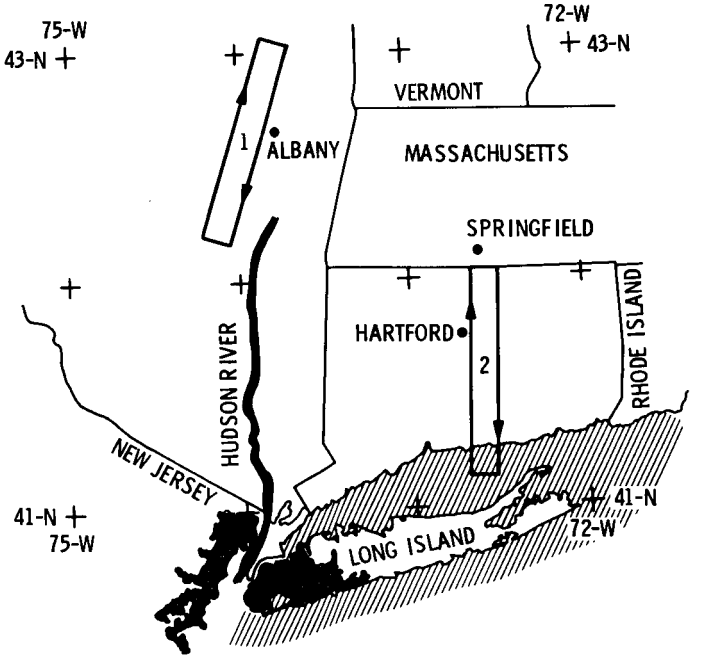

Figure 6-17. Track Plots for the (1) Cockaponset Forest, Connecticut and (2) Albany, New York Sites. These sites were flown first on 840920 supporting Sir-B and were flown in opposite directions. When revisited on 850713, the Albany site was flown with a heading of 16 deg and the Cockaponset site was flown with a heading of 180 deg (due south).

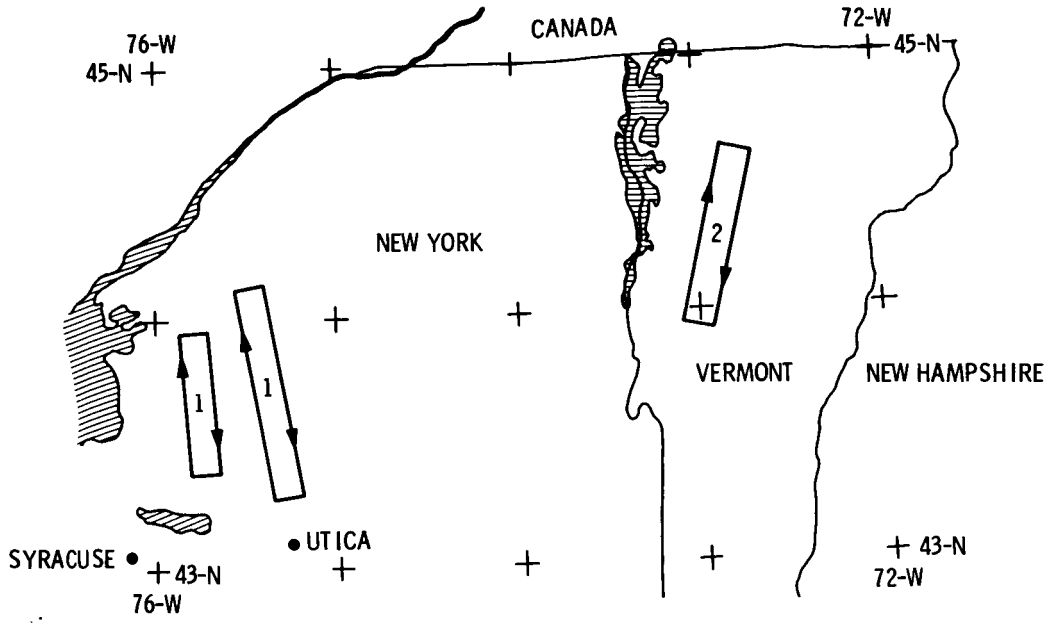

Figure 6-18. Track Plots for Upstate New York(1) and Vermont Forest(2) Sites. The Upstate New York Sites were flown on 840920 and 850713. The Vermont Site was flown on 850713 with six legs. All of these sites were flown in opposite directions on parallel tracks.

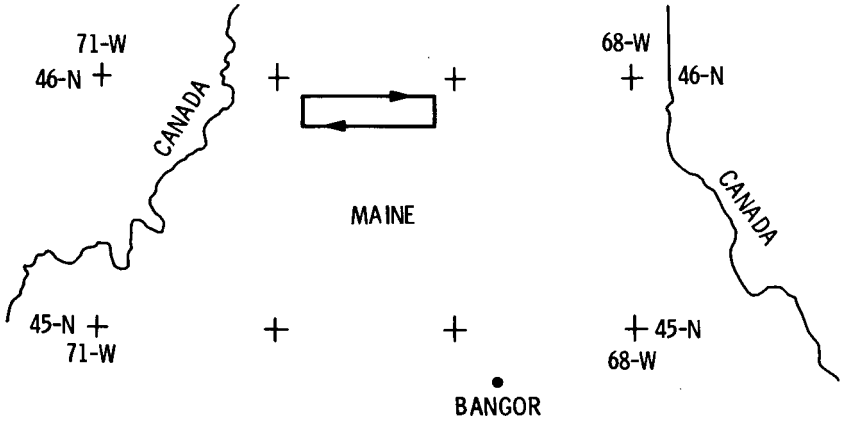

Figure 6-19. Track Plots for Moosehead Lake, Maine. This site was flown on 850713. There were two westbound legs and one eastbound leg.

B. OPTICAL SURVEY MOSAICS

Some sense of radar scattering from natural targets is provided by the optical survey mosaics shown in Figures 6-20 through 6-23. These were constructed by mosaicking SCP's of optical survey images for those targets observed from closely spaced parallel paths. Although many sites were observed with parallel tracks, only six mosaics are included here. The width of each optical survey image is about 10 km. Thus, the widths of these optical survey mosaics are 10 to 30 km; their lengths are 50 to 100 km. Like the track plots, these are presented in a west-to-east manner. Table 6-4 gives background information on these mosaics.

The Cima volcanic site shown in Figure 6-20 is located east of Los Angeles and is shown in track plots in Figure 6-6. The scattering modulations respond primarily to topography and differences in small scale (centimeter-to-meter) roughness as there is little vegetation here.

The Supersite in Figure 6-21 is primarily agricultural fields, and the primary modulation of radar echoes comes from field-to-field differences in vegetation. The Traverse City site in Figure 6-22 is a mixture of agricultural fields, forests, and lakes. In almost all of the sites with lakes, the smooth surface provides little if any echo power, and the lakes appear as the dark areas in the images. The Winchester site in Figure 6-23 is heavily forested. The slopes of mountain sides provide the primary modulation of the radar image.

The Cima volcanic site is shown in the example of the optical survey image of Figure 4-4, in the optical survey mosaic of Figure 6-20, and in an example of a digital image of Figure 6-24. A comparison of these three examples of aircraft SAR data will give users a sense of the scale of these image products. The semicircular feature in the center of these three images is 3 km x 5 km.

Table 6-4. Summary of Optical Survey Mosaics

Figure	Target	Date	Investigator
6-20	Cima Volcanics, CA	850627	Tom Farr (JPL)
6-21	Supersite, IL	841008	Dobson (U. of MI)
6-22	Traverse City, MI	850617	Dobson (U. of MI)
6-23	Winchester, VA	840916	Masuoka (GSFC)

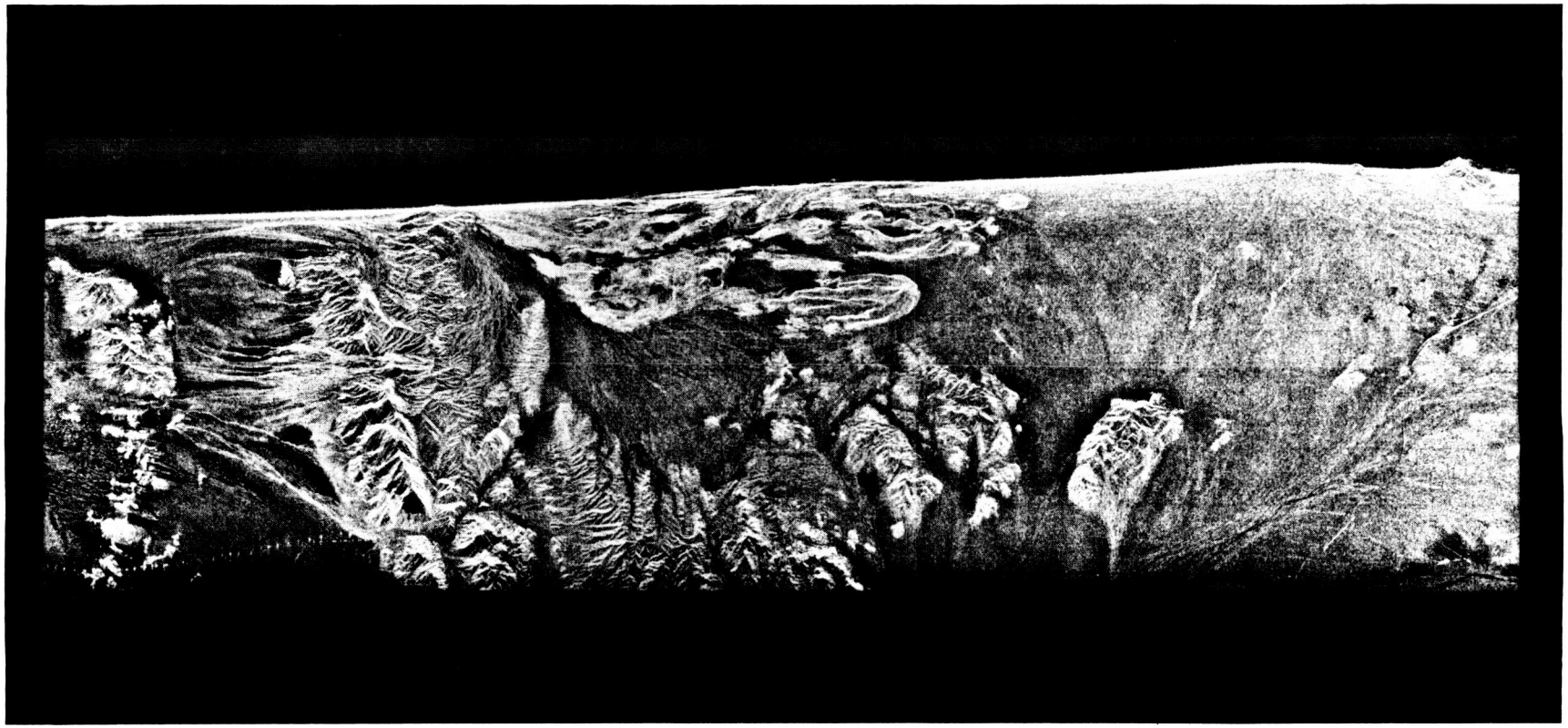

Figure 6-20. Optical Survey Mosaic for Cima Volcanic Site in the Mojave Desert in Southern California. (See track plot, Figure 6-6.) Here echo modulation is controlled primarily by differences in surface roughness as this desert area has little vegetation.

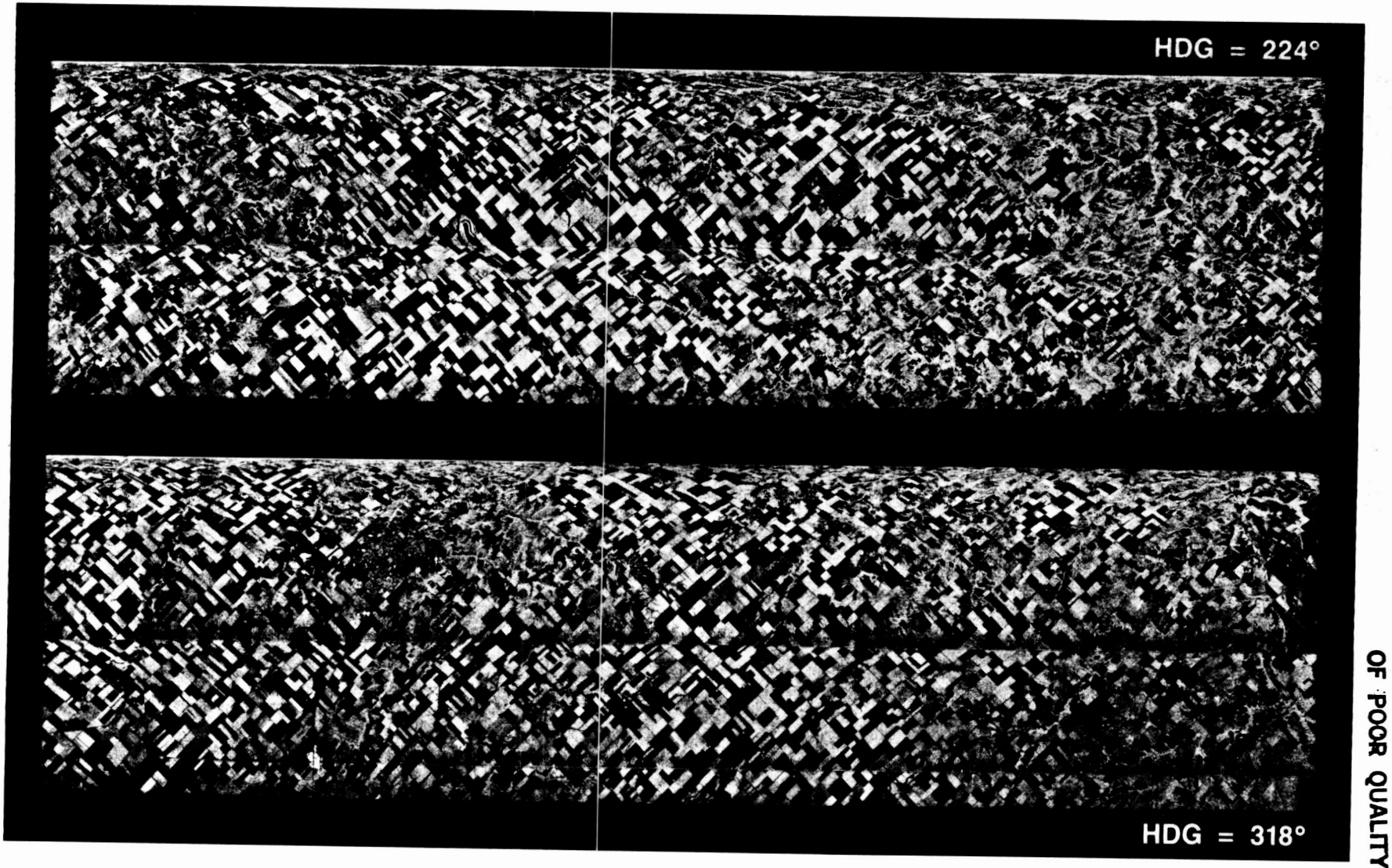

Figure 6-21. Optical Survey Mosaic of the Supersite Located in South Central Illinois Where the Ascending and Descending Passes of the SIR-B Overlap. (See track plot, Figure 6-11.) This site is primarily agricultural fields and was observed on 841008 with six tracks, three each with ground tracks of 224 deg and 318 deg. Echo modulation depends in large part upon state of cultivation.

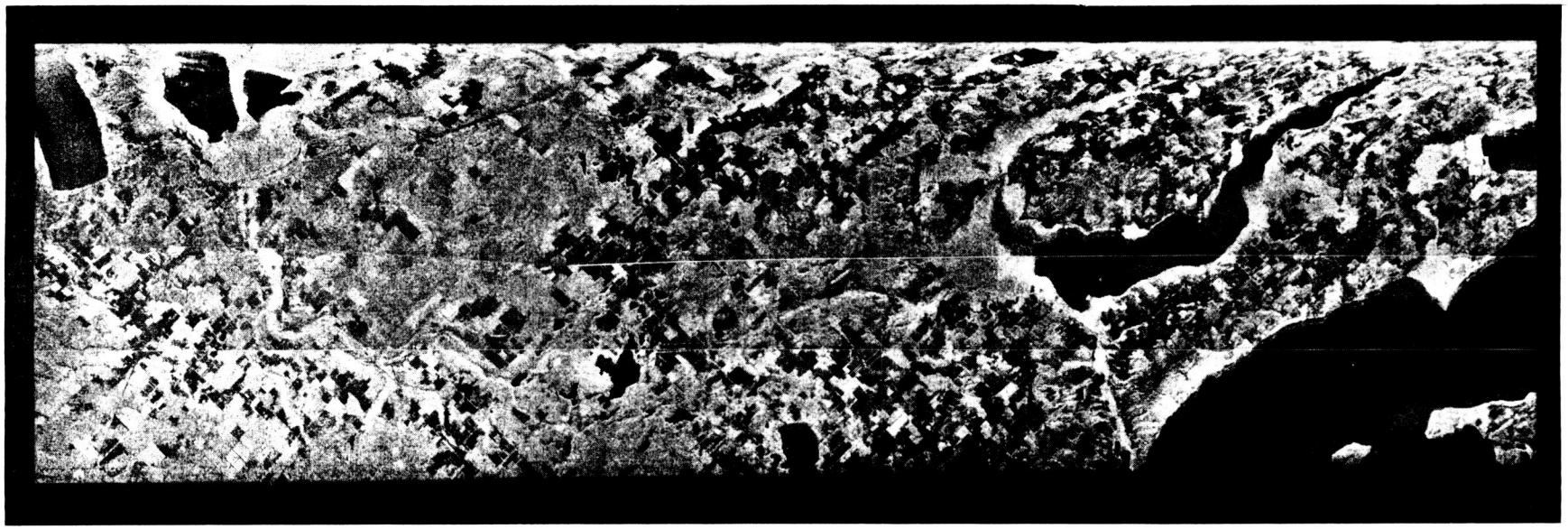

Figure 6-22. Optical Survey Mosaic of the Traverse City, Michigan Site on the Eastern Shore of Lake Michigan East of Green Bay Wisconsin. (See track plot, Figure 6-12.) This is a mixture of agricultural fields, forests, and lakes. The darkest areas are smooth lakes, which act as mirrors and reflect little, if any, energy back toward the aircraft.

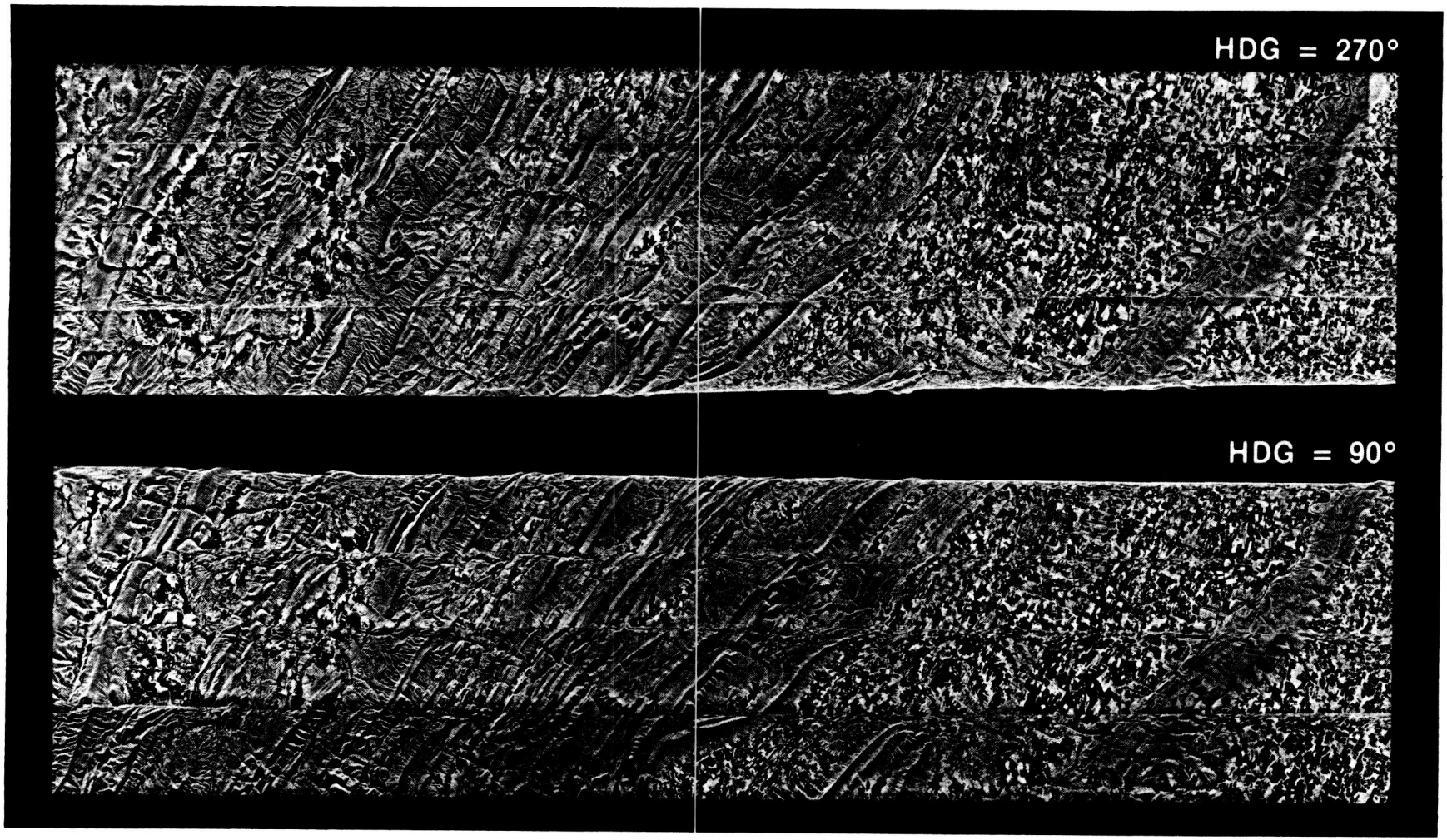

Figure 6-23. Optical Survey Mosaic for the Winchester, Virginia Site Located West of Washington, DC. (See track plots, Figure 6-14.) The site is in the Appalachian Mountains; it was flown on 840916 with eight tracks, four headings each of due east (90 deg) and due west (270 deg). Echo modulation is controlled in large part by the slopes of the mountain sides.

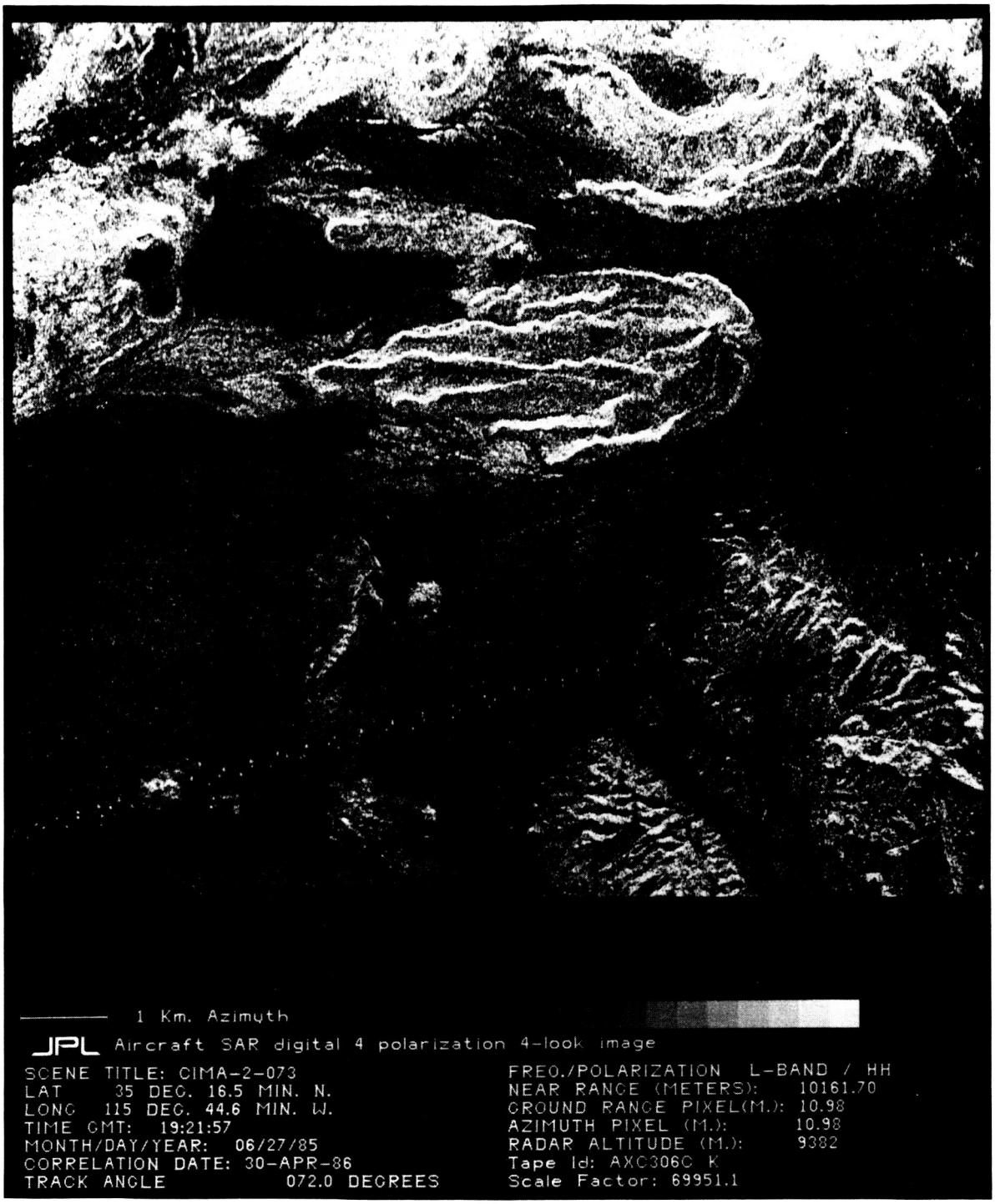

Figure 6-24. Digital HH Image of the Cima Volcanics Located in the Mojave Desert East of Los Angeles. There is little vegetation, so backscatter is controlled by slope and surface roughness. The bright area in the scene center is a young volcanic flow rougher than the adjacent sandy desert floor. Figure 6-20 shows the optical mosaic of this site. This scene is in the middle of the Figure 4-4 optical survey image.

C. DIGITAL DATA EXAMPLES

Some sense of the radar scattering from natural targets as they appear in digital images is given in Figures 6-24 through 6-27. These figures show the digital radar images in HH polarization for areas which are 11 km across. There are 1024 azimuth pixels with a pixel spacing of 10.98 m, and they are geometrically rectified. There are as many as 1024 range pixels with a spacing of 10.98 m. These digital images to first order are nearly 10 km by 10 km with resolutions and pixel spacings of 10 m. Several of these digital scenes are located in the optical survey mosaic described above.

The Cima site (Figure 6-24) is located in the Mojave desert east of Los Angeles. Here there is little vegetation, and radar backscatter is controlled by surface slope and/or roughness at centimeter-to-meter scales. The bright area in the center of the scene is a young, rough lava flow. The optical mosaic for this site is given in Figure 6-20; the track plot is given in Figure 6-5.

The Supersite image in Figure 6-25 is an agricultural area located in southern Illinois. This area was observed within a few hours of SIR-B data acquisition of the same area. The large rectangular bright and dark areas in this scene are fields in different stages of cultivation. The radar dark fields are likely fallow and have little backscatter; they appear like mirrors which reflect the radar pulses away from the radar. The radar bright fields have standing crops which scatter radar energy back toward the aircraft and the radar receivers. Several stream patterns are also visible in this scene. Here trees along the stream banks have strong echoes and outline the dendritic stream beds. The quasi-rectangular pattern in the upper right hand corner of this scene is the small town of Macomb, Illinois. The optical mosaic for this site is given in Figure 6-21; the track plot is given in Figure 6-11.

The Jacks Forest scene in Figure 6-26 is a mixed forestry site located west of Jacksonville, Florida. This area, like the Supersite site, was also observed with the SIR-B radar. Here the forested areas have stronger echoes than the nonforested areas. The dark stripe running top to bottom is a cleared area for an interstate highway; this radar smooth area has little backscatter. The track plot for this site is given in Figure 6-15.

The NOSC Tower image in Figure 6-27 shows an ocean area just west of San Diego, California. An ocean swell pattern is visible via differences in the number of small ocean waves between the peak and trough of the larger ocean waves. Here the backscatter is controlled by the Bragg conditions where the ocean wave must have wavelengths that match the radar wavelength [i.e., ocean wavelength = radar wavelength/2 • sin(angle of incidence)].

An example of digital imagery for an urban area is given in the frontispiece, which shows the false-color three-polarization composite and phase difference images of San Francisco. City buildings often create double-bounce corner-reflector geometries which have strong polarized backscatter.

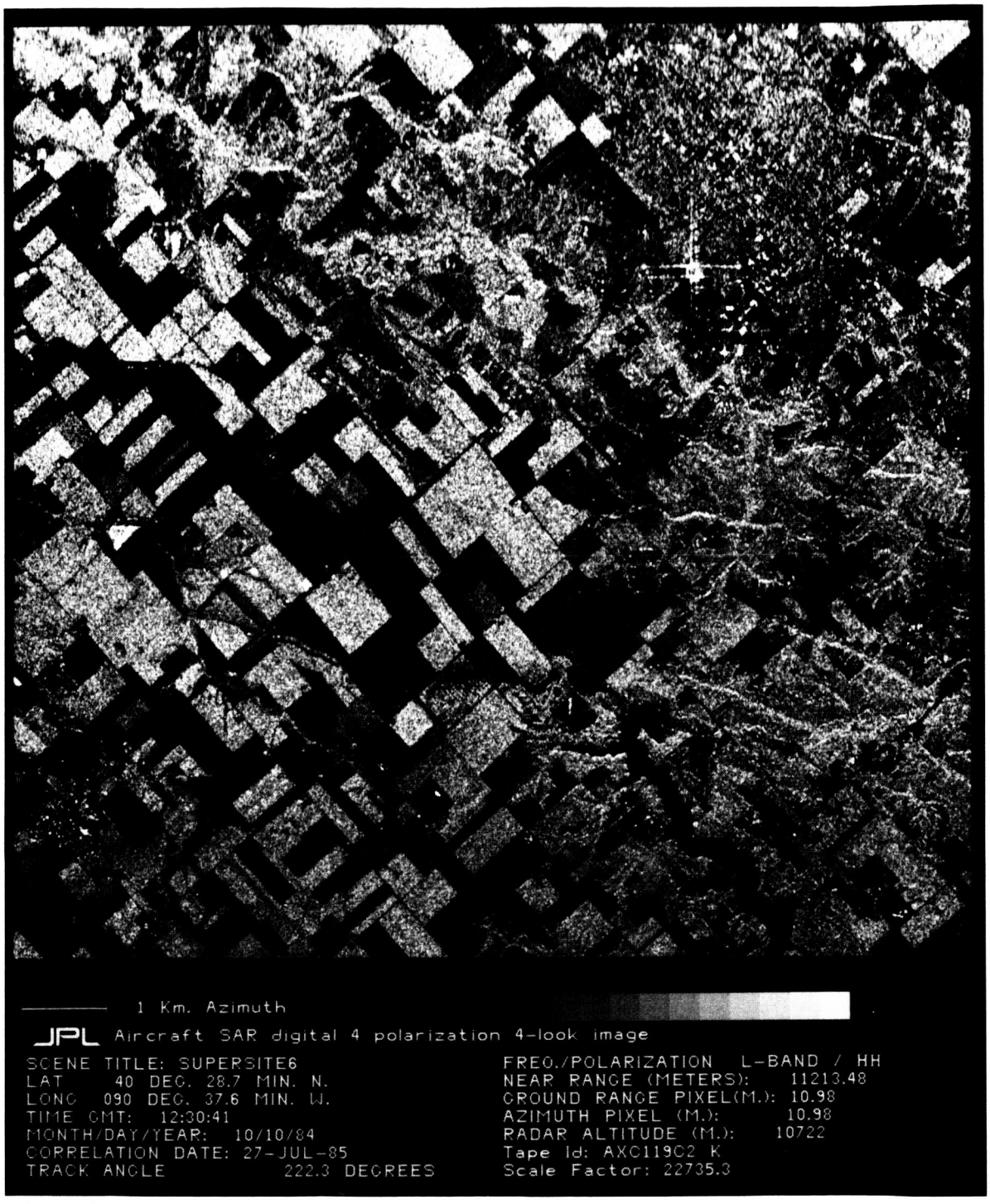

Figure 6-25. Digital HH Image of the Supersite, Illinois Observed Within a Few Hours of SIR-B Data Acquisition. The radar backscatter is controlled by the amount of cultivation of the fields. Also, dendritic patterns associated with streams are outlined by the trees that line the stream beds. The quasi-rectangular pattern in the upper right corner is the town of Macomb, Illinois. Figure 6-21 gives the optical mosaic for this site.

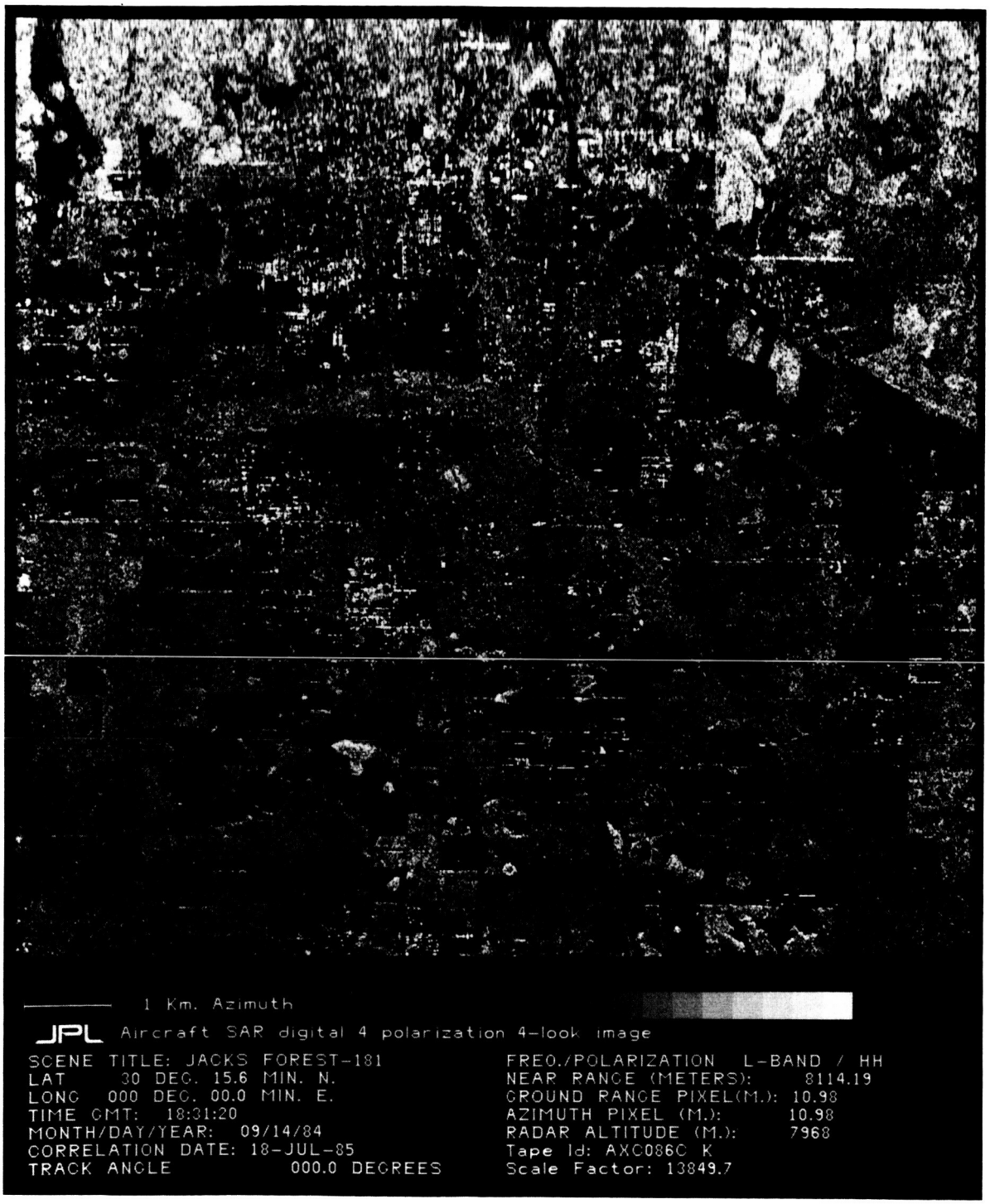

Figure 6-26. Digital HH Image of the Jacks Forest Site, Just West of Jacksonville, Florida. The bright areas are forested, and the dark stripe running top to bottom is an interstate highway where the pavement and shoulders reflect most radar energy away from the receivers on board the aircraft.

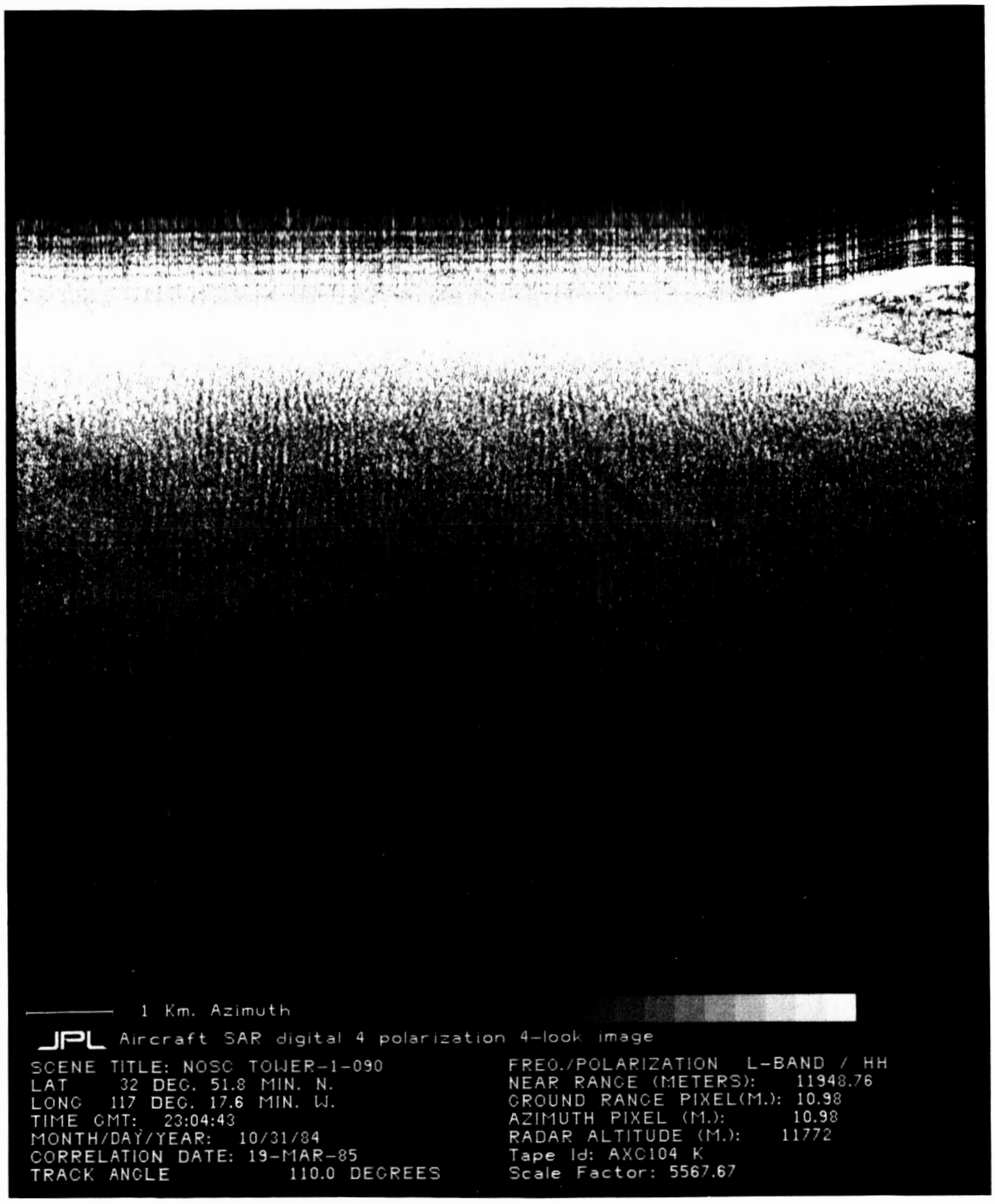

Figure 6-27. Digital HH Image of the NOSC Tower Area Located in the Ocean West of San Diego. An ocean swell pattern is visible from radar echo modulation from differences in the number of small ocean waves between the peak and trough of the larger ocean waves associated with the swell. Backscatter from the ocean is controlled by those small ocean waves that satisfy the Bragg condition.

SECTION VII

SUMMARY

This report has described how JPL acquired aircraft digital radar data during four expeditions in 1983 through 1985. We have described data acquisition as it was performed until the NASA/JPL Aircraft SAR was destroyed by fire on the night of 17 July 1985. These past operations will serve as a model for future work when the radar is rebuilt and airborne again.

This report has also provided an overview to when and where data were acquired in the Fall-84 and Summer-85 Expeditions when the highest quality data were obtained. This was done with the track plots, optical survey mosaics, and examples of digital imagery shown in Section VI. Appendixes A and B provide listings for digital data acquisitions since the first flight of the Summer-83 Expedition in August 1983 through the last data flight of the Summer-85 Expedition in July 1985. Appendix C lists all of the digital image data currently archived at JPL in the Reference Notebook system. Appendix D gives the addresses for various users who have obtained aircraft SAR data. These data, which are being archived in the JPL Radar Data Center, are excellent source material for multiple-polarization studies and provide background information for the SIR Program. Queries regarding the data can be addressed to either of the following:

Aircraft Radar Coordinator

T.W. Thompson
Mail Stop 183-701
NASA/Jet Propulsion Laboratory
4800 Oak Grove Drive
Pasadena, CA 91109
(818) 354-3792 Commercial
792-3792 FTS

Radar Data Center Manager

D. Harrison
Mail Stop 183-701
NASA/Jet Propulsion Laboratory
4800 Oak Grove Drive
Pasadena, CA 91109
(818) 354-2386 Commercial
792-2396 FTS

REFERENCES

1. Brown, W. E., Jr., "Radar Studies of the Earth," Proc. of the IEEE, Vol. 57, No. 4 , April, 1969, pp. 612-620.

2. Donovan, N., Evans, D., and Held, D., NASA/JPL Aircraft SAR Workshop Proceedings Feb. 4-5, 1985, Pasadena, CA, JPL Publication 85-39, Jet Propulsion Laboratory, Pasadena, California, June 15, 1985.

3. Evans, D. L., Farr, T. G., Ford, J. P., Thompson, T. W., and Werner, C. L., "Multipolarization Radar Images for Geologic Mapping and Vegetation Discrimination," IEEE Trans. on Geoscience and Remote Sensing, Vol. GE-24, No. 2, March 1986, pp. 246-257.

4. Thompson, T. W., A User's Manual for the NASA/JPL Synthetic Aperture Radar and the NASA/JPL L- and C-Band Scatterometers, JPL Publication 83-38, Jet Propulsion Laboratory, Pasadena, California, June 1, 1983.

BIBLIOGRAPHY

Brown, W.E., Jr., Elachi, C., and Thompson, T.W., "Radar Imaging of Ocean Surface Patterns," J. Geophys. Res., Vol. 81, No. 15, May 20, 1976, pp. 2657-2667.

Thompson, T. W., Weissman, D. E., and Gonzalez, F. I., "L-Band Radar Backscatter Dependence upon Surface Wind Stress: A Summary of New Seasat-1 and Aircraft Observations," J. Geophys. Res., Vol. 88, No. C3, Feb. 28, 1983, pp. 1727-1735.

Thompson, T. W., The Radar Operations: Marineland/GASP Test Series 25 November to 16 December 1975, JPL Internal Document 622-13, Jet Propulsion Laboratory, Pasadena, California, April 1, 1976.

Thompson, T. W., McMillan, E. S., and King, D. B., Jr., JPL Radar Operations Summer '76 Hurricane Expedition for the period 17 August to 3 October 1976, JPL Internal Document 622-18, Jet Propulsion Laboratory, Pasadena, California, Dec. 10, 1976.

Weissman, D. E., King, D. B., and Thompson, T. W., "Relationship Between Hurricane Surface Winds and L-Band Radar Backscatter from the Sea Surface", J. Applied Meteorology, Vol. 18, No. 8, Aug., 1979, pp. 1023-1034.

Zebker, H. A. and Goldstein, R. M., "Topographic Mapping from Interferometric Synthetic Aperture Radar Observations", J. Geophys. Res., Vol. 91, No. B5, April 10, 1986, pp. 4993-4999.

APPENDIX A

FLIGHT SUMMARIES

Table A-1. Flight Summary for Summer-83 Expedition

Sensor Checkout

830811 - Moffett-to-Moffett: Sensor Checkout
830812 - Moffett-to-Moffett: Sensor Checkout
830824 - Moffett-to-Moffett: Sensor Checkout
830830 - Moffett-to-Moffett: Sensor Checkout

Western U.S.

830826 - Moffett-to-Moffett: Southern Calif. Calibration
830828 - Moffett-to-Moffett: Southern Calif. Geology
830901 - Moffett-to-Moffett: Rockies Geology
830914 - Moffett-to-Moffett: Southern Calif. Abort
830916 - Moffett-to-Moffett: Southern Calif. Calibration

Eastern U. S. Deployment

830906 - Moffett-to-New Orleans: Transit Anadarko Basin, OK
830907 - New Orleans-to-New Orleans: Alabama and Mississippi
830908 - New Orleans-to-New Orleans: Alabama and Kentucky

Number of Data Flights = 12

Table A-2. Flight Summary for Winter-84 Expedition

Sensor Checkout	
840217 - Moffett-to-Moffett:	Sensor Checkout
Eastern U. S. Deployment	
840328 - Moffett-to-Houston:	Transit (East Texas)
840229 - Houston-to-Houston:	North Texas
840301 - Houston-to-Langley:	Transit (Savannah River Plant Swamp (GA and SC) and Cedar Island (NC))
840303 - Langley-to-Langley:	Virginia and Maryland
Western U.S.	
840306 - Moffett-to-Moffett:	SIR-B Calibration
Alaskan Deployment	
840309 - Moffett-to-Anchorage:	Gulf of Alaska
840311 - Anchorage-to-Anchorage:	Gulf of Alaska
840313 - Anchorage-to-Anchorage:	Gulf of Alaska
840314 - Anchorage-to-Anchorage:	Gulf of Alaska
840315 - Anchorage-to-Anchorage:	Gulf of Alaska

Number of Data Flights = 11

Table A-3. Flight Summary for Fall-84 (SIR-B Underflight) Expedition

Sensor Checkout

840816 - Moffett-to-Moffett: Sensor Checkout
840831 - Moffett-to-Moffett: Sensor Checkout
840906 - Moffett-to-Moffett: Sensor Checkout

Eastern U.S. Deployment

840910 - Moffett-to-Houston: SIR-B, Meteor Crater and Tucson, AZ
840911 - Houston-to-Houston: NASA-NSTL, MS
840913 - Houston-to-McQuire: SIR-B, Jacksonville Forest, FL
840916 - McQuire-to-McQuire: Winchester, VA and Blackwater River, MD
840920 - McQuire-to-Duluth: SIR-B, Connecticut and Upstate New York
840921 - Duluth-to-Moffett: Ely Pines, MN

Premission SIR-B

840926 - Moffett-to-Moffett: Northern California SIR-B
840928 - Moffett-to-Moffett: California-Nevada SIR-B

Mission Support for SIR-B (7)

841006 - Moffett-to-Moffett: Northern California Bistatic
841008 - Moffett-to-Topeka: Bistatic and Supersite, IL
841009 - Topeka-to-Topeka: Bistatic and Supersite, IL
841010 - Topeka-to-Topeka: Bistatic and Supersite, IL
841011 - Topeka-to-Topeka: Bistatic and Supersite, IL
841012 - Topeka-to-Topeka: Bistatic and Supersite, IL
841013 - Topeka-to-Moffett: Wind River, WY

Postmission SIR-B and RTOP

841017 - Moffett-to-Moffett: NOSC Tower and Raisin City, CA
841018 - Moffett-to-Moffett: Wind and Sanke Rivers, WY and ID
841019 - Moffett-to-Moffett: Raisin City, CA
841024 - Moffett-to-Moffett: Northern California
841025 - Moffett-to-Moffett: Southern California
841031 - Moffett-to-Moffett: NOSC Tower, CA
841104 - Moffett-to-Moffett: NOSC Tower and Los Angeles, CA
841106 - Moffett-to-Moffett: Southern California
841107 - Moffett-to-Moffett: NOSC Tower and Monterey Bay, CA

Number of Data Flights = 27

Table A-4. Flight Summary for Spring- and Summer-85 Expeditions

	Spring - 85 Sensor Checkout	
850308	Moffett-to-Moffett:	Sensor Checkout
850314	Moffett-to-Moffett:	Sensor Checkout
850323	Moffett-to-Moffett:	Artificial Comet Piggyback
	Spring - 85 Western U. S. Data	
850319	Moffett-to-Moffett:	First NOSC Tower Flight, CA
850327	Moffett-to-Moffett:	Second NOSC Tower Flight, CA
850424	Moffett-to-Moffett:	California Geobotany
	Spring - 85 Costa Rica Deployment	
850329	Moffett-to-Houston:	Transit, California and Arizona
850331	San Jose-to-San Jose:	Costa Rica: East-West Survey
850401	San Jose-to-San Jose:	Costa Rica Study Areas
	Summer - 85 Sensor Checkout	
850521	Moffett-to-Moffett:	Sensor Checkout
850610	Moffett-to-Moffett:	Sensor Checkout
	Summer - 85 First Eastern U. S. Deployment	
850612	Moffett-to-Omaha:	Transit, Konza, KS
850014	Omaha-to-New Jersey:	Transit, Konza, KS and Ann Arbor, MI
850616	New Jersey-to-New Jersey:	Wetlands and Forests, Maryland, New York and Vermont
850617	New Jersey-to-Omaha:	Transit, Traverse City, MI and Konza, KS
850618	Omaha-to-Moffett:	Transit, Konza, KS
	Summer - 85 Western U. S. Data	
850621	Moffett-to-Moffett:	Wind, WY and Snake, ID Rivers Geology
850627	Moffett-to-Moffett:	California - Nevada Geology
	Summer - 85 Second Eastern U. S. Deployment	
850710	Duluth-to-New Jersey:	Transit, Ely, MN and Traverse City, MI
850713	New Jersey-to-New Jersey:	Wetlands and Forests, Maryland and New England
850714	New Jersey-to-Moffett:	Transit, Raisin City, CA

Number of Data Flights = 9 (Spring-85)
12 (Summer-85)
21 (Spring and Summer-85)

APPENDIX B

DIGITAL DATA ACQUISITIONS

Table B-1. Digital Data for Summer-83 Expedition

HDDT No.(s)	Site Location	User(s)
	830811 Moffett-to-Moffett - Sensor Checkout 1	
8301-8303	Death Valley (8), CA	Brown, Schaber
	Pisgah, Amboy, CA	Brown
	San Joaquin Valley, CA	Brown
	830812 Moffett-to-Moffett - Sensor Checkout 2	
8304-8306	Death Valley (9), CA	Brown, Schaber
	Pisgah, Amboy, CA	Kobrick
	Means Valley (2), CA	Farr, Blom
	San Joaquin Valley, CA	Brown
	830824 Moffett-to-Moffett - Sensor Checkout 2	
8307-8307	Death Valley (8), CA	Brown, Thompson, Held
	830826 Moffett-to-Moffett - S. California Calibration	
8309-8312	Pisgah (7), CA	Held, Brown,
	Death Valley (3), CA	Kobrick
	Means Valley (2), CA	Kobrick
	Los Angeles, CA	Bryan
	Rose Bowl, CA	Roth
	830829 Moffett-to-Moffett - S. California Geology	
8313-8315	Owens Valley, CA	Farr
	Death Valley (3), CA	Evans
	Pisgah (4), CA	Blom
	Means Valley (2), CA	Kobrick
	830830 Moffett-to-Moffett - Sensor Checkout 4	
8316-8317	Death Valley (6), CA	Brown, Held,
	San Francisco Bay (2), CA	Thompson

( ) = number of data runs

Table B-1 (continued)

HDDT No.(s)	Site Location	User(s)
	830901 Moffett-to-Moffett - Rockies Geology	
8319-8322	Wind River (4), WY	Evans
	Patrick Draw (4), CO	Evans
	Capitol Reefs (2), UT	Farr
	Paradox Basin, NV	Farr
	830906 Moffett-to-New Orleans - Transit	
8322-8324	Anadarko Basin (3), OK	Dixon, Stern
	830907 New Orleans-to-New Orleans 1 - Alabama/Mississippi	
	No digital data on this flight	
	830908 New Orleans-to-New Orleans 2 - Kentucky/Alabama	
8325-8327	Hazard, KY (3),	Ford
	Mobile, AL (2)	Wu, Paris
	830914 Moffett-to-Moffett - S. Califfornia Abort	
8328	Pisgah (2), CA	Held, Werner
	830916 Moffett-to-Moffett - California Calib./Geology	
8329-8334	Pisgah (7), CA	Held, Werner
	Coso Hills (2), CA	Dixon
	Coastal Range (3), CA	Dixon
	San Francisco Bay (4), CA	Goldstein
	Napa Valley, CA	Dixon

( ) = number of data runs
Total number HDDTs = 32
Total digital along-track coverage = 6400 km
Number sites = 31
Number of users = 17

Table B-2. Digital Data for Winter-84 Expedition

HDDT No.(s)	Site Location	User(s)
	840217 Moffett-to Moffett: Sensor Checkout	
8402-8406	Death Valley (9), CA	Kobrick/Brown
	San Joaquin Valley, CA	Brown
	San Francisco (2), CA	Brown
	840328 Moffett-to-Houston: East Texas	
8408-8409	East Texas (7)	Demel
	840229 Houston-to-Houston: North Texas Soil Moisture	
8410-8414	North Texas (9)	Schmugge
	840301 Houston-to-Langley-Transit	
8414-8419	SRP Swamp (10), GA and SC	Ford
	Cedar Island (6), NC	Ormsby/Blanchard
	840303 Langley-to-Langley: Virginia and Blackwater	
8419-8425	G. Washington Forest (4), VA	Masuoka
	Winchester (5), VA	Masuoka
	Blackwater River (6), MD	Ormsby/Blanchard
	840306 Moffett-to-Moffett: SIR-B Calibration	
8425-8430	Death Valley (3), CA	Held/Werner
	Pisgah (3), CA	Held/Werner
	Raisin City (5), CA	Paris
	San Francisco (2), CA	Held

( ) = number of data runs
Total Number HDDTs = 28
Total Along-Track Coverage = 5600 km
Number of sites = 14
Number of users = 11

Table B-3. Digital Data Fall-84 (SIR-B Underflight) Expedition

HDDT No.(s)	Site Location	User(s)
	840816 Moffett-to-Moffett: Sensor Checkout	
8450-8455	Mono Lake (1), CA	Brown
	Death Valley (5), CA	Brown
	Bistatic Tests (1), CA	Goldstein
	Cinder Cones (2), CA	Blom
	San Francisco Bay, CA	Bicknell
	840831 Moffett-to-Moffett: Sensor Checkout	
8460-8463	Owens Valley (1), CA	Farr
	Death Valley (1), CA	Held
	Raisin-Fresno (1), CA	Paris
	San Joaquin Valley (2), CA	Brown
	Bistatic Tests (2)	Goldstein
	Cinder Cones (4), CA	Blom
	Golden Gate (4), CA	Goldstein
	840910 Moffett-to-Houston: Transit	
8476-8478	Meteor Crater (4), AZ	Mouginis-Mark
	Tucson SIR-B, AZ	Farr
	Imaging Tests (2)	Brown
	840911 Houston-to-Houston: NSTL	
8479-8481	NASA-NSTL (8), MS	Wu
	840914 Houston-to-McQuire: Transit	
8484-8485	Jacksonville, SIR-B (6), FL	Hoffer
	840916 McQuire-to-McQuire: Winchester and Blackwater	
8486-8491	Winchester (8), VA	Mosuoka
	Blackwater River (8), MD	Ormsby
	840921 McQuire-to-Duluth: SIR-B New England	
8494-8497	Connecticut SIR-B (2)	Paris
	Upstate New York SIR-B (5)	Paris

( ) = number of data runs

Table B-3 (continued)

HDDT No.(s)	Site Location	User(s)
	840922 Duluth-to-Moffett: Ely Pines	
8497-8498	Ely (3), MN	Pitts
	840926 Moffett-to-Moffett: Northern California SIR-B	
8499-84103	Shasta SIR-B (6), CA	Simonett
	Medicine Lake SIR-B (6), CA	Kaupp/Farr
	Northern Calif. SIR-B (2), CA	Farr
	Golden Gate (2), CA	Goldstein
	840928 Moffett-to-Moffett: California-Nevada SIR-B	
84103-84110	Imaging Test (1)	Brown
	Owen's Valley (1), CA	Farr/Gillespie
	Death Valley (2), CA	Farr/Gillespie
	Amargosa SIR-B (1), NV	Taranik
	Goldfield SIR-B (3), NV	Parr
	Soda Springs SIR-B (2), NV	Taranik
	Candeleria SIR-B (2), NV	Taranik
	Raisin-Fresno SIR-B (2), CA	Paris
	841006 Moffett-to-Moffett: Bistatic	
84111	Bistatic, Lava Flows (2), CA	Goldstein
	841008 Moffett-to-Topeka: Transit and SIR-B Supersite	
84112-84114	Bistatic, Evansville (2), IL	Goldstein
	SIR-B Supersite (6), IL	Dobson
	841009 Topeka-to-Topeka: SIR-B Supersite	
84115-84116	Bistatic, Evansville (2), IL	Goldstein
	SIR-B Supersite (6), IL	Dobson

( ) = number of data runs

Table B-3 (continued)

HDDT No.(s)	Site Location	User(s)
	841010 Topeka-to-Topeka: SIR-B Supersite	
84117-84119	Bistatic, St. Louis (2), MO	Goldstein
	SIR-B Supersite (6), IL	Dobson
	Imaging Test (1)	Brown
	841011 Topeka-to-Topeka: SIR-B Supersite	
84120-84121	Supersite (6), IL	Dobson
	841012 Topeka-to-Topeka: SIR-B Supersite	
84122-84124	Bistatic-Sioux City (2), IA	Goldstein
	SIR-B Supersite (6)	Dobson
	841013 Topeka-to-Moffett: Transit and Wind River	
84125	Wind River (5), WY	Evans
	841017 Moffett-to-Moffett: First NOSC Tower Flight	
82126-84129	Los Angeles, (1), CA	Brown
	NOSC Tower (14), CA	Shemdin
	Raisin City SIR-B (4), CA	Held
	841018 Moffett-to-Moffett: Wind and Snake River	
84130-84132	Imaging Test (1)	Brown
	Wind River (4), WY	Evans
	Snake River SIR-B (4), ID	Farr
	841019 Moffett-to-Moffett: Raisin City SIR-B	
84133-84134	Raisin City (4), CA	Held/Wang
	Raisin - Fresno SIR-B (2), CA	Paris/Schmugge

( ) = number of data runs

Table B-3 (continued)

HDDT No.(s)	Site Location	User(s)
	841024 Moffett-to-Moffett: Northern California SIR-B	
84135-84140	Glass Mountain SIR-B (6), CA	Simonett
	Bistatic Lava SIR-B (1), CA	Goldstein
	Newberry Crater (1), OR	Farr
	Shasta SIR-B (6), CA	Simonett
	Cinder Cones (3), CA	Blom
	841025 Moffett-to-Moffett: Southern California	
841419-84145	Imaging Test (1)	Brown
	Goldstone (2), CA	Evans
	Cima (2), CA	Farr
	Kelso Dunes (4), CA	Blom
	Pisgah (6), CA	Evans
	Means Valley, CA	Evans
	841031 Moffett-to-Moffett: Second NOSC Flight	
84146-84148	Catalina (1), CA	Brown
	NOSC Tower (14), CA	Shemdin
	841104 Moffett-to-Moffett: Third NOSC Flight	
84149-84151	Palmdale (1), CA	Brown
	NOSC Tower (9), CA	Shemdin
	Los Angeles (3), CA	Bryan
	841106 Moffett-to-Moffett: Southern California	
84152-84152	Imaging Test (1)	Brown
	Goldstone (3), CA	Held/Evans
	Cima (1), CA	Farr
	Kelso (2), CA	Blom
	Monterey Bay, CA	Zebker

( ) = number of data runs

Table B-3 (continued)

HDDT No.(s)	Site Location	User(s)
	841107 Moffett-to-Moffett: Fourth (Last) NOSC Tower	
84154-84157	Palmdale (1), CA	Brown
	NOSC Tower (14), CA	Shemdin
	Los Angeles (1), CA	Brown
	Monterey Bay (2), CA	Zebker

( ) = number of data runs
Total number of HDDT's = 89
Total along-track digital coverage = 17,800 km
Number of sites = 79
Number of users = 23

Table B-4. Digital Data for Spring-85 Expedition

HDDT No.(s)	Site Location	User(s)
	850308 Moffett-to-Moffett: Sensor Checkout 1	
8505-8508	Mina (1), NV	Thompson
	Death Valley (5), CA	Thompson
	Silver Lake (1), CA	Farr
	NOSC Tower (6), CA	Brown
	Wing-Wing Interferometer (1)	Zebker
	850314 Moffett-to-Moffett: Sensor Checkout 2	
8510-8513	Winnemucca (5), NV	Thompson
	San Andreas Interferometer (4), CA	Zebker
	In Transit Imaging (2)	Thompson
	850319 Moffett-to-Moffett: First NOSC Tower	
8514-8517	In Transit Imaging (2)	Thompson
	NOSC Tower (17), CA	Brown
	Raisin City (1), CA	Paris
	850323 Moffett-to-Moffett: Artificial Comet Piggyback	
8519	In Transit Imaging (2)	Thompson
	Fore-Aft Interferometer (1)	Zebker
	850327 Moffett-to-Moffett: Second NOSC Tower	
8520-8524	NOSC Tower (15), CA	Brown
	Pisgah Calibration (2), CA	Thompson
	Raisin City (1), CA	Paris
	850329 Moffett-to-Houston: Transit	
8525	Vidal Junction (1), CA-AZ	Farr
	Tucson (1), AZ	Farr
	Marker Test (1)	Thompson

( ) = number of data runs

Table B-4 (continued)

HDDT No.(s)	Site Location	User(s)
	850331 San Jose-to-San Jose: Costa Rica E-W-Survey	
8526-8531	Costa-Rica E-W Survey	Joyce
	850401 San Jose-to-San Jose: Costa Rica Study Areas	
8532-8537	Costa Rica Study Area-A (8)	Joyce
	Costa Rica Study Area-B (6)	Joyce
	Costa Rica Topography (6)	Joyce
	850424 Moffett-to-Moffett: California Geobotany	
8538-8545	Raisin City (1), CA	Paris
	Owens Valley (6), CA	Rock
	Lake Tahoe Topo (1), NV	Zebker
	Mount Shasta Topo (2), CA	Zebker
	Mount Shasta Stereo (6), CA	Kobrick
	San Francisco Topo (1), CA	Zebker

( ) = number of data runs
Number of HDDTs = 39
Along-track digital coverage = 7,800 km
Number of sites = 29
Number of users = 8

Table B-5. Digital Data for Summer-85 Expedition

HDDT No.(s)	Site Location	User(s)
	850521 Moffett-to-Moffett: Sensor Checkout 1	
8546-8548	San Joaquin Valley (2)	Brown
	Goldstone (2), CA	Brown
	San Francisco (1), CA	Brown
	850610 Moffett-to-Moffett: Sensor Checkout 2	
8551-8553	San Joaquin Valley (10), CA	Brown
	850612 Moffett-to-Omaha Transit: Kansas 1	
8554-8555	Konza Grasslands (6), KS	Schmugge
	850614 Omaha-to-New Jersey Transit: Kansas 2	
8555-8558	Konza Grasslands (4), KS	Schmugge
	Ann Arbor (8), MI	Dobson
	Enroute Imaging (2)	Thompson
	850616 New Jersey-to-New Jersey: Eastern U.S.	
8558-8563	Blackwater River (14), MD	Ormsby
	Vermont (6)	Paris
	Enroute Imaging (2)	Thompson
	850617 New Jersey-to-Omaha Transit: Kansas 3	
8564-8566	Traverse City (7), MI	Dobson/Ulaby
	Konza Grasslands (4), KS	Schmugge
	Enroute Imaging (2)	Thompson
	850618 Omaha-to-Moffett Transit: Kansas 4	
8567-8568	Konza Grasslands (7), KS	Schmugge
	Test Calibration (1)	Miller

( ) = number of data runs

Table B-5 (continued)

HDDT No.(s)	Site Location	User(s)
	850621 Moffett-to-Moffett: Wind and Snake Rivers	
8569-8572	Wind River (5), WY	Evans
	Snake River (7), ID	Farr
	Enroute Imaging (3)	Brown
	850627 Moffett-to-Moffett: California Geobotany	
8573-8578	Owens Valley (6), CA	Rock
	Rhodes (2), NV	Taranik
	Death Valley (1), CA	Farr
	Cima Volcanics (2), CA	Farr
	Vidal Junction (2), AZ-CA	Farr
	Pisgah Calib (2), CA	Held
	Raisin City (2), CA	Paris
	Sine Wave Test (1)	Miller
	850710 Duluth-to-New Jersey Transit: Eastern U.S.	
8579-8582	Ely Forests (5), MN	Pitts
	Ottawa National Forest (2), MI-MN	Hoffer
	Traverse City (3), MI	Dobson
	850713 New Jersey-to-New Jersey: Eastern U.S.	
8582-8587	Blackwater River (8), MD	Ormsby
	Upstate New York (2)	Paris
	Maine Forest (2)	Hoffer
	Fore-Aft Interferometer (2)	Goldstein
	Connecticut (1)	Paris
	850714 New Jersey-to-Moffett Transit: Raisin City	
8587-8588	Enroute Imaging (2)	Brown
	Raisin City (2), CA	Paris

( ) = number of data runs
Number of HDDT's = 45 (Summer), 84 (Spring and Summer)
Total Along-track coverage = 9,000 km (Summer),
16,800 (Spring and Summer)
Number of users = 16 (Summer), 24 (Spring and Summer)
Number of sites = 37 (Summer), 66 (Spring and Summer)

APPENDIX C

AIRCRAFT SAR DIGITAL IMAGE SUMMARY

All of the digital images produced at JPL are archived in the Reference Notebook System, which is described via a data base on the Section 324 VAX Computer. The following pages are listings from that data base. Table C-1 (p. C-2) is a listing by site title; Table C-2 (p. C-15) is a listing by correlation date. Users should be aware that the later correlations with the AXC serial numbers are likely of better quality than the earlier correlations with the AXK serial numbers.

Table C-1. SAR Imagery Sorted by Title

Book No.	Page No.	Correlation Date	CCT	Title
1				
	1	11/19/83	AXK901	HAZARD KY1 (HAZARD, KENTUCKY)
	2	11/28/83	AXK902	MEANS VAL SIR2 (MEANS VALLEY, CALIFORNIA)
	3	12/01/83	AXK903	ROSE BOWL (JPL, PASADENA, CALIFORNIA)
	4	12/06/83	AXK910	PISGAH CAL3 (PISGAH, CALIFORNIA)
	5	12/07/83	AXK911	PISGAH CAL3 (PISGAH, CALIFORNIA)
	6	12/11/83	AXK912	PISGAH CAL2 (PISGAH, CALIFORNIA)
	7	12/13/83	AXK913	PISGAH CAL4 (PISGAH, CALIFORNIA)
	8	12/14/83	AXK914	WIND RIVER2 (WIND RIVER, WYOMING)
	9	12/15/83	AXK915	PISGAH CAL6 (PISGAH, CALIFORNIA)
	10	12/16/83	AXK916	PISGAH CAL4 (PISGAH, CALIFORNIA)
	11	12/18/83	AXK917	PISGAH CAL5 (PISGAH, CALIFORNIA)
	12	12/20/83	AXK918	JAMAICA8 (JAMAICA, WEST INDIES)
	13	12/23/83	AXK919	SF BAY1 (SAN FRANCISCO BAY, CALIFORNIA)
	14	01/04/84	AXK920	ROSE BOWL (PASADENA, CALIFORNIA)
	15	01/06/84	AXK921	DTH VAL USGS5 (DEATH VALLEY, CALIFORNIA)
	16	01/07/84	AXK922	SF BAY2 (GOLDEN GATE BRIDGE, CALIFORNIA)
2				
	1	01/11/84	AXK923	COSO HILLS1 (RAISIN CITY AGRICULTURAL FIELDS, CALIFORNIA)
	2	01/12/84	AXK924	PISGAH CAL7 (PISGAH, CALIFORNIA)
	3	01/13/84	AXK925	WIND RIVER4 (SPRING CREEK, WYOMING)
	4	01/14/84	AXK926	SF BAY2 (SAN FRANCISCO, TOMALES, AKA BODEGA BAY, CALIFORNIA)
	5	01/18/84	AXK927	WIND RIVER4 (DEAD MAN BUTTE, WYOMING)
	6	01/19/84	AXK928	MOBILE/BLDWN1 (BALDWIN COUNTY, ALABAMA)
	7	01/20/84	AXK930	SF BAY1 (SAN FRANCISCO BAY, CALIFORNIA, PACIFIC OCEAN WAVES)
	8	01/20/84	AXK931	COSO HILLS90 (COSO HILLS, CALIFORNIA)
	9	01/21/84	AXK929	SF BAY1 (TOMALES BAY 2, CALIFORNIA)
	10	01/26/84	AXK932	SF BAY1 (SAN FRANCISCO BAY, CALIF., PACIFIC OCEAN WAVES 2)
	11	01/27/84	AXK933	DTH VAL USGS2 (DEATH VALLEY SAND DUNES, CALIFORNIA)
	12	01/31/84	AXK934	PISGAH CAL5 (PISGAH, CALIFORNIA)
	13	02/01/84	AXK935	PISGAH CAL5 (PISGAH, CALIFORNIA)
	14	02/14/84	AXK936	ANADARKO BASN4 (ANADARKO 1, OKLAHOMA)
	15	02/16/84	AXK937	ANADARKO BASN4 (ANADARKO 2, OKLAHOMA)
	16	02/17/84	AXK938	SF BAY2 (MOFFETT FIELD, CALIFORNIA)

Table C-1 (Continued)

Book No.	Page No.	Correlation Date	CCT	Title
	17	02/20/84		DTH VAL ENG161 (DEVIL'S GOLF COURSE, DEATH VALLEY, CA)
	18	02/21/84	AXK940	DTH VAL TOPO158 (DEATH VALLEY TOPO 3, PANAMINT RANGE, CA)
3				
	1	02/22/84	AXK941	DTH VAL TOPO157 (DEATH VALLEY TOPO 2, PANAMINT RANGE, CA)
	2	02/24/84	AXK942	OWENS VALLEY, CALIFORNIA
	3	02/28/84	AXK944	PISGAH CAL1 (PISGAH, CALIFORNIA)
	4	02/29/84	AXK945	PISGAH CAL1 (PISGAH, CALIFORNIA)
	5	03/01/84	AXK946	HAZARD KY3 (ELKHORN CITY, KENTUCKY)
	6	03/02/84	AXK947	MOBILE/BLDWN1 (BALDWIN COUNTY 2, ALABAMA)
	7	03/03/84	AXK948	HAZARD KY5 (ZEBULON, KENTUCKY)
	8	03/05/84	AXK950	DTH VAL TOPO156 (DEATH VALLEY TOPO 1, PANAMINT RANGE, CA)
	9	03/06/84	AXK943	WIND RIVER4 (DEAD MAN BUTTE WEST, WYOMING)
	10	03/07/84	AXK951	OWENS VALLEY, CALIFORNIA 2
	11	03/08/84	AXK952	SF-FARLON77 (SAN FRANCISCO SHIPS, PACIFIC OCEAN WAVES)
	12	03/13/84	AXK953	RAISIN CITY003 (AGRICULTURAL FIELDS, CALIFORNIA)
	13	03/14/84	AXK954	RAISIN CITY270 (AGRICULTURAL FIELDS, CALIFORNIA)
	14	03/14/84	AXK955	RAISIN CITY315 (AGRICULTURAL FIELDS, CALIFORNIA)
	15	03/16/84	AXK957	RAISIN CITY270 (AGRICULTURAL FIELDS, CALIFORNIA)
	16	03/20/84	AXK958	RAISIN CITY003 (AGRICULTURAL FIELDS, CALIFORNIA)
	17	03/22/84	AXK959	SRP SWAMP302 PEN BRANCH, SAVANNAH RIVER PLANT, SC
	18	03/23/84	AXK960	RAISIN CITY003 (AGRICULTURAL FIELDS, CALIFORNIA)
4				
	1	03/27/84	AXK961	SRP SWAMP125, SAVANNAH RIVER PLANT SWAMP SAND HILLS, SC
	2	03/27/84	AXK962	RAISIN CITY003 (AGRICULTURAL FIELDS, CALIFORNIA)
	3	03/29/84	AXK963D	RAISIN CITY270 (AGRICULTURAL FIELDS, CALIFORNIA)
	4	03/29/84	AXK964	NORTH TEXAS184 (NORTH TEXAS 2)
	5	03/30/84	AXK965	G WASH FRST271 (LITTLE N MTN, G WASHINGTON FOREST, VA)
	6	04/03/84	AXK966	PALASTINE TX91, PALESTINE 3, TEXAS
	7	04/04/84	AXK968	SHIP PASS 007, GULF OF ALASKA
	8	04/06/84	AXK967	SHIP PASS 007, EXTENDED SHIP WAKE, GULF OF ALASKA
	9	04/08/84	AXK969	PISGAH CAL4, CALIFORNIA

C-2

Table C-1 (Continued)

Book No.	Page No.	Correlation Date	CCT	Title
	10	04/14/84	AXK970	SHIP PASS 004, GULF OF ALASKA
	11	04/15/84	AXK971	BLACK RVR REF2, LOWER HOOPER ISLAND, VIRGINIA
	12	04/17/84	AXK972	SRP SWAMP123, ELLENTON BAY, SOUTH CAROLINA
	13	04/18/84	AXK973	NORTH TEXAS181, SAND HILLS 1
	14	04/20/84	AXK974	SHIP PASS 006, GULF OF ALASKA
	15	04/24/84	AXK975	NORTH TEXAS002, CASTRO COUNTY LINE
	16	05/03/84	AXK976	BLACK RVR REF181, LOWER HOOPER ISLAND 2, VIRGINIA
	17	05/04/84	AXK977	BLACK RVR REF181, MONEY STUMP SWAMP, VIRGINIA
	18	05/11/84	AXK978	PISGAH CAL 4
	19	05/14/84	AXK979	PISGAH CAL 4
	20	05/30/84	AXK980	SAN ANDREAS317 (SF BAY WAVES)
	21	06/01/84	AXK981	WINCHSTR VA 292
	22	06/05/84	AXK982	G WASH FRST92, GREAT NORTH MT, GEORGE WASHINGTON FOREST, VA
	23	06/05/84	AXK983	SHIP PASS 010 (CROSS WAKE-#5), GULF OF ALASKA
	24	06/06/84	AXK985	SHIP PASS 004, GULF OF ALASKA
	25	06/07/84	AXK986	SHIP PASS 002, GULF OF ALASKA
	26	06/08/84	AXK984	SHIP PASS 005, GULF OF ALASKA
	26A	06/11/84	AXK987	SHIP PASS 013, GULF OF ALASKA
	27	06/13/84	AXK990	OWENS VALLEY, CALIFORNIA
	28	06/15/84	AXK991	SRP SWAMP 124 (DUMBARTON BAYS)
	29	06/20/84	AXK989	SHIP PASS 003, GULF OF ALASKA
	30	07/01/84	AXK993	DEATH VAL ENG161 (COTTON BALL BASIN) CALIFORNIA
	31	07/02/84	AXK994	DEATH VAL ENG90 (SAND DUNES)
	32	07/03/84	AXK995	DTH VAL ENG342
	33	07/04/84	AXK988	SHIP PASS 001 (GULF OF ALASKA)
	34	07/06/84	AXK996	SAN ANDREAS137 (SOUTH SFO BAY)
	35	07/07/84	AXK997	CAP REEF1 (SAN RAFEAL SWELL)UTAH
	37	07/10/84	AXK998	BLACK RVR REF181 (MONEY STUMP SWAMP NORTH)
	38	07/10/84	AXK999	BLACK RIVER REF181 (MONEY STUMP SWAMP SOUTH)
	39	07/11/84	AXC001	NORTH TEXAS001 (SOUTH OF SPADE)
	40	07/11/84	AXC002	SAN ANDREAS137 (SFO-NORTH)
	41	07/12/84	AXC003	BRAZOS TEXAS-DEMEL
	41	07/12/84	AXC004	BRAZOS TEXAS - DEMEL
	42	07/14/84	AXC005	MOBILE BLDWN1 (BALDWIN CO. EAST OF AXK947)
	43	07/17/84	AXC006	SAN ANDREAS137 (SAN FRANCISCO-URBAN)CALIFORNIA
	44	07/18/84	AXC007	SHEMDIN'S LAST SHIP PASS
	45	07/20/84	AXC008	DTH VAL ENG342 (DEATH VALLEY) CALIFORNIA
	46	07/21/84	AXC009	DTH VAL ENG342 (DEATH VALLEY, CALIFORNIA)

Table C-1 (Continued)

Book No.	Page No.	Correlation Date	CCT	Title
5				
	1	07/24/84	AXC010	G WASH FRST272, STEVEN'S CITY, GEORGE WASHINGTON FOREST, VA
	2	07/25/84	AXC011	G WASH FRST272, MIDDLETON-1, GEORGE WASHINGTON FOREST, VA
	3	07/26/84	AXC012	PISGAH CAL7 (EARLY) CALIFORNIA
	4	07/27/84	AXC013	PISGAH CAL7 (LATE) CALIFORNIA
	5	08/05/84	AXC014	PISGAH CAL7 (SIGMA 0 AND CALIBRATION)
	6	08/12/84	AXC015	NORTH TEXAS181
	7	08/15/84	AXC016	WIND RIVER4 (WIND RIVER REDO)
	8	08/18/84	AXC020	DEATH VALLEY ENG. 162
	9	08/18/84	AXC021	DEALTH VALLEY ENG. 340
	10	08/29/84	AXC022	DTH VANG342 (DEATH VALLEY COTTONBALL BASIN)
	11	08/31/84	AXC023	JUST A TEST (MONO LAKE)
	12	09/27/84	AXC024	BLCKWTER RVR-092 (MONEYSTUMP SWAMP-3
	13	10/01/84	AXC025	BLCKWTER RVR-271 (MONEYSTUMP SWAMP)
	14	10/04/84	AXC026	BLKWTER RVR-091 (LOWER HOOPER ISLAND)
	15	10/04/84	AXC027	OWENS VALLEY-166 (INDEPENDENCE, CA)
	16	10/08/84	AXC028	NASA-NSTL-003
	17	10/08/84	AXC029	NASA-NSTL-003 (NASA NSTL-B, NORTH-EAST)
	18	10/10/84	AXC030	NASA-NSTL-004 (NASTL-C, SOUTHWEST)
	19	10/10/84	AXC031	NASA-NSTL-004
	20	10/19/84	AXC032	SUPERSITE4
	21	10/20/84	AXC033	SUPERSITE2
	22	10/23/84	AXC034	SUPERSITE4
	23	10/25/84	AXC035	SUPERSITE2
	24	10/26/84		SUPERSITE2
	25	11/02/84	AXC036	ELY PINES-291 (ELY PINES-1)
	26	11/02/84	AXC037	ELY PINES-291 (ELY PINES-4)
	27	11/03/84	AXC038	ELY PINES-291
	28	11/03/84	AXC039	ELY PINES-291
	29	11/11/84	AXC040	PISGAH CAL4
	30	11/11/84	AXK041	PISGAH CAL7
	31	11/15/84	AXC042	RAISIN CITY003
	32	11/15/84	AXC043	RAISIN CITY 315
	33	11/16/84	AXC045	NOSC TOWER-1-090
	34	11/20/84	AXC046	SRP SWAMP302
	35	12/05/84	AXC044	NORTH TEXAS181 (SAND HILL)
	36	12/14/84	AXC053	CANDELARIA-174
	37	12/17/84	AXC054	CANDELARIA-354
	38	12/17/84	AXC055	RAISIN CITY270
	39	12/26/84	AXC052	NORTH TEXAS002 (SAND HILLS-A)
	39A	12/27/84	AXC052	NORTH TEXAS002
	40	01/08/85	AXC056	GLASS MTN-354

Table C-1 (Continued)

Book No.	Page No.	Correlation Date	CCT	Title
	41	01/08/85	AXC057	OWENS VALLEY
	42	01/10/85	AXC059	WINCHSTER VA-272 (WALDENSVILLE-1)
	43	01/11/85	AXC058	WINCHSTER VA-272 (STEVENS CITY)
	44	01/11/85	AXC060	CIMA-255
	45	01/13/85	AXC061	CIMA-255
	46	01/13/85	AXC062	KELSO DUNES-270
	47	01/14/85	AXC063	MEDICINE LAKE-2
	48	01/15/85	AXC064	MEDICINE LAKE-4
6				
	1	01/15/85	AXC065	MEDICINE LAKE-2
	2	01/16/85	AXC066	MEDICINE LAKE-5
	3	01/16/85	AXC067	GLASS MTN-355
	4	01/19/85	AXC068	GOLDFIELD-321
	5	01/19/85	AXC069	GOLDFIELD-045
	6	01/20/85	AXC070	GOLDFIELD-321
	7	01/20/85	AXC071	SUPERSITE2
	8	01/20/85	AXC072	SUPERSITE2
	9	01/23/85	AXC074	WIND RIVER4
	10	01/24/85	AXC075	SUPERSITE4
	11	01/25/85	AXC076	SUPERSITE6
	12	01/26/85	AXC077	NOSC TOWER-1-090
	13	01/26/85	AXC078	NOSC TOWER-1-270
	14	01/27/85	AXC079	NOSC TOWER-1-240
	15	01/28/85	AXC073	GLASS MTN-174
	16	01/29/85	AXC080	NOSC TOWER-1-090
	17	01/30/85	AXC082	JACKS FOREST-182
	18	01/31/85	AXC081	JACKS FOREST-003
	19	01/31/85	AXC083	WINCHSTER VA-091
	20	02/01/85	AXC084	WINCHSTER VA-091
	21	02/02/85	AXC085	JACKS FOREST-002
	22	02/02/85	AXC086	JACKS FOREST-181
	23	02/08/85	AXC087	MEDICINE LAKE-1
	24	02/08/85	AXC088	MEDICINE LAKE-1
	25	02/14/85	AXC089	GOLDFIELD-321
	26	02/18/85	AXC090	GOLDEN GATE-180
	27	02/19/85	AXC091	GOLDEN GATE-270
	28	02/22/85	AXC092	TWT AQUEDUCT
	29	02/24/85	AXC093	BURBANK-CHTSWRTH
	30	02/25/85	AXC094	CANDELARIA-174
	31	02/28/85	AXC095	CANDELARIA-354
	32	02/28/85	AXC096	SODA SPRING-127
	33	02/28/85	AXC097	BURBANK-CHTSWRTH
	34	03/01/85	AXC098	BLACKWATER RVR-274
	35	03/01/85	AXC099	BLACKWATER RVR-274
	36	03/05/85	AXC100	BLACKWATER RVR-092
	37	03/06/85	AXC101	WINCHESTER VA-094
	38	03/10/85	AXC200	NOSC 38KFT-6-180
	39	03/12/85	AXC102	NOSC TOWER-A-090
	40	03/13/85	AXC103	NOSC TOWER-1-090
	41	03/19/85	AXC104	NOSC TOWER-1-090
	42	03/20/85	AXC201	RAISIN FRESNO-270

Table C-1 (Continued)

Book No.	Page No.	Correlation Date	CCT	Title
	43	03/22/85	AXC105	NOSC TOWER-1-270
7				
	1	03/24/85	AXC106	NOSC TOWER-1-090
	2	03/24/85	AXC202	NOSC 38KFT-1-090
	3	03/26/85	AXC108	NOSC TOWER-1-240
	4	03/27/85	AXC107C	NOSC TOWER-1-090
	5	03/28/85	AXC203	AMPTE fore-aft
	6	03/30/85	AXC109	NOSC TOWER-1-270
	8	03/31/85	AXC101C	WINCHSTER VA-094
	7	03/31/85	AXC101C	WINCHSTER VA-094
	9	04/03/85	AXC110	NOSC TOWER-1-300
	10	04/10/85	AXC111	NOSC TOWER-1-240
	11	04/11/85	AXC112	NOSC TOWER-1-240
	12	04/11/85	AXC113	NOSC TOWER-1-300
	13	04/13/85	AXC115	NOSC TOWER-1-090
	14	04/15/85	AXC114	NOSC TOWER-1-090
	15	04/17/85	AXC116	NOSC TOWER-1-090
	16	04/18/85	AXC076C	SUPERSITE6
	17	04/19/85	AXC204	COSTA RICA-B-320
	18	04/22/85	AXC117	SUPERSITE6
	19	04/23/85	AXC117C	SUPERSITE6
	20	04/24/85	AXC118C	SUPERSITE6
	21	04/25/85	AXC119C	SUPERSITE6
	22	04/26/85	AXC205	COSTA TOPO-090
	23	04/26/85	AXC206	COSTA TOPO-270
	24	05/01/85	AXC085C	JACKS FOREST-002
	25	05/01/85	AXC120C	SUPERSITE6
	26	05/02/85	AXC064C	MEDICINE LAKE-4
	27	05/02/85	AXC121C	GLASS MTN-354
	28	05/08/85	AXC105C	NOSC TOWER-1-270
	29	05/08/85	AXC122C	GLASS MTN-354
	30	05/09/85	AXC123C	GLASS MTN-355
	31	05/09/85	AXC124C	GLASS MTN-355
	32	05/13/85	AXC125	SRP SWAMP303
	33	05/13/85	AXC125C	SRP SWAMP303
	34	05/13/85	AXC126	SRP SWAMP124
	35	05/13/85	AXC126C	SRP SWAMP124
8				
	1	05/16/85	AXC129	SODA SPRING-307
	2	05/17/85	AXC127C	CINDER CONE-048
	3	05/17/85	AXC128C	CINDER CONE-228
	4	05/17/85	AXC130C	CINDER CONE-047
	5	05/20/85	AXC131C	CINDER CONE-229
	6	05/21/85	AXC132C	SRP SWAMP 122
	7	05/21/85	AXC133C	SRP SWAMP 122
	8	05/24/85	AXC134C	NORTH TEXAS003
	9	05/24/85	AXC135C	NORTH TEXAS003
	10	05/27/85	AXC136C	NASA-NSTL-184
	11	05/27/85	AXC137C	NASA-NSTL-184
	12	05/29/85	AXC207	SAN JOAQUIN ENG
	13	05/31/85	AXC207C2	SAN JOAQUIN ENG
	14	05/31/85	AXC208C2	SAN JOAQUIN ENG

Table C-1 (Continued)

Book No.	Page No.	Correlation Date	CCT	Title
	15	06/01/85	AXC140C	SHASTA-308
	16	06/01/85	AXC209C	SAN JOAQUIN
	17	06/01/85	AXC210C	JUST A TEST
	18	06/05/85	AXC211C	OWENS VALLEY-346
	19	06/05/85	AXC212C	OWENS VALLEY-346
	20	06/06/85	AXC213C	OWENS VALLEY-346
	21	06/07/85	AXC214C	RAISIN FRSNO-270
	22	06/07/85	AXC215C	RAISIN FRESNO-270
	23	06/08/85	AXC217C	OWENS VALLEY-347
	24	06/11/85	AXC218C	SAN JOAQUIN ENG.
	25	06/11/85	AXC219CC	C-BAND ONLY TEST
	26	06/12/85	AXC220CC	RAISIN CBAND260
	27	06/13/85	AXC216C	RAISIN-FRSNO-090
9				
	1	06/27/85	AXC221C	OWENS VALLEY-347
	2	06/27/85	AXC222CC	KONZA L/C-BAND-1
	3	06/27/85	AXC223CC	C-BAND OHIO
	4	06/27/85	AXC224C	OWENS VALLEY-347
	5	06/30/85	AXC138C	MEDICINE LAKE-5
	6	06/30/85	AXC139C	MEDICINE LAKE-5
	7	07/03/85	AXC225CC	RHODES L/C-BAND
	8	07/10/85	AXC226C	COSTA RICA-B-141
	9	07/15/85	AXC227C	SNAKE RIVER-151
	10	07/15/85	AXC228C	SNAKE RIVER-151
	11	07/16/85	AXC207C3	SAN JOAQUIN ENG.
	12	07/16/85	AXC229C	WIND RIVER-355
	13	07/18/85	AXC086C	JACKS FOREST-181
	14	07/22/85	AXC081C	JACKS FOREST-003
	15	07/22/85	AXC085C2	JACKS FOREST-002
	16	07/24/85	AXC082C	JACKS FOREST-182
	17	07/25/85	AXC117C2	SUPERSITE6
	18	07/25/85	AXC118C2	SUPERSITE6
	19	07/25/85	AXC141C	NASA-NSTL-183
	20	07/27/85	AXC119C2	SUPERSITE6
	21	07/27/85	AXC120C2	SUPERSITE6
10				
	1	07/29/85	AXC230C	RHODES NEV-000
	2	07/30/85	AXC231C	TRAV CITY-140'
	3	07/30/85	AXC232C	WIND RIVER-355
	4	07/31/85	AXC233C	WIND RIVER-355
	5	07/31/85	AXC234	KONZA GRASS-182
	6	08/01/85	AXC235C	KONZA GRASS-270
	7	08/02/85	AXC236C	KONZA GRASS-090
	8	08/03/85	AXC237C	SHASTA-STER-136
	9	08/03/85	AXC238C	SHASTA-STER-137
	10	08/04/85	AXC239	SHASTA-TOPO-135
	11	08/05/85	AXC240C	OWENS VALLEY-168
	12	08/06/85	AXC241C	PISGAH CAL-7
	13	08/06/85	AXC242C	BLCKWTER RVR-060
	14	08/08/85	AXC243C	COSTA RICA-A-022
	15	08/15/85	AXC244C	COSTA-RICA-A-202
	16	08/15/85	AXC245C	COSTA RICA-A-020

Table C-1 (Continued)

Book No.	Page No.	Correlation Date	CCT	Title
	17	08/16/85	AXC246C	KONZA GRASS-181
	18	08/16/85	AXC247C	KONZA GRASS-002
	19	08/18/85	AXC248C	GOLDSTONE340
	20	08/19/85	AXC249C	RAISIN CITY-325
	21	08/19/85	AXC250C	KONZA GRASS-270
	22	08/20/85	AXC251C	GOLDSTONE339
	23	08/21/85	AXC252	LAKE TAHOE TOPO
	24	08/27/85	AXC254C	TRAV-CITY-046 (TRAVERSE CITY, MICHIGAN)
	25	08/28/85	AXC143C	SRP SWAMP302 (SAVANNAH RIVER PLANT SWAMP)
	26	08/28/85	AXC255C	TRAV-CITY-047 (TRAVERSE CITY, MICHIGAN)
11				
	1	09/01/85	AXC142C	SRP SWAMP302 (SAVANNAH RIVER PLANT SWAMP)
	2	09/01/85	AXC253C	WIND RIVER-355 (WIND RIVER, WYOMING)
	3	09/03/85	AXC056C	GLASS MTN-354 (GLASS MOUNTAIN FLOW, MEDICINE LAKE, CA)
	4	09/03/85	AXC067C	GLASS MTN-355 (GLASS MOUNTAIN FLOW, MEDICINE LAKE, CA)
	5	09/04/85	AXC147C	NOSC TOWER-1-270
	6	09/05/85	AXC145C	NOSC TOWER-1-270
	7	09/06/85	AXC144C	NOSC TOWER-1-270
	8	09/10/85	AXC109C	NOSC TOWER-1-270
	9	09/10/85	AXC256C	WIND RIVER-155
	10	09/11/85	AXC146C2	GOLDSTONE-340
	11	09/12/85	AXC257C	KONZA GRASS-090
	12	09/14/85	AXC258C	KONZA GRASS-002
	13	09/16/85	AXC259C	ANN ARBOR-001
	14	09/19/85	AXC260C	ANN ARBOR-002
	15	09/21/85	AXC261C	ANN ARBOR-003
	16	09/21/85	AXC262C	TRAV-CITY-046
	16A	09/25/85	AXC065C	MEDICINE LAKE-2
	16B	09/26/85	AXC066C	MEDICINE LAKE-5
	16C	09/26/85	AXC087C	MEDICINE LAKE-1
	17	10/01/85	AXC265C	NOSC 38KFT-2-270
	18	10/01/85	AXC267C	SNAKE RIVER-150
	19	10/02/85	AXC266C	NOSC 38KFT-4-240
12				
	1	11/06/85	AXC268	MAINE FORE-AFT
	2	11/07/85	AXC269C	COSTA RICA-A-022
	3	11/12/85	AXC270C	COSTA RICA-A-021
	4	11/13/85	AXC249C2	RAISIN CITY-325
	5	11/14/85	AXC148C	RAISIN-FRESNO-034
	6	11/16/85	AXC150C	RAISIN-FRESNO-034
	7	11/18/85	AXC271C	BLCKWTER RVR-274
	8	11/19/85	AXC272C	BLCKWTER RVR-274
	9	11/26/85	AXC273C	NOSC 38KFT-7-300
	10	12/02/85	AXC274C	NOSC 38KFT-1-090
	11	12/10/85	AXC275C	NOSC 20KFT-2-270

Table C-1 (Continued)

Book No.	Page No.	Correlation Date	CCT	Title
	12	12/12/85	AXC276C	NOSC 20KFT-1-090
	13	12/17/85	AXC227C	NOSC 20KFT-6-180
	14	12/19/85	AXC278C	NOSC 20KFT-1-090
	15	01/06/86	AXC279	LAKE TAHOE TOPO
	16	01/07/86	AXC280	SHASTA-STER-135
	17	01/09/86	AXC281	SHASTA-STER-137 (SHASTA-STEREO-2B)
	18	01/10/86	AXC282	SHASTA-STER-136
	19	01/16/86	AXC283C	MAINE WOODS-271
	20	01/21/86	AXC151C	MEDICINE LAKE-1
	21	01/22/86	AXC284C	OTTAWA WOODS-181
	22	01/23/86	AXC152C	SHASTA-126
	23	01/23/86	AXC153C	SHASTA-127
	24	01/30/86	AXC154C	SHASTA-308
	25	02/06/86	AXC285C	OWENS VALLEY-168
13				
	1	02/07/86	AXC286C	OWENS VALLEY-168 (OWENS VALLEY-85-2)
	2	02/09/86	AXC287C	OWENS VALLEY-168 (OWENS VALLEY-85-3)
	3	02/10/86	AXC288C	OWENS VALLEY-168 (OWENS VALLEY-85-4)
	4	02/11/86	AXC289C	COSTA RICA-A-202 (COSTA RICA-A-3-b)
	5	02/16/86	AXC290C	COSTA RICA-B-141 (COSTA RICA-B-5)
	6	02/20/86	AXC292C	COSTA RICA-B-322 (COSTA RICA-B-6)
	7	03/05/86	AXC295C	TUG HILL-356
	8	03/05/86	AXC296C	RAISIN FRSNO-270 (RAISIN CITY-85-1)
	9	03/12/86	AXC297C	TRANSMITTER OFF TEST
	10	03/17/86	AXC299C	VERMONT-195 (CAMELBACK-85-1)
	11	03/26/86	AXC300C	SNAKE RIVER-150 (SNAKE RIVER-150-1)
	12	03/26/86	AXC301C	SNAKE RIVER-150-2
	13	03/27/86	AXC074C	WIND RIVER4
	14	04/03/86	AXC291C	COSTA RICA-B-321 (COSTA RICA-B-7)
	15	04/05/86	AXC303C	CIMA-3-000 (CIMA-1-LEFT)
	16	04/05/86	AXC304C	CIMA-3-000 (CIMA-1-RIGHT)
	17	04/28/86	AXC155C	BLCKWTER RVR-274
	18	04/28/86	AXC156C	BLCKWTER RVR-274
	19	04/28/86	AXC305C	CIMA-2-073 (CIMA-2-LEFT)
	20	04/28/86	AXC306C	CIMA-2-073 (CIMA-2-RIGHT)
	21	05/07/86	AXC307C	SNAKE RIVER-331
	22	05/07/86	AXC308C	SNAKE RIVER-331
	23	05/15/86	AXC309C	JACKS FOREST-003
	24	05/15/86	AXC310C	JACKS FOREST-003
	25	07/03/86	AXC311C	SAN JOAQUIN ENG

Table C-1 (Continued)

Book No.	Page No.	Correlation Date	CCT	Title
7				
	5	03/28/85	AXC203	AMPTE fore-aft
2				
	14	02/14/84	AXK936	ANADARKO BASN4 (ANADARKO 1, OKLAHOMA)
	15	02/16/84	AXK937	ANADARKO BASN4 (ANADARKO 2, OKLAHOMA)
11				
	13	09/16/85	AXC259C	ANN ARBOR-001
	14	09/19/85	AXC260C	ANN ARBOR-002
	15	09/21/85	AXC261C	ANN ARBOR-003
4				
	38	07/10/84	AXK999	BLACK RIVER REF181 (MONEY STUMP SWAMP SOUTH)
	37	07/10/84	AXK998	BLACK RVR REF181 (MONEY STUMP SWAMP NORTH)
	16	05/03/84	AXK976	BLACK RVR REF181, LOWER HOOPER ISLAND 2, VIRGINIA
	17	05/04/84	AXK977	BLACK RVR REF181, MONEY STUMP SWAMP, VIRGINIA
	11	04/15/84	AXK971	BLACK RVR REF2, LOWER HOOPER ISLAND, VIRGINIA
6				
	36	03/05/85	AXC100	BLACKWATER RVR-092
	34	03/01/85	AXC098	BLACKWATER RVR-274
	35	03/01/85	AXC099	BLACKWATER RVR-274
10				
	13	08/06/85	AXC242C	BLCKWTER RVR-060
5				
	12	09/27/84	AXC024	BLCKWTER RVR-092 (MONEYSTUMP SWAMP-3
	13	10/01/84	AXC025	BLCKWTER RVR-271 (MONEYSTUMP SWAMP)
12				
	7	11/18/85	AXC271C	BLCKWTER RVR-274
	8	11/19/85	AXC272C	BLCKWTER RVR-274
13				
	17	04/28/86	AXC155C	BLCKWTER RVR-274
	18	04/28/86	AXC156C	BLCKWTER RVR-274
5				
	14	10/04/84	AXC026	BLKWTER RVR-091 (LOWER HOOPER ISLAND)
4				
	41	07/12/84	AXC004	BRAZOS TEXAS - DEMEL
	41	07/12/84	AXC003	BRAZOS TEXAS-DEMEL
6				
	29	02/24/85	AXC093	BURBANK-CHTSWRTH
	33	02/28/85	AXC097	BURBANK-CHTSWRTH
9				
	3	06/27/85	AXC223CC	C-BAND OHIO
8				
	25	06/11/85	AXC219CC	C-BAND ONLY TEST

Table C-1 (Continued)

Book No.	Page No.	Correlation Date	CCT	Title
5	36	12/14/84	AXC053	CANDELARIA-174
6	30	02/25/85	AXC094	CANDELARIA-174
5	37	12/17/84	AXC054	CANDELARIA-354
6	31	02/28/85	AXC095	CANDELARIA-354
4	35	07/07/84	AXK997	CAP REEF1 (SAN RAFEAL SWELL)UTAH
13	19	04/28/86	AXC305C	CIMA-2-073 (CIMA-2-LEFT)
	20	04/28/86	AXC306C	CIMA-2-073 (CIMA-2-RIGHT)
5	44	01/11/85	AXC060	CIMA-255
	45	01/13/85	AXC061	CIMA-255
13	15	04/05/86	AXC303C	CIMA-3-000 (CIMA-1-LEFT)
	16	04/05/86	AXC304C	CIMA-3-000 (CIMA-1-RIGHT)
8	4	05/17/85	AXC130C	CINDER CONE-047
	2	05/17/85	AXC127C	CINDER CONE-048
	3	05/17/85	AXC128C	CINDER CONE-228
	5	05/20/85	AXC131C	CINDER CONE-229
2	1	01/11/84	AXK923	COSO HILLS1 (RAISIN CITY AGRICULTURAL FIELDS, CALIFORNIA)
	8	01/20/84	AXK931	COSO HILLS90 (COSO HILLS, CALIFORNIA)
10	16	08/15/85	AXC245C	COSTA RICA-A-020
12	3	11/12/85	AXC270C	COSTA RICA-A-021
10	14	08/08/85	AXC243C	COSTA RICA-A-022
12	2	11/07/85	AXC269C	COSTA RICA-A-022
13	4	02/11/86	AXC289C	COSTA RICA-A-202 (COSTA RICA-A-3-b)
9	8	07/10/85	AXC226C	COSTA RICA-B-141
13	5	02/16/86	AXC290C	COSTA RICA-B-141 (COSTA RICA-B-5)
7	17	04/19/85	AXC204	COSTA RICA-B-320
13	14	04/03/86	AXC291C	COSTA RICA-B-321 (COSTA RICA-B-7)
	6	02/20/86	AXC292C	COSTA RICA-B-322 (COSTA RICA-B-6)

Table C-1 (Continued)

Book No.	Page No.	Correlation Date	CCT	Title
7				
	22	04/26/85	AXC205	COSTA TOPO-090
	23	04/26/85	AXC206	COSTA TOPO-270
10				
	15	08/15/85	AXC244C	COSTA-RICA-A-202
5				
	9	08/18/84	AXC021	DEALTH VALLEY ENG. 340
4				
	30	07/01/84	AXK993	DEATH VAL ENG161 (COTTON BALL BASIN) CALIFORNIA
	31	07/02/84	AXK994	DEATH VAL ENG90 (SAND DUNES)
5				
	8	08/18/84	AXC020	DEATH VALLEY ENG. 162
2				
	17	02/20/84		DTH VAL ENG161 (DEVIL'S GOLF COURSE, DEATH VALLEY, CA)
4				
	32	07/03/84	AXK995	DTH VAL ENG342
	45	07/20/84	AXC008	DTH VAL ENG342 (DEATH VALLEY) CALIFORNIA
	46	07/21/84	AXC009	DTH VAL ENG342 (DEATH VALLEY, CALIFORNIA)
3				
	8	03/05/84	AXK950	DTH VAL TOPO156 (DEATH VALLEY TOPO 1, PANAMINT RANGE, CA)
	1	02/22/84	AXK941	DTH VAL TOPO157 (DEATH VALLEY TOPO 2, PANAMINT RANGE, CA)
2				
	18	02/21/84	AXK940	DTH VAL TOPO158 (DEATH VALLEY TOPO 3, PANAMINT RANGE, CA)
	11	01/27/84	AXK933	DTH VAL USGS2 (DEATH VALLEY SAND DUNES, CALIFORNIA)
1				
	15	01/06/84	AXK921	DTH VAL USGS5 (DEATH VALLEY, CALIFORNIA)
5				
	10	08/29/84	AXC022	DTH VANG342 (DEATH VALLEY COTTONBALL BASIN)
	27	11/03/84	AXC038	ELY PINES-291
	28	11/03/84	AXC039	ELY PINES-291
	25	11/02/84	AXC036	ELY PINES-291 (ELY PINES-1)
	26	11/02/84	AXC037	ELY PINES-291 (ELY PINES-4)
4				
	5	03/30/84	AXK965	G WASH FRST271 (LITTLE N MTN, G. WASHINGTON FOREST, VA)
5				
	2	07/25/84	AXC011	G WASH FRST272, MIDDLETON-1, GEORGE WASHINGTON FOREST, VA
	1	07/24/84	AXC010	G WASH FRST272, STEVEN'S CITY, GEORGE WASHINGTON FOREST, VA
4				

Table C-1 (Continued)

Book No.	Page No.	Correlation Date	CCT	Title
	22	06/05/84	AXK982	G WASH FRST92, GREAT NORTH MT, GEORGE WASHINGTON FOREST, VA
6				
	15	01/28/85	AXC073	GLASS MTN-174
5				
	40	01/08/85	AXC056	GLASS MTN-354
7				
	27	05/02/85	AXC121C	GLASS MTN-354
	29	05/08/85	AXC122C	GLASS MTN-354
11				
	3	09/03/85	AXC056C	GLASS MTN-354 (GLASS MOUNTAIN FLOW, MEDICINE LAKE, CA)
6				
	3	01/16/85	AXC067	GLASS MTN-355
7				
	30	05/09/85	AXC123C	GLASS MTN-355
	31	05/09/85	AXC124C	GLASS MTN-355
11				
	4	09/03/85	AXC067C	GLASS MTN-355 (GLASS MOUNTAIN FLOW, MEDICINE LAKE, CA)
6				
	26	02/18/85	AXC090	GOLDEN GATE-180
	27	02/19/85	AXC091	GOLDEN GATE-270
	5	01/19/85	AXC069	GOLDFIELD-045
	4	01/19/85	AXC068	GOLDFIELD-321
	6	01/20/85	AXC070	GOLDFIELD-321
	25	02/14/85	AXC089	GOLDFIELD-321
11				
	10	09/11/85	AXC146C2	GOLDSTONE-340
10				
	22	08/20/85	AXC251C	GOLDSTONE339
	19	08/18/85	AXC248C	GOLDSTONE340
1				
	1	11/19/83	AXK901	HAZARD KY1 (HAZARD, KENTUCKY)
3				
	5	03/01/84	AXK946	HAZARD KY3 (ELKHORN CITY, KENTUCKY)
	7	03/03/84	AXK948	HAZARD KY5 (ZEBULON, KENTUCKY)
6				
	21	02/02/85	AXC085	JACKS FOREST-002
7				
	24	05/01/85	AXC085C	JACKS FOREST-002
9				
	15	07/22/85	AXC085C2	JACKS FOREST-002
6				
	18	01/31/85	AXC081	JACKS FOREST-003
9				
	14	07/22/85	AXC081C	JACKS FOREST-003
13				
	23	05/15/86	AXC309C	JACKS FOREST-003
	24	05/15/86	AXC310C	JACKS FOREST-003
6				

Table C-2. SAR Imagery Sorted by Correlation Date

Book No.	Page No.	Correlation Date	CCT	Title
	22	02/02/85	AXC086	JACKS FOREST-181
9				
	13	07/18/85	AXC086C	JACKS FOREST-181
6				
	17	01/30/85	AXC082	JACKS FOREST-182
9				
	16	07/24/85	AXC082C	JACKS FOREST-182
1				
	12	12/20/83	AXK918	JAMAICA8 (JAMAICA, WEST INDIES)
8				
	17	06/01/85	AXC210C	JUST A TEST
5				
	11	08/31/84	AXC023	JUST A TEST (MONO LAKE)
	46	01/13/85	AXC062	KELSO DUNES-270
10				
	18	08/16/85	AXC247C	KONZA GRASS-002
11				
	12	09/14/85	AXC258C	KONZA GRASS-002
10				
	7	08/02/85	AXC236C	KONZA GRASS-090
11				
	11	09/12/85	AXC257C	KONZA GRASS-090
10				
	17	08/16/85	AXC246C	KONZA GRASS-181
	5	07/31/85	AXC234	KONZA GRASS-182
	6	08/01/85	AXC235C	KONZA GRASS-270
	21	08/19/85	AXC250C	KONZA GRASS-270
9				
	2	06/27/85	AXC222CC	KONZA L/C-BAND-1
10				
	23	08/21/85	AXC252	LAKE TAHOE TOPO
12				
	15	01/06/86	AXC279	LAKE TAHOE TOPO
	1	11/06/85	AXC268	MAINE FORE-AFT
	19	01/16/86	AXC283C	MAINE WOODS-271
1				
	2	11/28/83	AXK902	MEANS VAL SIR2 (MEANS VALLEY, CALIFORNIA)
6				
	23	02/08/85	AXC087	MEDICINE LAKE-1
	24	02/08/85	AXC088	MEDICINE LAKE-1
11				
	16C	09/26/85	AXC087C	MEDICINE LAKE-1
12				
	20	01/21/86	AXC151C	MEDICINE LAKE-1
5				
	47	01/14/85	AXC063	MEDICINE LAKE-2
6				
	1	01/15/85	AXC065	MEDICINE LAKE-2
11				
	16A	09/25/85	AXC065C	MEDICINE LAKE-2
5				

Table C-2 (Continued)

Book No.	Page No.	Correlation Date	CCT	Title
	48	01/15/85	AXC064	MEDICINE LAKE-4
7				
	26	05/02/85	AXC064C	MEDICINE LAKE-4
6				
	2	01/16/85	AXC066	MEDICINE LAKE-5
9				
	5	06/30/85	AXC138C	MEDICINE LAKE-5
	6	06/30/85	AXC139C	MEDICINE LAKE-5
11				
	16B	09/26/85	AXC066C	MEDICINE LAKE-5
4				
	42	07/14/84	AXC005	MOBILE BLDWN1 (BALDWIN CO. EAST OF AXK947)
3				
	6	03/02/84	AXK947	MOBILE/BLDWN1 (BALDWIN COUNTY 2, ALABAMA)
2				
	6	01/19/84	AXK928	MOBILE/BLDWN1 (BALDWIN COUNTY, ALABAMA)
5				
	16	10/08/84	AXC028	NASA-NSTL-003
	17	10/08/84	AXC029	NASA-NSTL-003 (NASA NSTL-B, NORTH-EAST)
	19	10/10/84	AXC031	NASA-NSTL-004
	18	10/10/84	AXC030	NASA-NSTL-004 (NASTL-C, SOUTHWEST)
9				
	19	07/25/85	AXC141C	NASA-NSTL-183
8				
	10	05/27/85	AXC136C	NASA-NSTL-184
	11	05/27/85	AXC137C	NASA-NSTL-184
4				
	39	07/11/84	AXC001	NORTH TEXAS001 (SOUTH OF SPADE)
5				
	39A	12/27/84	AXC052	NORTH TEXAS002
	39	12/26/84	AXC052	NORTH TEXAS002 (SAND HILLS-A)
4				
	15	04/24/84	AXK975	NORTH TEXAS002, CASTRO COUNTY LINE
8				
	8	05/24/85	AXC134C	NORTH TEXAS003
	9	05/24/85	AXC135C	NORTH TEXAS003
5				
	6	08/12/84	AXC015	NORTH TEXAS181
	35	12/05/84	AXC044	NORTH TEXAS181 (SAND HILL)
4				
	13	04/18/84	AXK973	NORTH TEXAS181, SAND HILLS 1
	4	03/29/84	AXK964	NORTH TEXAS184 (NORTH TEXAS 2)
12				
	12	12/12/85	AXC276C	NOSC 20KFT-1--090
	14	12/19/85	AXC278C	NOSC 20KFT-1-090
	11	12/10/85	AXC275C	NOSC 20KFT-2-270

Table C-2 (Continued)

Book No.	Page No.	Correlation Date	CCT	Title
	13	12/17/85	AXC227C	NOSC 20KFT-6-180
7				
	2	03/24/85	AXC202	NOSC 38KFT-1-090
12				
	10	12/02/85	AXC274C	NOSC 38KFT-1-090
11				
	17	10/01/85	AXC265C	NOSC 38KFT-2-270
	19	10/02/85	AXC266C	NOSC 38KFT-4-240
6				
	38	03/10/85	AXC200	NOSC 38KFT-6-180
12				
	9	11/26/85	AXC273C	NOSC 38KFT-7-300
5				
	33	11/16/84	AXC045	NOSC TOWER-1-090
6				
	12	01/26/85	AXC077	NOSC TOWER-1-090
	16	01/29/85	AXC080	NOSC TOWER-1-090
	40	03/13/85	AXC103	NOSC TOWER-1-090
	41	03/19/85	AXC104	NOSC TOWER-1-090
7				
	1	03/24/85	AXC106	NOSC TOWER-1-090
	4	03/27/85	AXC107C	NOSC TOWER-1-090
	13	04/13/85	AXC115	NOSC TOWER-1-090
	14	04/15/85	AXC114	NOSC TOWER-1-090
	15	04/17/85	AXC116	NOSC TOWER-1-090
6				
	14	01/27/85	AXC079	NOSC TOWER-1-240
7				
	3	03/26/85	AXC108	NOSC TOWER-1-240
	10	04/10/85	AXC111	NOSC TOWER-1-240
	11	04/11/85	AXC112	NOSC TOWER-1-240
6				
	13	01/26/85	AXC078	NOSC TOWER-1-270
	43	03/22/85	AXC105	NOSC TOWER-1-270
7				
	6	03/30/85	AXC109	NOSC TOWER-1-270
	28	05/08/85	AXC105C	NOSC TOWER-1-270
11				
	5	09/04/85	AXC147C	NOSC TOWER-1-270
	6	09/05/85	AXC145C	NOSC TOWER-1-270
	7	09/06/85	AXC144C	NOSC TOWER-1-270
	8	09/10/85	AXC109C	NOSC TOWER-1-270
7				
	9	04/03/85	AXC110	NOSC TOWER-1-300
	12	04/11/85	AXC113	NOSC TOWER-1-300
6				
	39	03/12/85	AXC102	NOSC TOWER-A-090
12				
	21	01/22/86	AXC284C	OTTAWA WOODS-181
5				
	41	01/08/85	AXC057	OWENS VALLEY
3				

Table C-2 (Continued)

Book No.	Page No.	Correlation Date	CCT	Title
	2	02/24/84	AXK942	OWENS VALLEY, CALIFORNIA
4				
	27	06/13/84	AXK990	OWENS VALLEY, CALIFORNIA
3				
	10	03/07/84	AXK951	OWENS VALLEY, CALIFORNIA 2
5				
	15	10/04/84	AXC027	OWENS VALLEY-166 (INDEPENDENCE, CA)
10				
	11	08/05/85	AXC240C	OWENS VALLEY-168
12				
	25	02/06/86	AXC285C	OWENS VALLEY-168
13				
	1	02/07/86	AXC286C	OWENS VALLEY-168 (OWENS VALLEY-85-2)
	2	02/09/86	AXC287C	OWENS VALLEY-168 (OWENS VALLEY-85-3)
	3	02/10/86	AXC288C	OWENS VALLEY-168 (OWENS VALLEY-85-4)
8				
	18	06/05/85	AXC211C	OWENS VALLEY-346
	19	06/05/85	AXC212C	OWENS VALLEY-346
	20	06/06/85	AXC213C	OWENS VALLEY-346
	23	06/08/85	AXC217C	OWENS VALLEY-347
9				
	1	06/27/85	AXC221C	OWENS VALLEY-347
	4	06/27/85	AXC224C	OWENS VALLEY-347
4				
	6	04/03/84	AXK966	PALASTINE TX91, PALESTINE 3, TEXAS
	18	05/11/84	AXK978	PISGAH CAL 4
	19	05/14/84	AXK979	PISGAH CAL 4
10				
	12	08/06/85	AXC241C	PISGAH CAL-7
3				
	3	02/28/84	AXK944	PISGAH CAL1 (PISGAH, CALIFORNIA)
	4	02/29/84	AXK945	PISGAH CAL1 (PISGAH, CALIFORNIA)
1				
	6	12/11/83	AXK912	PISGAH CAL2 (PISGAH, CALIFORNIA)
	4	12/06/83	AXK910	PISGAH CAL3 (PISGAH, CALIFORNIA)
	5	12/07/83	AXK911	PISGAH CAL3 (PISGAH, CALIFORNIA)
5				
	29	11/11/84	AXC040	PISGAH CAL4
1				
	7	12/13/83	AXK913	PISGAH CAL4 (PISGAH, CALIFORNIA)
	10	12/16/83	AXK916	PISGAH CAL4 (PISGAH, CALIFORNIA)
4				
	9	04/08/84	AXK969	PISGAH CAL4, CALIFORNIA
1				
	11	12/18/83	AXK917	PISGAH CAL5 (PISGAH, CALIFORNIA)
2				
	12	01/31/84	AXK934	PISGAH CAL5 (PISGAH, CALIFORNIA)

Table C-2 (Continued)

Book No.	Page No.	Correlation Date	CCT	Title
	13	02/01/84	AXK935	PISGAH CAL5 (PISGAH, CALIFORNIA)
1				
	9	12/15/83	AXK915	PISGAH CAL6 (PISGAH, CALIFORNIA)
5				
	30	11/11/84	AXK041	PISGAH CAL7
	5	08/05/84	AXC014	PISGAH CAL7 (SIGMA 0 AND CALIBRATION)
	3	07/26/84	AXC012	PISGAH CAL7 (EARLY) CALIFORNIA
	4	07/27/84	AXC013	PISGAH CAL7 (LATE) CALIFORNIA
2				
	2	01/12/84	AXK924	PISGAH CAL7 (PISGAH, CALIFORNIA)
8				
	26	06/12/85	AXC220CC	RAISIN CBAND260
5				
	32	11/15/84	AXC043	RAISIN CITY 315
10				
	20	08/19/85	AXC249C	RAISIN CITY-325
12				
	4	11/13/85	AXC249C2	RAISIN CITY-325
5				
	31	11/15/84	AXC042	RAISIN CITY003
3				
	12	03/13/84	AXK953	RAISIN CITY003 (AGRICULTURAL FIELDS, CALIFORNIA)
	16	03/20/84	AXK958	RAISIN CITY003 (AGRICULTURAL FIELDS, CALIFORNIA)
	18	03/23/84	AXK960	RAISIN CITY003 (AGRICULTURAL FIELDS, CALIFORNIA)
4				
	2	03/27/84	AXK962	RAISIN CITY003 (AGRICULTURAL FIELDS, CALIFORNIA)
5				
	38	12/17/84	AXC055	RAISIN CITY270
3				
	13	03/14/84	AXK954	RAISIN CITY270 (AGRICULTURAL FIELDS, CALIFORNIA)
	15	03/16/84	AXK957	RAISIN CITY270 (AGRICULTURAL FIELDS, CALIFORNIA)
4				
	3	03/29/84	AXK963D	RAISIN CITY270 (AGRICULTURAL FIELDS, CALIFORNIA)
3				
	14	03/14/84	AXK955	RAISIN CITY315 (AGRICULTURAL FIELDS, CALIFORNIA)
6				
	42	03/20/85	AXC201	RAISIN FRESNO-270
8				
	22	06/07/85	AXC215C	RAISIN FRESNO-270
	21	06/07/85	AXC214C	RAISIN FRSNO-270
13				
	8	03/05/86	AXC296C	RAISIN FRSNO-270 (RAISIN CITY-85-1)

Table C-2 (Continued)

Book No.	Page No.	Correlation Date	CCT	Title
12				
	5	11/14/85	AXC148C	RAISIN-FRESNO-034
	6	11/16/85	AXC150C	RAISIN-FRESNO-034
8				
	27	06/13/85	AXC216C	RAISIN-FRSNO-090
9				
	7	07/03/85	AXC225CC	RHODES L/C-BAND
10				
	1	07/29/85	AXC230C	RHODES NEV-000
1				
	3	12/01/83	AXK903	ROSE BOWL (JPL, PASADENA, CALIFORNIA)
	14	01/04/84	AXK920	ROSE BOWL (PASADENA, CALIFORNIA)
4				
	43	07/17/84	AXC006	SAN ANDREAS137 (SAN FRANCISCO-URBAN)CALIFORNIA
	40	07/11/84	AXC002	SAN ANDREAS137 (SFO-NORTH)
	34	07/06/84	AXK996	SAN ANDREAS137 (SOUTH SFO BAY)
	20	05/30/84	AXK980	SAN ANDREAS317 (SF BAY WAVES)
8				
	16	06/01/85	AXC209C	SAN JOAQUIN
	12	05/29/85	AXC207	SAN JOAQUIN ENG
	13	05/31/85	AXC207C2	SAN JOAQUIN ENG
	14	05/31/85	AXC208C2	SAN JOAQUIN ENG
13				
	25	07/03/86	AXC311C	SAN JOAQUIN ENG
8				
	24	06/11/85	AXC218C	SAN JOAQUIN ENG.
9				
	11	07/16/85	AXC207C3	SAN JOAQUIN ENG.
2				
	10	01/26/84	AXK932	SF BAY1 (SAN FRANCISCO BAY, CALIF., PACIFIC OCEAN WAVES 2)
1				
	13	12/23/83	AXK919	SF BAY1 (SAN FRANCISCO BAY, CALIFORNIA)
2				
	7	01/20/84	AXK930	SF BAY1 (SAN FRANCISCO BAY, CALIFORNIA, PACIFIC OCEAN WAVES)
	9	01/21/84	AXK929	SF BAY1 (TOMALES BAY 2, CALIFORNIA)
1				
	16	01/07/84	AXK922	SF BAY2 (GOLDEN GATE BRIDGE, CALIFORNIA)
2				
	16	02/17/84	AXK938	SF BAY2 (MOFFETT FIELD, CALIFORNIA)
	4	01/14/84	AXK926	SF BAY2 (SAN FRANCISCO, TOMALES, AKA BODEGA BAY, CALIFORNIA)
3				
	11	03/08/84	AXK952	SF-FARLON77 (SAN FRANCISCO SHIPS, PACIFIC OCEAN WAVES)

Table C-2 (Continued)

Book No.	Page No.	Correlation Date	CCT	Title
12				
	22	01/23/86	AXC152C	SHASTA-126
	23	01/23/86	AXC153C	SHASTA-127
8				
	15	06/01/85	AXC140C	SHASTA-308
12				
	24	01/30/86	AXC154C	SHASTA-308
	16	01/07/86	AXC280	SHASTA-STER-135
10				
	8	08/03/85	AXC237C	SHASTA-STER-136
12				
	18	01/10/86	AXC282	SHASTA-STER-136
10				
	9	08/03/85	AXC238C	SHASTA-STER-137
12				
	17	01/09/86	AXC281	SHASTA-STER-137 (SHASTA-STEREO-2B)
10				
	10	08/04/85	AXC239	SHASTA-TOPO-135
4				
	44	07/18/84	AXC007	SHEMDIN'S LAST SHIP PASS
	33	07/04/84	AXK988	SHIP PASS 001 (GULF OF ALASKA)
	25	06/07/84	AXK986	SHIP PASS 002, GULF OF ALASKA
	29	06/20/84	AXK989	SHIP PASS 003, GULF OF ALASKA
	10	04/14/84	AXK970	SHIP PASS 004, GULF OF ALASKA
	24	06/06/84	AXK985	SHIP PASS 004, GULF OF ALASKA
	26	06/08/84	AXK984	SHIP PASS 005, GULF OF ALASKA
	14	04/20/84	AXK974	SHIP PASS 006, GULF OF ALASKA
	8	04/06/84	AXK967	SHIP PASS 007, EXTENDED SHIP WAKE, GULF OF ALASKA
	7	04/04/84	AXK968	SHIP PASS 007, GULF OF ALASKA
	23	06/05/84	AXK983	SHIP PASS 010 (CROSS WAKE-#5), GULF OF ALASKA
	26A	06/11/84	AXK987	SHIP PASS 013, GULF OF ALASKA
11				
	18	10/01/85	AXC267C	SNAKE RIVER-150
13				
	11	03/26/86	AXC300C	SNAKE RIVER-150 (SNAKE RIVER-150-1)
	12	03/26/86	AXC301C	SNAKE RIVER-150-2
9				
	9	07/15/85	AXC227C	SNAKE RIVER-151
	10	07/15/85	AXC228C	SNAKE RIVER-151
13				
	21	05/07/86	AXC307C	SNAKE RIVER-331
	22	05/07/86	AXC308C	SNAKE RIVER-331
6				
	32	02/28/85	AXC096	SODA SPRING-127
8				
	1	05/16/85	AXC129	SODA SPRING-307
	6	05/21/85	AXC132C	SRP SWAMP 122
	7	05/21/85	AXC133C	SRP SWAMP 122

Table C-2 (Continued)

Book No.	Page No.	Correlation Date	CCT	Title
4				
	28	06/15/84	AXK991	SRP SWAMP 124 (DUMBARTON BAYS)
	12	04/17/84	AXK972	SRP SWAMP123, ELLENTON BAY, SOUTH CAROLINA
7				
	34	05/13/85	AXC126	SRP SWAMP124
	35	05/13/85	AXC126C	SRP SWAMP124
4				
	1	03/27/84	AXK961	SRP SWAMP125, SAVANNAH RIVER PLANT SWAMP SAND HILLS, SC
5				
	34	11/20/84	AXC046	SRP SWAMP302
10				
	25	08/28/85	AXC143C	SRP SWAMP302 (SAVANNAH RIVER PLANT SWAMP)
11				
	1	09/01/85	AXC142C	SRP SWAMP302 (SAVANNAH RIVER PLANT SWAMP)
3				
	17	03/22/84	AXK959	SRP SWAMP302 PEN BRANCH, SAVANNAH RIVER PLANT, SC
7				
	32	05/13/85	AXC125	SRP SWAMP303
	33	05/13/85	AXC125C	SRP SWAMP303
5				
	21	10/20/84	AXC033	SUPERSITE2
	23	10/25/84	AXC035	SUPERSITE2
	24	10/26/84		SUPERSITE2
6				
	7	01/20/85	AXC071	SUPERSITE2
	8	01/20/85	AXC072	SUPERSITE2
5				
	20	10/19/84	AXC032	SUPERSITE4
	22	10/23/84	AXC034	SUPERSITE4
6				
	10	01/24/85	AXC075	SUPERSITE4
	11	01/25/85	AXC076	SUPERSITE6
7				
	16	04/18/85	AXC076C	SUPERSITE6
	18	04/22/85	AXC117	SUPERSITE6
	19	04/23/85	AXC117C	SUPERSITE6
	20	04/24/85	AXC118C	SUPERSITE6
	21	04/25/85	AXC119C	SUPERSITE6
	25	05/01/85	AXC120C	SUPERSITE6
9				
	17	07/25/85	AXC117C2	SUPERSITE6
	18	07/25/85	AXC118C2	SUPERSITE6
	20	07/27/85	AXC119C2	SUPERSITE6
	21	07/27/85	AXC120C2	SUPERSITE6
13				
	9	03/12/86	AXC297C	TRANSMITTER OFF TEST
10				

Table C-2 (Continued)

Book No.	Page No.	Correlation Date	CCT	Title
	2	07/30/85	AXC231C	TRAV CITY-140'
11				
	16	09/21/85	AXC262C	TRAV-CITY-046
10				
	24	08/27/85	AXC254C	TRAV-CITY-046 (TRAVERSE CITY, MICHIGAN)
	26	08/28/85	AXC255C	TRAV-CITY-047 (TRAVERSE CITY, MICHIGAN)
13				
	7	03/05/86	AXC295C	TUG HILL-356
6				
	28	02/22/85	AXC092	TWT AQUEDUCT
13				
	10	03/17/86	AXC299C	VERMONT-195 (CAMELBACK-85-1)
6				
	37	03/06/85	AXC101	WINCHESTER VA-094
	19	01/31/85	AXC083	WINCHSTER VA-091
	20	02/01/85	AXC084	WINCHSTER VA-091
7				
	8	03/31/85	AXC101C	WINCHSTER VA-094
	7	03/31/85	AXC101C	WINCHSTER VA-094
5				
	43	01/11/85	AXC058	WINCHSTER VA-272 (STEVENS CITY)
	42	01/10/85	AXC059	WINCHSTER VA-272 (WALDENSVILLE-1)
4				
	21	06/01/84	AXK981	WINCHSTR VA 292
11				
	9	09/10/85	AXC256C	WIND RIVER-155
9				
	12	07/16/85	AXC229C	WIND RIVER-355
10				
	3	07/30/85	AXC232C	WIND RIVER-355
	4	07/31/85	AXC233C	WIND RIVER-355
11				
	2	09/01/85	AXC253C	WIND RIVER-355 (WIND RIVER, WYOMING)
1				
	8	12/14/83	AXK914	WIND RIVER2 (WIND RIVER, WYOMING)
6				
	9	01/23/85	AXC074	WIND RIVER4
13				
	13	03/27/86	AXC074C	WIND RIVER4
5				
	7	08/15/84	AXC016	WIND RIVER4 (WIND RIVER REDO)
3				
	9	03/06/84	AXK943	WIND RIVER4 (DEAD MAN BUTTE WEST, WYOMING)
2				
	5	01/18/84	AXK927	WIND RIVER4 (DEAD MAN BUTTE, WYOMING)

Table C-2 (Continued)

Book No.	Page No.	Correlation Date	CCT	Title
	3	01/13/84	AXK925	WIND RIVER4 (SPRING CREEK, WYOMING)

APPENDIX D

PARTICIPANT ADDRESSES

John Reller
George Grant
George Alger
NASA/Ames Research Center
Medium Altitude Mission Branch
Mail Code 211-12
Moffett Field, CA 94035
(415) 694-5392/5525/5342
FTS 464-5392/5525/5342

Jim Ormsby
Code 624
NASA/Goddard Spce Flight Center
Greenbelt, MD 20771
(301) 286-6811
FTS 888-6811

Ed Masuoka
Code 622
NASA/Goddard Spaceflight Center
Greenbelt, MD 20771
(301) 286-4743
FTS 888-4743

Jim Wang
Mail Code 675
NASA Goddard
Greenbelt, MD 20771
(301) 864-8949
FTS 888-8949

JET PROPULSION LABORATORY

Walter Brown, Jr. (MS 183-701) X 2110
Diane Evans (MS 183-701) X 2418
Tom Farr (MS 183-701) X 2418
Dick Goldstein (MS 183-701) X 6999
Dan Held (MS 183-701) X 7763
Mike Kobrick (MS 183-701) X 4631
Harold Lang (MS 183-501) X 3440
Jack Paris (MS 183-501) X 6936
Barry Rock (MS 183-501) X 6229
Tommy Thompson (MS 183-701) X 3792
Howard Zebker (MS 183-701) X 8780

4800 Oak Grove Drive
Pasadena, CA 91109
(818) 354-XXXX
FTS 792-XXXX

Dave Pitts
Mail Code SN-3
NASA/Johnson Space Center
Houston, TX 77058
(713) 483-5171
FTS 525-5171

Jules Lehmann
Bob Murphy
Diane Wickland
Code EEL
NASA Headquarters
Washington, DC 20546
(202) 453-1720
FTS 453-1720

Armond Joyce
NASA/National Space Technology Lab.
Mail Code HA10
NSTL Station, MS 39529
FTS 494-3830

Steve Wu
NASA/National Space Technology Lab.
Mail Code HA20
NSTL Station, MS 39529
FTS 494-1922

Tom Schmugge
USDA/ARS Hydrology Laboratory
Room 139, Bldg. 007 BARC-West
Beltsville, MD 20705
(301) 344-1554
FTS 344-1554

Peter Mouginis-Mark
Planetary Geosciences Division
Hawaii Institute of Geophysics
2525 Correa Road
Honolulu, HI 96822
(808) 948-6490

Fawwaz Ulaby
Craig Dobson
University of Michigan
Radiation Laboratory
Department of Electrical &
Computer Engineering
4072 E. Engineering Building
Ann Arbor, MI 48109
(313) 764-0500

Jim Taranik
Marcus Borengasser
Mackay School of Mines
University of Nevada-Reno
Reno, MV 89557-0047
(702) 784-6987/4263

Verne Kaupp
University of Arkansas
Dept. of Electrical Engineering
Fayetteville, AR 72701
(501) 575-6582

Roger Hoffer
Purdue University
Dept. of Forestry
Laboratory for Applications of
Remote Sensing
West Lafayette, IN 47907
(317) 494-3605

Dave Simonett
University of California
Santa Barbara
Dept. of Geography
Santa Barbara, CA 93106
(805) 961-2013

Thomas Parr
The Analytic Sciences Corp.
One Jacob Way
Reading, MA 01867
(617) 944-6850

Ron Wasowski
Department of Earth Sciences
University of Notre Dame
Notre Dame, IN 46556
(219) 239-6492

APPENDIX E

ABBREVIATIONS/NOMENCLATURE/ACRONYMS

A/C	aircraft
ADC	analog-to-digital converter
ADDAS	Airborne Digital Data Acquisition System
ASCII	American Standard Code for Information Interchange
az.	azimuth, along-track dimension
BP FILT	bandpass filter
bpi	bits per inch
Bpi	bytes per inch
C-band	microwave frequency range (4,000 to 8,000 MHz)
CCT	computer-compatible tape
CV-990	Convair jet airliner, Model 990
CW	continuous wave
DA	drift angle
dB	decibel
DICO	Dicomed media conversion unit (CCT to photographic negative)
D-log E	film-density logarithm (exposure)
DN	digital number
Fairchild M-80	Fairchild brand HDDR model number 80
FOV	field of view
FPS	Floating Point Systems
GMT	Greenwich Mean Time
GS	ground speed
GSFC	NASA/Goddard Space Flight Center
HDDR	high-density digital recorder
HDDT	high-density digital tape
HH	transmit horizontal, receive horizontal polarizations
HP-9845	Hewlett-Packard computer model number 9845
HV	transmit horizontal, receive vertical polarizations
INS	Inertial Navigation System
IPL	Image Processing Laboratory (at JPL)
I/O	input/output
IRIG	interrange instrumentation group
IR	infrared
JPL	Jet Propulsion Laboratory
JSC	NASA/Johnson Space Center
KS-87	small-format (12.7-cm, 5-in. film) airborne camera
kt	knot (nautical mi/h)
L-band	microwave-frequency range (1,000 to 2,000 MHz)
LO	local oscillator
MAMB	Medium Altitude Missions Branch, NASA/Ames Research Center
M-80	Fairchild model 80 HDDR
μs	microsecond

NASA	National Aeronautics and Space Administration
NSTL	National Space Technology Laboratory
NOSC	Naval Ocean Science Center
OSSA	Office of Space Science Applications, NASA Headquarters
PI	principal investigator
pixel	picture element
PRF	pulse-repetition frequency
Quad-Pol	four polarization data: HH, HV, VH, and VV
RAM	random access memory
Ramtek	Ramtek brand high-resolution color image display unit
rf	radio frequency
RMS	root mean square
RS-8 or RS-9	large-format (22.9-cm, 9-in. film) airborne camera
Sabre III	Sabre brand HDDR, model 3
SAR	synthetic aperture radar
SCP	strip contact print
SIR	Spaceborne Imaging Radar
SNR	signal-to-noise ratio
STALO	stable local oscillator
STC	sensitivity time control
TWT	traveling-wave tube
UCSB	University of California, Santa Barbara
VAX	Digital Equipment Corporation computer model line
VH	transmit vertical, receive horizontal polarizations
VV	transmit vertical, receive vertical polarizations
X-band	microwave-frequency range (8,000 to 12,000 MHz)